

Polymer tensiometers to characterize  
unsaturated zone processes in dry soils

**Promotor:**

Prof. dr. ir. R.A. Feddes

Hoogleraar Bodemnatuurkunde,  
Agrohydrologie en  
Grondwaterbeheer,  
Wageningen Universiteit

**Copromotor:**

Dr. ir. G.H. de Rooij

Universitair hoofddocent  
bij de leerstoelgroep  
Bodemnatuurkunde, Ecohydrologie  
en Grondwaterbeheer,  
Wageningen Universiteit

**Promotiecommissie:**

Prof. dr. P.A. Ferré

Prof. dr. M.A. Cohen Stuart

Prof. dr. ir. P.C. Struik

Prof. dr. H. Vereecken

University of Arizona, Verenigde Staten

Wageningen Universiteit

Wageningen Universiteit

Forschungszentrum Jülich, Duitsland

Dit onderzoek is uitgevoerd binnen de onderzoeksschool SENSE.

# Polymer tensiometers to characterize unsaturated zone processes in dry soils

Martine J. van der Ploeg

Proefschrift  
ter verkrijging van de graad van doctor  
op gezag van de rector magnificus  
van Wageningen Universiteit,  
Prof. dr. M.J. Kropff  
in het openbaar te verdedigen  
op vrijdag 19 december 2008  
des namiddags te vier uur in de Aula.

Van der Ploeg, M.J.

Polymer tensiometers to characterize unsaturated zone processes in dry soil.  
[Doctoral thesis, Wageningen University, 2008]

ISBN 978-90-8585-257-5

---

# Abstract

---

More frequent and intense droughts due to global climate change, together with an increasing agricultural water use emphasize the importance of understanding root water uptake by plants under water-stressed conditions. Root water uptake is driven by potential gradients between water in the soil and in the root. In unsaturated soil, the soil water matric potential is often the largest component of the total soil water potential. Tensiometers are commonly used to measure the pressure-equivalent of the matric potential. Unfortunately, the water-filled reservoir of conventional tensiometers limits their applicability to soil water matric pressures above approximately  $-0.09$  MPa. Using tensiometers filled with a polymer solution instead of water extends the measurement range beyond a matric pressure of  $-1.6$  MPa (almost twenty times more than water-filled tensiometers). This thesis deals with the development of such polymer tensiometers, which consists of a wide-range pressure transducer with a temperature sensor, a stainless steel casing, and a ceramic plate with a membrane to prevent leakage of the polymer solution.

The polymer tensiometers were tested under laboratory conditions for long-term operation, the effects of temperature, response times, and performance in repacked sandy loam, sand, and loam. Several months of continuous operation caused a gradual drop in the osmotic pressure, for which a suitable correction was developed. The osmotic potential of polymer solutions is temperature-dependent, and requires calibration before installation in the soil. The response times to ambient temperature variations were found to be affected by polymer chamber height and polymer type. By minimizing the volume of polymer solution inside the tensiometer while at the same time maximizing the ceramic area in contact with that polymer solution, response times dropped to acceptable ranges for laboratory

and field conditions. Contact with the soil has been improved by using cone-shaped solid ceramics instead of flat ceramics.

By combining polymer tensiometer and time domain reflectometry readings, *in situ* moisture retention curves could be measured over the range permitted by both instruments. Independently determined soil moisture retention curves were used to convert soil moisture content measurements from time domain reflectometry probes to matric potentials. It was shown that at low moisture contents, the accuracy of the time domain reflectometry probes, and the accuracy of the conversion had a large influence. The comparison between matric potentials measured by polymer tensiometers and potentials obtained indirectly by time domain reflectometry thus highlights the risk of using the latter method at low soil moisture contents.

Subsequently, the suitability of polymer tensiometers to monitor soil matric potentials in the presence of root water uptake was evaluated in a cropped lysimeter experiment. Three irrigation intensities created severe, intermediate, and no water stress conditions in lysimeters with growing maize (*Zea mays*, L.) plants. In the lysimeter experiment soil water matric potentials measured by polymer tensiometers yielded more accurate levels of local water stress than would have resulted using conventional methods. The predefined stress levels were located at the steep dry end of the moisture retention curve, where volumetric moisture measurements for this particular loam soil were less informative compared to matric potential measurements. Observation of matric potentials by polymer tensiometers showed the ability of maize plants to take up water under extremely dry conditions, and to shift water uptake areas to lower, relatively wetter soil layers. This shift in water uptake to deeper layers seems to occur when the steep dry end of the retention curve is reached at a shallower depth. Observations made in rhizotubes during the experiment showed that water stress provoked root growth deeper in the soil profile, and showed the dynamic response of root growth during periods of water stress and resumed irrigation.

Polymer tensiometers are currently the only field instruments that can reliably measure the steep dry end of the soil moisture retention curve. The results presented in this thesis demonstrate that polymer tensiometers are an important instrumental addition when characterizing soil physical processes in dry soils.

---

## Preface

---

My Ph.D. *adventure* could not have been *la dolce vita* without the help, support and friendship of many.

As my supervisor at the time of my M.Sc thesis, Sylvi Haldorsen showed me that *science* is not only *serious business*, but also great *fun*. Toon Leijnse stuurde mij naar een wetenschappelijk congres om eens rond te gaan kijken waar ik *de smaak van water* pas echt te pakken kreeg.

Op dit congres kwam ik Ger de Rooij tegen die, tot zijn eigen verbazing vermoed ik, mij enthousiast kreeg voor een promotieonderzoek in de bodemfysica. Ger had *great expectations*, werd waarschijnlijk *knetter* van mijn eigenwijze *karakter* en leukte de werkdagen op met *big fish*-verhalen. Nadat Sinterklaas zijn kantoor had geherdecoreerd hoorde ik al snel bij de *usual suspects* wanneer er iets gebeurde, wat vaak ook terecht was. Ik wil je bedanken dat je mij in een vroeg stadium naar congressen hebt gestuurd, omdat het juist voor een jonge onderzoeker belangrijk is een netwerk op te bouwen. Verder ben ik je, ondanks mijn gemopper, dankbaar voor het commentaar op mijn *pulp fiction*, wat bij het schrijven van dit proefschrift goed van pas kwam.

Reinder volgde het project gedurende het grootste deel enthousiast vanaf een afstandje. De laatste maanden was hij erg betrokken bij het proefschrift en zette met een *eagle eye* de puntjes op de i.

Dit onderzoek werd gefinancierd door de Technologiestichting STW, als onderdeel van NWO en het technologie programma van EZ. Ik dank Lia, Rene, Cindy, Luuk, Henk en de leden van de gebruikerscommissie voor de prettige samenwerking tijdens dit project.

Veel dank gaat naar de familie Van Bentem voor het belangeloos beschikbaar stellen van de bodem voor het lysimeter experiment. Dank aan Ko voor het advies en de literatuur. Dank aan Bart Timmermans en Peter van der Putten voor het advies op het gebied van wortelbemonstering en CWE voor het gebruik van de

faciliteiten. Stavroula, thank you, it was amazing you were willing to take over the root washing and scanning procedures from me. Joke, dankjewel dat ik je naaimachine mocht lenen voor enkele experimentele onderdelen en voor *de vriendschap*.

Pat and Kris, thank you for making me feel at *home*, showing me all the two-and-a-half-hour-drive-wonders of Riverside, and saving me from seeing too many *Saw IV* type movies. John, thank you for teaching me how to drive *cars*, even though you knew I had hardly driven before. *June*, thank you for the terrific *dinner* on *Thanksgiving*, and all the other things. Many thanks to Ranvir and Gina, and family, especially for the ‘grapes’ at New Year’s Eve. Rien, Pete, Jack, Joann, Eran and Jirka, thank you for *the hours* you spend to help me with what sometimes seemed like a *labyrinth*.

I thank the people of the Forschungszentrum Jülich for giving me the opportunity to stay a month to work on root water uptake modeling. Mathieu and Tom, it is great fun working with you.

*Another day at the office* hoeft geen *Walhalla* te zijn, maar fijne collega’s helpen veel. Harm en Hidde, dank voor de gesprekken over Alles en Nogwat. Ik ben heel blij dat jullie mijn paranimfen zijn. Gerben, als *third man* zorgde jij voor levendige donderdagen. Esther en Franck, het was leuk! Sjoerd en Klaas, dank dat jullie af en toe vanaf de zijlijn meekeken. Henny, dankjewel voor de hulp met experimentele zaken en met de kaft van het proefschrift. Johan en Herman, dank voor jullie altijd prachtig uitgevoerde opstellingen. Dank aan alle (oud)medewerkers van SEG en HWM.

*Het echte leven* ziet er soms als een *ratatouille* uit, maar er zijn gelukkig altijd *happy go lucky heroes* die er de moed in te houden. *Sterren stralen overal*. Lot, we lijken vaak *als twee druppels water*. Ik ben blij met *zo’n fijne familie*. Bedankt pa en ma. Lieve Dennis, *Leef! een gelukkige tijd* alsof *het alle dagen feest* is, desnoods *met een lach en een traan*. Wanneer ik mezelf een *Frankenweenie* voel vind je dat niet erg. Het dankwoord is dan ook van begin tot eind vooral voor jou geschreven, maar dat had je vast al gezien.



---

## List of symbols and abbreviations

---

The symbols and abbreviations are listed in the table below, together with a short description, and units where applicable.

Symbol	Short description	Dimensions	Units
$\alpha$	Parameter to scale $h_m$	$L^{-1}$	$m^{-1}$
$\chi$	Flory–Huggins interaction parameter	-	-
$\phi$	Volume fraction	-	-
$\mu$	Soil water potential	$L^2t^{-2}$	$J\ kg^{-1}$
$\mu_j$	Chemical potential	$L^2t^{-2}$	$J\ kg^{-1}$
$\pi$	Osmotic pressure of the polymer solution	$ML^{-1}t^{-2}$	Pa
$\pi_t$	Osmotic pressure at time $t$	$ML^{-1}t^{-2}$	Pa
$\Theta$	Normalized volumetric moisture content	-	-
$\theta$	Volumetric moisture content	$L^3L^{-3}$	$m^3\ m^{-3}$
$\theta_{\text{grav}}$	Gravimetric moisture content	$L^3L^{-3}$	$m^3\ m^{-3}$
$\theta_r$	Residual volumetric moisture content	$L^3L^{-3}$	$m^3\ m^{-3}$
$\theta_s$	Saturated volumetric moisture content	$L^3L^{-3}$	$m^3\ m^{-3}$
$\theta_{\text{TDR}}$	Volumetric moisture content as measured by TDR	$L^3L^{-3}$	$m^3\ m^{-3}$
$\rho_d$	Dry bulk density of the soil	$ML^{-3}$	$kg\ m^{-3}$
$\rho_w$	Density of water	$ML^{-3}$	$kg\ m^{-3}$

Symbol	Short description	Dimensions	Units
$\tau$	Pressure decay parameter	t	days
$\omega$	Pressure transducer sensitivity	$ML^{-4}t^{-2}$	$Pa\ m^{-3}$
$\psi$	Soil water potential	$ML^{-1}t^{-2}$	Pa
$\psi_g$	Gravitational potential	$ML^{-1}t^{-2}$	Pa
$\psi_m$	Matric potential	$ML^{-1}t^{-2}$	Pa
$\psi_o$	Osmotic potential	$ML^{-1}t^{-2}$	Pa
$\psi_p$	Pressure potential	$ML^{-1}t^{-2}$	Pa
$\psi_{tot}$	Total soil water potential	$ML^{-1}t^{-2}$	Pa
$A$	Fitting parameter	$ML^{-1}t^{-1}\ T^{-1}$	$Pa\ d\ ^\circ C^{-1}$
$b$	Fitting parameter	$ML^{-1}t^{-2}$	Pa
$C_i$	Fitting parameter with $i = 1,2,3$	-	-
$c$	Fitting parameter	-	-
$G$	Gibbs free energy	$ML^2t^{-2}$	J
$\Delta G_m$	Gibbs free energy change for mixing a polymer with a solvent	$ML^2t^{-2}$	J
$g$	Gravitational acceleration	$Lt^{-2}$	$m\ s^{-2}$
$h$	Hydraulic head	L	m
$h_m$	Matric head	L	m
$I$	Interaction between various water potentials	$ML^{-1}t^{-2}$	Pa
$K_c$	Ceramic conductivity	$L^4M^{-1}$	$m^3\ s^{-1}Pa^{-1}$
$K_s(\psi)$	Unsaturated soil conductivity	$L^3tM^{-1}$	$m^2\ Pa^{-1}\ d^{-1}$
$L_r$	Root length density	$L^{-2}$	$m\ m^{-3}$
$L_{r,avg}$	Average root length density	$L^{-2}$	$m\ m^{-3}$
$L_{r,z}$	Cumulative root length density	$L^{-1}$	$m\ m^{-2}$
$l$	Polymer chain length	-	-
$m$	Van Genuchten parameter	-	-
$M$	Mass	M	kg
$N$	Number of samples	-	-
$N_r$	Number of roots	-	-
$n$	Van Genuchten parameter	-	-
x			

Symbol	Short description	Dimensions	Units
$n_j$	Mass of component j	M	kg
$\hat{n}_j$	Mass of all components except j	M	kg
$n_m$	Number of moles	-	mol
$P$	Pressure of a system	$ML^{-1}t^{-2}$	Pa
$P_{\text{ext}}$	External pressure of a system	$ML^{-1}t^{-2}$	Pa
$P_{\text{int}}$	Internal pressure of a system	$ML^{-1}t^{-2}$	Pa
$P_T$	Pressure at temperature $T$	$ML^{-1}t^{-2}$	Pa
$P_0$	Pressure at temperature $T_0$	$ML^{-1}t^{-2}$	Pa
$R^2$	Coefficient of determination	-	-
$q$	Heat flow	$ML^2t^{-2}$	J
$q_p$	Heat flow in a constant pressure process	$ML^2t^{-2}$	J
$R$	Gas constant	$ML^2t^{-2}T^{-1}$	$J \text{ mol}^{-1} \text{ K}^{-1}$
$S$	Entropy	$ML^2t^{-2}T^{-1}$	$J \text{ K}^{-1}$
$T$	Temperature	T	$^{\circ}\text{C}$
$T_0$	Reference temperature	T	$^{\circ}\text{C}$
$t$	Time	t	days
$U$	Energy content of a system	$ML^2t^{-2}$	J
$V$	Volume	$L^3$	$\text{m}^3$
$v_s$	Solution molair volume	$L^3$	$\text{m}^3$
$w$	Work	$ML^2t^{-2}$	J
$X_i$	Generalized force	$MLt^{-2}$	N
$x$	$x$ coordinate	L	m
$x_i$	Generalized displacement	L	m
$y$	$y$ coordinate	L	m
$Z$	Some property of a gas	$MLt^{-2}T^{-1}$	$J \text{ K}^{-1}$
$z$	$z$ coordinate	L	m

---

Abbreviation	Short description
CT	Conventional tensiometer
CV	Coefficient of variation
EB	Evaporation box
POT	Polymer tensiometer
RH	Relative Humidity
TDR	Time domain reflectometry

---

# Contents

---

<b>Abstract</b>	<b>v</b>
<b>Preface</b>	<b>vii</b>
<b>List of symbols and abbreviations</b>	<b>ix</b>
<b>1 Introduction</b>	<b>1</b>
1.1 Introduction	1
1.2 Root water uptake	2
1.3 Soil water potential theory	3
1.4 Instrumentation	5
1.4.1 Water-filled tensiometers	5
1.4.2 Thermocouple psychrometry	6
1.4.3 Indirect methods	7
1.4.4 Osmotic tensiometers	7
1.5 Thesis outline	8
<b>2 New polymer tensiometers: Measuring matric potentials down to wilting point</b>	<b>11</b>
2.1 Introduction	12
2.2 Design	13
2.3 Water reservoir tests	16
2.4 Block and sinusoidal temperature waves	19
2.5 Long-term behavior and rewetting	26
2.6 Repacked soil experiment	29
2.7 Conclusions	31
<b>3 Polymer tensiometers with ceramic cones: performance in drying soils</b>	<b>33</b>
3.1 Introduction	34
3.2 Design and operational procedures	36
	xiii

3.3 Temperature response times	40
3.4 Evaporation experiments	41
3.4.1 Soil drying process	45
3.4.2 Comparison of polymer tensiometers, time domain reflectometry probes and conventional tensiometers for sand and loam	46
3.4.3 Comparison of moisture retention curves	54
3.5 Conclusions	62
<b>4 Performance of polymer tensiometers in root water uptake studies in dry soil</b>	<b>63</b>
4.1 Introduction	64
4.2 Setup of the lysimeter experiment	65
4.3 Experimental conditions	71
4.4 Comparison of polymer tensiometers and time domain reflectometry probes	73
4.5 Conclusions	88
<b>5 Water uptake strategies by maize plants under varying levels of water stress</b>	<b>89</b>
5.1 Introduction	90
5.2 Experimental Setup	92
5.3 Root water uptake strategies	95
5.3.1 Matric potentials measurements by polymer tensiometers	95
5.3.2 Rhizotube observations and root length density	104
5.4 Conclusions	112
<b>6 Synthesis</b>	<b>113</b>
6.1 Conclusions	113
6.2 Outlook	116
6.2.1 Polymer tensiometers	116
6.2.2 Salinity	117
6.2.3 Plant responses to water stress	118
6.2.4 Modeling root water uptake	119
<b>A Derivation of soil water potential theory</b>	<b>121</b>
<b>B Flory-Huggins solution theory</b>	<b>125</b>

<b>Bibliography</b>	<b>127</b>
<b>Samenvatting</b>	<b>141</b>
<b>Curriculum Vitae</b>	<b>145</b>





# Chapter 1

---

## Introduction

---

### 1.1 Introduction

Water is the key component of life, and organisms exhibit various adaptation mechanisms for surviving and thriving within water-limited environments (Wood, 2005). Terrestrial organisms, like plants, are constantly losing water to the surrounding environment because they are in disequilibrium with the atmosphere (Wood and Jenks, 2007).

In many regions of the world plant growth and productivity are limited by water deficits. In developed agriculture, losses due to poor nutrition and plant health have been greatly reduced to the extent that crop losses relating to water availability exceed those from all other sources (Kramer 1980, Passioura 2002). Under the influence of climate change, droughts are becoming more frequent and intense, and as a result the area of land characterized as ‘very dry’ has more than doubled since the 1970s (Dai et al. 2004, Huntington 2006). Although 70-85% of the world’s consumable water is currently allotted to agriculture, increasing urban demands for potable water due to population growth will continue to compete with agricultural water use (Somerville and Briscoe 2001, Foley et al. 2005). Moreover, the new demands for alternative energy sources and the production of biofuels will create an even greater demand on the world’s limited water resources (Hill et al. 2006). As aquifers are depleted to supply irrigation for expanding agricultural production worldwide, crop losses as a consequence of drought will become more likely. Development of sustainable irrigation is highly necessary, and irrigation

practices must shift from land productivity to water productivity. The need to understand plant responses to water deficits has never been more acute.

## 1.2 Root water uptake

Periods of soil and atmospheric water deficit often occur within a plant's life cycle, even in temperate deciduous forests (Wilson et al. 2001) as well as in tropical rain forests (Grace 1999). Cell expansion, cell-wall synthesis and protein synthesis are among the processes most sensitive to water deficits (Hsiao et al. 1976, Hsiao et al. 1985, Lawlor and Leach 1985).

At microscopic scale, plants respond to water deficits by reduced leaf expansion, stomatal closure and other non-stomatal effected reductions in photosynthesis (Boyer 1970, Hsiao et al. 1985, Chaves 1991, Chaves et al. 2002). Stomata close in response to a decline in leaf turgor and/or water potential (e.g. Ludlow 1980) or to a low-humidity atmosphere (Schulze et al. 1987, Maroco et al. 1997). Leaf water potential was traditionally used by plant physiologists to describe plant responses to water deficits (Sadras and Milroy 1996). Various experiments however, have shown that roots are able to sense soil water status, and produce signals that trigger changes in leaf expansion rate and stomatal conductance (Blackman and Davies 1985, Gollan et al. 1986, Gowing et al. 1990, Davies and Zhang 1991, Mansfield and De Silva 1994, Sadras and Milroy 1996). Hence, the response of a plant to water deficit in the soil seems to be controlled by its roots.

Water in the soil is mostly absorbed by root hairs. It was demonstrated that the rate of root water uptake is not proportional to the amount of water stress (Cailloux 1972), and that the amount of roots in a particular layer of soil may change over time. This makes quantification of water absorption by roots a complex phenomenon involving root metabolism. Magnetic resonance imaging emerges as a potential method to study dynamic water uptake patterns of single roots (Pohlmeier et al. 2008, Segal et al. 2008). Instead of quantifying metabolisms of single roots, it is also possible and necessary to measure at a more macroscopic scale, and to observe the response to water deficit at the level of the plant.

Looking macroscopically, when water transpires from the leaves, the amount of water in the leaves will drop, causing water deficit. Consequently, water will move from tissues that hold more water to tissues that experience water deficit. As a consequence water will move throughout the plant and the soil along a series of frictional resistances, and against the force of gravity (Begg and Turner 1976). The water uptake rate by roots from the soil depends on the water conducting properties of the soil and the plant, and on the potential gradient between soil and plant. The background of this potential gradient will be explained in section 1.3.

To mathematically describe water flow through the soil-plant-atmosphere system an electrical analogue can be used (Van den Honert 1948, Kirkham 2002). The general approach in unsaturated zone hydrology however, is to add a sink term to the Richards' equation (Feddes and Raats 2004, Green et al. 2006). This sink term can be formulated such that it describes microscale physics of water flow (e.g Gardner 1960), or comprises an empirical macroscale function that describes root water uptake based on a response to water potentials (e.g Feddes et al. 1978).

A third category consists of models that are a hybrid approach of the two mentioned above, and include root density, root permeability, and root water extraction in the extraction relationship (Green et al. 2006). Extensive overviews of root water uptake models have been given by Hopmans and Bristow (2002), Feddes and Raats (2004), and Green et al. (2006).

### 1.3 Soil water potential theory

The driving force for root water uptake is the gradient in total water potential  $\psi_{\text{tot}}$  ( $\text{Pa} = \text{N m}^{-2}$ ) between soil and root xylem (e.g. Steudle and Peterson 1998). The water potential concept is derived from thermodynamic principles (See Appendix A). Corey and Klute (1985) provide a historical overview of the potential concept. Most plants can take up water down to potentials of about  $-1.6$  MPa, while some specialized plants such as cacti may survive much lower potentials (Wood 2005).

The water potential may be expressed as energy per unit mass  $\mu$  ( $\text{J kg}^{-1}$ ), energy per unit volume  $\psi$  ( $\text{N m}^{-2}$ ) or energy per unit weight  $h$  (m). Although only  $\mu$  has the actual unit of potential, the various expressions are equivalent under the

assumption of a constant density of water  $\rho_w$  ( $\text{kg m}^{-3}$ ). The expressions are widely used in a generic sense in the soil and plant sciences, and are related by (Warrick 2000):

$$\mu = \frac{\psi}{\rho_w} = gh \quad (1-1)$$

where  $g$  ( $\text{m s}^{-2}$ ) is the gravitational acceleration. Throughout this thesis the soil water potential is expressed as the pressure equivalent  $\psi$ .

Total water potential can be partitioned in several potentials:

$$\psi_{\text{tot}} = \psi_p + \psi_m + \psi_g + \psi_o + I \quad (1-2)$$

The pressure potential  $\psi_p$  is a result of the turgor pressure acting outward on the cell walls and internal membranes in a plant, or the hydrostatic pressure in the soil. The matric potential  $\psi_m$  describes the forces of capillarity in plant and soil, in addition to molecule imbibition forces associated with cell walls in plants, and colloidal surfaces that bind some of the water in the soil. In unsaturated soil,  $\psi_m$  is often the largest component of  $\psi_{\text{tot}}$ . The gravitational potential  $\psi_g$  defines the gravitational forces on the water, and the osmotic potential  $\psi_o$  denotes the influence of dissolved solutes. Finally, an interaction term  $I$  can be acknowledged (Begg and Turner 1976, Grant and Bachmann 2002), which emphasizes that the components of  $\psi_{\text{tot}}$  are not independent of each other and thus not strictly additive. In practice however, this concept is omitted, and interactive forces are generally assigned to each respective component of  $\psi_{\text{tot}}$ . Depending on specific situations, other potentials can be recognized. These are negligible in this thesis.

The definition of  $\psi_{\text{tot}}$  and the various terms in its expression have been continuously debated (eg. Groenevelt and Bolt 1969, Bolt 1976, Corey and Klute 1985, Iwata et al. 1988, Nitao and Bear 1996, Corey and Logsdon 2005). Problems in the definition arise from potentials referring to the soil solution and potentials referring to the water as a component of the soil solution.

During the experiments described in this thesis demineralized or non-chlorinated tap water low in dissolved solutes was used, therefore a negligible  $\psi_o$

of the soil solution is assumed in this thesis. During water bath experiments  $\psi_p$  was negligible. As the experiments in soil were most of the time unsaturated,  $\psi_p$  was assumed to be zero. As  $\psi_g$  was constant throughout experiments,  $\psi_p = 0$ , and  $\psi_o = 0$ , it is possible to determine plant responses to water stress by measuring  $\psi_m$  in the vicinity of roots.

## 1.4 Instrumentation

Components of  $\psi_{tot}$  can be measured by various instruments. A comprehensive overview can be found in Klute (1986a, Chapter 22-25), and Dane and Topp (2002, Chapter 3.2). Below a short overview is given.

### 1.4.1 Water-filled tensiometers

Tensiometers are widely used instruments to monitor  $\psi_m$ , and have been used for almost 100 years (Or 2001, Young and Sisson 2002). Bolt (1976) noted that readings obtained by tensiometers refer to potentials of the solution phase, and Edlefsen and Anderson (1943) pointed out that it is not possible to separate  $\psi_m$  from  $\psi_p$ . As in unsaturated soils,  $\psi_p$  is usually negligible, it is assumed that tensiometers measure  $\psi_m$ . All tensiometers consist of three elements (see Fig. 1-1): a ceramic that is in contact with the soil, a water reservoir in equilibrium with the soil water, and a pressure measurement device that measures this equilibrium accordingly. Unfortunately, the measurement of matric potentials by water-filled tensiometers is hampered by cavitation, and measurements are thus limited to above approximately  $-0.09$  MPa.

Attempts have been made to circumvent cavitation of tensiometers and to extend their measurement range. Tamari et al. (1993) used microtensiometers that could measure until approximately  $-0.14$  MPa for short time periods. Nucleation particles were removed by purging the tensiometers extensively with demineralized water, and this created the possibility of having the liquid in a metastable state. For geotechnical applications Ridley and Burland (1993) constructed a tensiometer that measured  $\psi_m$  down to  $-1.5$  MPa, but the instrument only worked for a few hours or less. This tensiometer, which was also studied by Tarantino and Mongiovi (2001) required a 24 hour pre-hydration phase in a high

pressure chamber at 4.0 MPa to dissolve air bubbles, and stopped working as soon as cavitation occurred. The tensiometer can only be used in the laboratory due to the elaborate preparation prior to use.

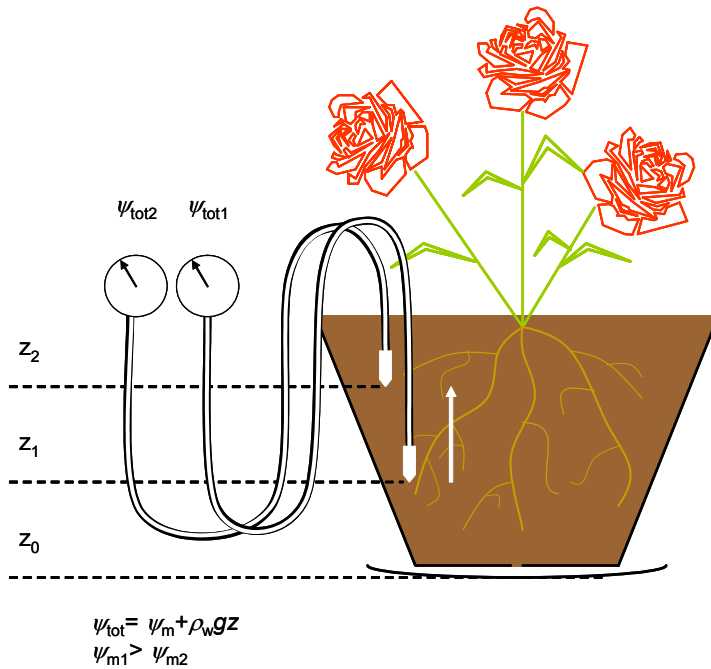


Figure 1-1. Setup of two tensiometers in a pot experiment. Water flow is directed upwards (white arrow).

### 1.4.2 Thermocouple psychrometry

Thermocouple psychrometry is a technique that infers the water potential of the liquid phase of a soil sample from relative humidity measurements within the vapor phase that is in equilibrium with the sample (Andraski and Scanlon 2002). As a result it measures both  $\psi_o$  and  $\psi_m$ . Most measurements in unsaturated zone hydrology lie within a humidity range of 0.06; from 0.94 (i.e.  $-8$  MPa) to 1.0 (0 MPa), which may make this method insensitive for use in wet to relatively dry soils. A second difficulty is the temperature influence on the measurements. Reece (1996) stated that field psychrometers have a measurement range between  $-0.5$  and  $-5$  MPa when used with sensitive instrumentation, and without temperature gradients, but did not give additional quantitative data. Under laboratory conditions

where temperature was controlled within  $\pm 0.001^\circ\text{C}$ , the water potential ( $\psi_o + \psi_m$ ) could be inferred with an accuracy of 0.01 MPa (Andraski and Scanlon 2002).

### 1.4.3 Indirect methods

Measurements of  $\psi_m$  between  $-0.09$  and  $-0.5$  MPa can be done by filter paper, electrical resistance (e.g. Time Domain Reflectometry), inference from soil moisture content  $\theta$  and soil moisture retention curve  $\theta(\psi_m)$ , and heat dissipation methods (e.g. Noborio et al. 1999, Andraski and Scanlon 2002, Agus and Schanz 2005). These methods are not derived from thermodynamic principles, but rely on calibrating sensor properties against known matric potentials (Campbell and Gee 1986). Difficulties arise from the non-uniqueness in the relationship between  $\psi_m$  and measured properties, as the latter also depend on other variables (Campbell 1988). Furthermore the relationship needs to be determined for each soil type, and implicitly assumes soil homogeneity.

### 1.4.4 Osmotic tensiometers

Peck and Rabbidge (1966, 1969) were the first to use a polymer solution in a tensiometer instead of water. Polymer solutions were already used to determine water stress in plants (Lawlor 1970, Tingey and Stockwell 1977, Whalley et al. 2000), but measurements were restricted to pot plant experiments. In a tensiometer, dry polymer is enclosed behind a membrane that is permeable to water, but not to polymer. Subsequently, the osmotic potential  $\pi$  (see Appendix B) of a hydrophilic polymer causes a build-up of pressure when the polymer is exposed to free water. When exposed to unsaturated soil, the pressure drop inside the instrument serves as a measure for the actual  $\psi_m$  in the soil. Peck and Rabbidge (1969) were able to measure down to  $-1.5$  MPa. Their instrument, later studied by Bocking and Fredlund (1979), suffered from gradual loss of pressure, unknown zero drift, temperature effects and slow equilibration times. Until the development of technically advanced ceramics (e.g. Biesheuvel et al. 1999), and the availability of high quality polymers and pressure transducers, progress could not be made.

## 1.5 Thesis outline

This thesis contains the development of a new polymer tensiometer (POT), and the investigation of root water uptake in dry soil as measured by these POTs. Chapters 2 to 5 will be based on papers that have been or will be published independently in international journals. Consequently, some duplication is unavoidable.

Chapters 2 and 3 will describe the development of a POT that has a potential measurement range of 0 to  $-1.6$  MPa. This measurement range is approximately 20 times more as compared to conventional tensiometers. To prevent or have an acceptable loss of pressure over time, the suitability of several polymers will be screened. To ensure long term use, any gradual pressure loss should be predictable. The osmotic pressure of polymer solutions has a relation with temperature that has been described by Flory-Huggins solution theory (see Appendix B). As temperature calibration during experiments is essential, temperature-pressure relationships were determined before and after experiments.

Chapter 3 will also deal with the use of a solid ceramic cone to enhance soil contact, and facilitate installation in soils. These POT designs will then be compared with Time Domain Reflectometry (TDR) probes for a sandy and a loamy soil in a laboratory setup. TDR is a popular method for measuring the bulk electrical permittivity of a soil as it has a close relationship with the soil moisture content. By using a soil specific calibrated permittivity-soil moisture curve, and an independently determined moisture retention curve, measurements from TDR will be converted to matric potentials.

The advantage of measuring the soil moisture content with TDR probes and matric potentials with POTs together is that the combined methods can assess soil moisture retention curves. These curves will be compared with independently determined moisture retention curves as well as with Van Genuchten (1980) fitted retention curves.

Chapter 4 will show the use of POTs for defining levels of local water stress in a lysimeter experiment. The limited applicability of soil moisture content measurements by TDR in studies concerning water stress in plants will be illuminated.



Chapters 4 and 5 will subsequently describe the response of maize plants to varying levels of water stress. In a 4 month experiment, three lysimeters were used to establish water stress in the root zone. We defined three irrigation treatments that were based on the soil water status: no stress (minimum  $\psi_m = -0.15$  MPa), intermediate stress (minimum  $\psi_m = -0.45$  MPa) and severe stress (minimum  $\psi_m = -0.80$  MPa). Minimum  $\psi_m$  represents the most negative matric potential (at any measurement location in the soil) that was allowed during the three irrigation treatments.

In Chapter 6 the conclusions that can be drawn throughout the thesis are summarized, and an outlook into future research possibilities with POTs will be given.



## Chapter 2

---

# New polymer tensiometers: Measuring matric potentials down to wilting point

---

This chapter is a modified version of: Bakker, G., M.J. van der Ploeg, G.H. de Rooij, C.W. Hoogendam, H.P.A. Gooren, C. Huiskes, L.K. Koopal, and H. Kruidhof. 2007. New polymer tensiometers: Measuring matric pressures down to the wilting point. *Vadose Zone Journal* 6: 196-202.

## 2.1 Introduction

Tensiometers are widely used for measuring soil water matric potentials ( $\psi_m$ ) in field and laboratory conditions. Its measurement principle is based on the use of a water-filled reservoir enclosed by a pressure transducer and a water-saturated ceramic tip that is in contact with the soil. Equilibrium between the liquid phase in the soil and in the tensiometer makes it possible to determine  $\psi_m$ . Direct measurement of  $\psi_m$  with conventional tensiometers is restricted to values greater than approximately  $-0.09$  MPa (Cassel and Klute 1986, Koorevaar et al. 1983, Young and Sisson 2002). Most plants can take up water down to a  $\psi_m$  of about  $-1.6$  MPa. To determine  $\psi_m$  below the tensiometer range, thermocouple psychrometers and relative humidity sensors can be used. However, thermocouple psychrometers have a slow response and are subject to significant measurement errors above  $-1.0$  MPa, while relative humidity sensors seem to be more suitable for measurements below  $-2.0$  MPa (Andraski and Scanlon 2002, Agus and Schantz 2005). Other field methods measure the volumetric moisture content ( $\theta$ ) and infer  $\psi_m$  from the soil moisture characteristic  $\theta(\psi_m)$  (Klute 1986b, Dane and Hopmans 2002).

Recognizing the desirability of direct  $\psi_m$  measurements over an extended range, Peck and Rabbidge (1966, 1969) proposed an osmotic tensiometer. Its principle is based on the osmotic potential of a highly concentrated hydrophilic polymer solution. The soluble polymer molecules are retained inside the osmotic tensiometer by a ceramic membrane that is permeable to the soil solution, but impermeable to the polymers. The osmotic potential ( $\pi$ ) of the polymer solution strongly reduces the total water potential inside the osmotic tensiometer (Hillel 1998). The reduction in the total water potential then causes a build-up of a positive pressure inside the tensiometer. Consequently the water in an osmotic tensiometer at equilibrium with a drying soil will cavitate at a much lower soil water potential than the essentially pure water in a conventional tensiometer. The positive pressure  $\pi$  inside the osmotic tensiometer can thus be related to the negative  $\psi_m$ .

Although Peck and Rabbidge (1966, 1969) were able to construct an osmotic tensiometer capable of measuring  $\psi_m$  in the range of 0 to  $-1.5$  MPa, their

instrument suffered from slow equilibration times (0.33 - 1.76 hours), temperature effects, unknown zero drift and gradual reduction in the osmotic potential inside the instrument ( $3.46 \times 10^{-4}$  to  $4.34 \times 10^{-4}$  MPa d<sup>-1</sup>). Since then progress has been limited (Peck and Rabbidge 1969, Bocking and Fredlund 1979), possibly because of technological limitations at that time (e.g. poorly defined size distributions of the polymer molecules). More recently, Biesheuvel et al. (1999, 2000) reported new osmotic tensiometer designs, which were tested in a limited set of laboratory experiments (no installation in soil material, only in a water bath).

The design of Peck and Rabbidge (1969) was used as a starting point for the development of the polymer tensiometer (POT). The term “polymer tensiometer” is used here to avoid frequent confusion with osmometers (e.g., Moses et al. 2003). Different polymers for durability and temperature behavior were used. The response time of the POT was minimized, and its operation in a soil was tested. The objective of this chapter is to present the main details of the POT design, describe operational procedures, present results of the various tests, and compare the results with previous instrument performance (Peck and Rabbidge 1969, Bocking and Fredlund 1979, Biesheuvel et al. 1999).

## 2.2 Design

The POT (Fig. 2-1) consists of a flat solid ceramic disc, a stainless steel polymer chamber cup, an aqueous polymer solution, and a pressure transducer. The porous inorganic ceramic disc was made of an  $\alpha$ -Al<sub>2</sub>O<sub>3</sub> support layer and a mesoporous  $\gamma$ -Al<sub>2</sub>O<sub>3</sub> membrane (Everett 1972, Alami-Younssi et al. 1995, De Vos and Verweij 1998). The  $\gamma$ -Al<sub>2</sub>O<sub>3</sub> membrane very efficiently prevented leakage of large polymers ( $> 20 \text{ kg mol}^{-1}$ ) from the polymer chamber (Biesheuvel et al. 1999). The ceramic was glued into the polymer chamber cup.

The pressure transducer (type PR55-20, Keller Instruments) registered a pressure relative to the atmospheric pressure. The transducer had a range of  $-0.175$  to  $2.201$  MPa, and an accuracy of  $2.38 \times 10^{-3}$  MPa. A temperature sensor (0-40 °C, accuracy 0.01 °C) measured temperatures just behind the polymer chamber. To

seal the connection between pressure transducer and the polymer chamber cup, we used a 0.2 mm synthetic ring inside the instrument.

The polymer chamber was filled with dry polymer. Upon placement in demineralized water of 20.0 °C, the ceramic saturated instantly and wetted the hydrophilic polymer, leading to a build-up of osmotic pressure and the release and dissolution of entrapped air. In principle, when the osmotic pressure of the polymer solution matched the pressure transducer range, POTs could measure down to a  $\psi_m$  of approximately  $-2.0$  MPa.

We selected polymers that were water-soluble in the temperature range relevant for plant growth. In order to minimize the effects of the salinity of the soil solution we selected polymers that had little or no charged groups in their molecules. We preferred synthetic over natural polymers to prevent bacterial breakdown. Polyethyleneglycol (PEG), Polyacrylamide (PAM), and Polyvinylpyrrolidone (PVP) were found acceptable for our applications. Table 2-1 lists selected properties of these polymers.

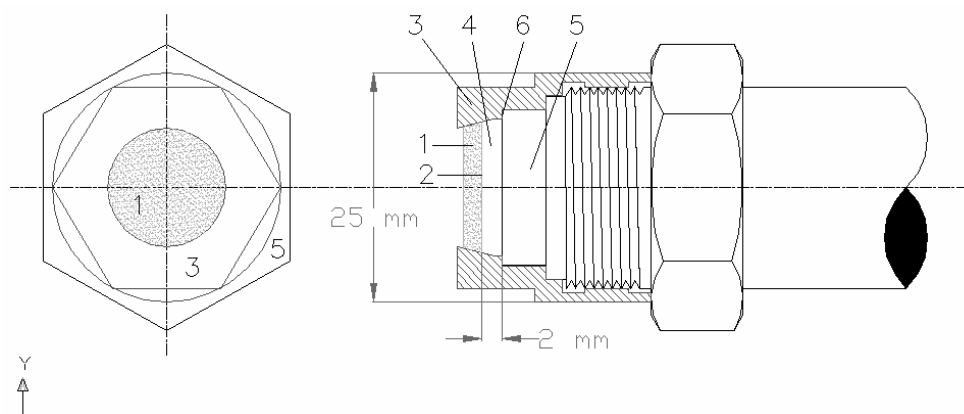


Figure 2-1. Polymer tensiometer with disc-shaped ceramic containing (1) an  $\alpha$ - $\text{Al}_2\text{O}_3$  support layer, (2) a  $\gamma$ - $\text{Al}_2\text{O}_3$  membrane, (3) a stainless steel cup, (4) a polymer chamber, (5) a pressure transducer, and (6) a synthetic ring. Different polymer chamber volumes were obtained by adjusting the length of the stainless steel cup between the two arrows.

Table 2-1. Properties of the polymers used in the polymer tensiometers

Polymer (trade name)	Polymer type	Average molar mass ( $\text{kg mol}^{-1}$ )	Percentage of anionic groups <sup>†</sup>	Phase separation when dissolved in water at <sup>‡</sup>
PAM FLUKA	Polyacrylamide (21.6% cross-linked)	500	1	$< -35\text{ }^\circ\text{C}$
PEG 4000	Polyethyleneglycol	4000	0	$< -15\text{ }^\circ\text{C}; > 95\text{ }^\circ\text{C}$
Praestol 2500	Polyacrylamide	2500	1	$< -35\text{ }^\circ\text{C}$
PVP 40000	Polyvinyl-pyrrolidone	40	0	$> 135\text{ }^\circ\text{C}$

<sup>†</sup>Davidson (1980), <sup>‡</sup>Molyneux (1983).

## 2.3 Water reservoir tests

We investigated temperature behavior, long-term stability, and rewetting behavior by filling the POTs with the polymers and placing them in a temperature-controlled water reservoir (accuracy  $\pm 0.1$  °C). Table 2-2 gives the properties of the POTs that were used. Pressures and temperatures inside each POT were recorded every 10 min. The schematic in Fig. 2-2 outlines our subsequent experiments.

Table 2-2. Overview of the polymer chamber geometry and the polymers used in six polymer tensiometers (POT).

POT	Chamber depth (cm)	Chamber volume (cm <sup>3</sup> )	Polymer	Mass of polymer (g)
1	1.0	2.1	PAM FLUKA	0.45
2	1.0	2.2	PVP40000	0.65
3	1.0	1.9	Praestol	0.66
4	0.20	0.7	Praestol	0.31
5	0.05	0.1	Praestol	0.072
6	0.05	0.1	PEG4000	0.044

The results of the water reservoir tests deal with the pressure inside the polymer chamber only, and are therefore given as positive pressure values. Figures 2-3 and 2-4 show the pressure build-up when the dry POTs were placed in water. The pressure peak probably resulted from enclosed air in the polymer chamber. The enclosed air reduced the volume of the polymer solution, thereby leading to a higher concentration. When air diffused out of the polymer chamber, the volume of the polymer solution increased, again leading to a drop in pressure. The subsequent gradual pressure decrease is possibly caused by polymer degradation, or by diffusion of some smaller-sized polymer molecules through the porous membrane (Caulfield et al. 2003).



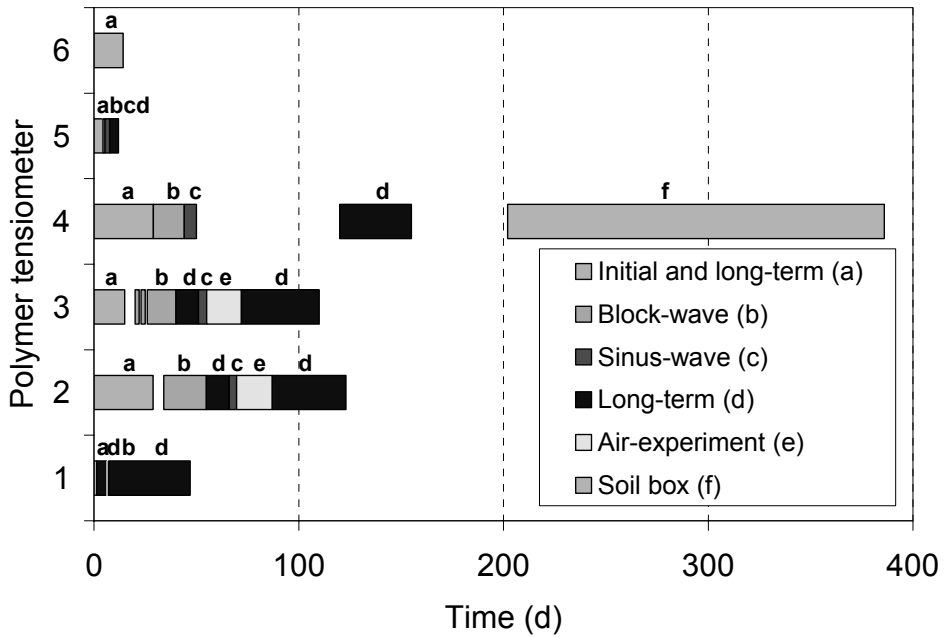


Figure 2-2. Overview of the various experiments with six polymer tensiometers (Table 2-2), involving temperature effects (2, 4), drying and rewetting (5), performance in soil material (6), and long-term stability (1, 3).

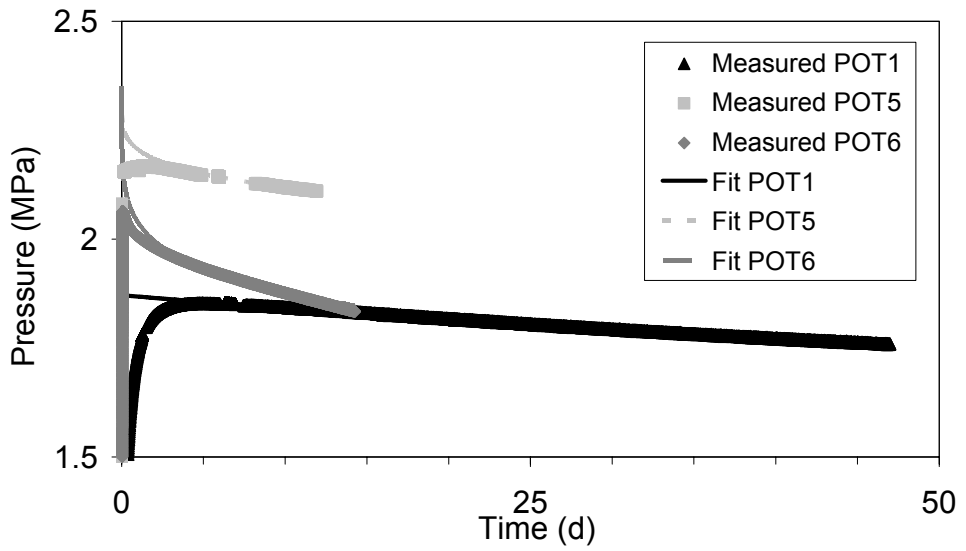


Figure 2-3. Initial pressure peaks and long-term pressure drops for polymer tensiometers (POT) 1, 5 and 6 (Table 2-2) when placed in water. Intermissions in the data are a result of other experiments carried out at that time (See Fig.2-2).

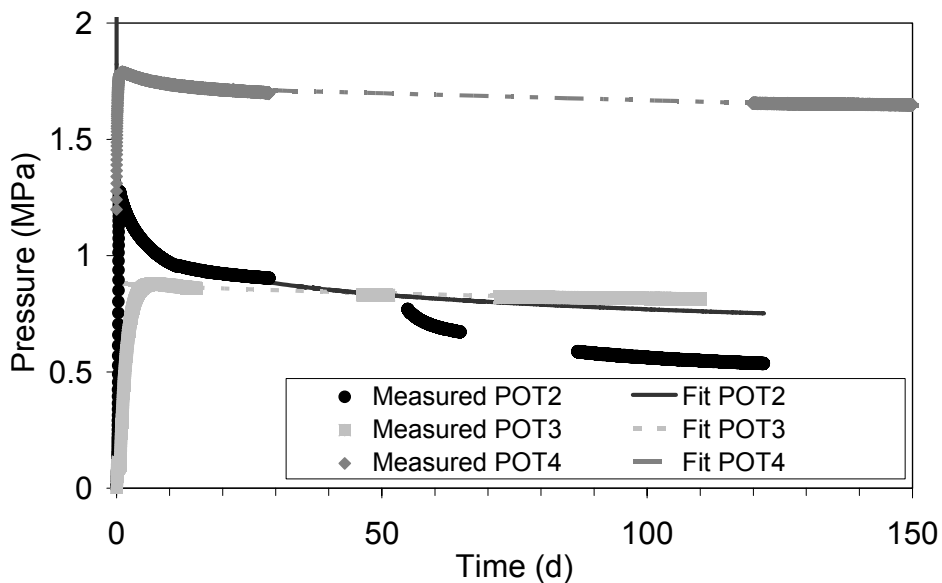


Figure 2-4. Initial pressure peaks and long-term pressure drops for polymer tensiometers (POT) 2, 3 and 4 (Table 2-2) when placed in water. Intermissions in the data are a result of other experiments carried out at that time (See Fig.2-2).

## 2.4 Block and sinusoidal temperature waves

The osmotic potential  $\pi$  of a polymer solution generally depends on temperature. A key parameter of the temperature dependency is the dimensionless Flory-Huggins interaction parameter (Flory 1941, 1942, Huggins 1942*a*, 1942*b*, Appendix B). A POT's response to temperature changes is determined by the temperature dependency of the osmotic pressure, together with various thermal expansion coefficients of POT components, and the dynamics of the temperature front traveling through the instrument. To determine the temperature coefficient we subjected the POTs to both abrupt (block-type) and sinusoidal temperature variations within the water bath (Table 2-3). The selected intervals between the imposed block-type temperature changes depended upon the POT's response time (up to a maximum of 7 days) and allowed in most cases the pressure to stabilize.

The various polymer types and concentrations of the individual POTs required different temperature ranges. The amplitude was chosen such that the maximum pressure in the polymer chamber would not exceed the range of the pressure transducer.

Table 2-3. Imposed temperature variations for the block- and sinus-wave temperature experiments using the polymer tensiometers (POT) of Table 2-2, including increments for the block-wave experiments and the periods for the sinus-wave experiments.

POT No.	Block wave			Sinus wave		
	Temperature		Increments	Temperature		Period
	Min (°C)	Max (°C)	(°C)	Min (°C)	Max (°C)	(h)
1	15.0	25.0	5.0	-	-	-
2	1.0	50.0	4.0, 5.0, 10.0	0.0	40.0	24
3	1.0	50.0	4.0, 5.0, 10.0	0.0	40.0	12
4	1.0	40.0	4.0, 5.0, 10.0	10.0	30.0	24
5	1.0	35.0	4.0, 5.0, 10.0	10.0	30.0	12
6	-	-	-	-	-	-

When the POTs were subjected to an abrupt temperature change, the pressure responded immediately and with high peaks (Fig. 2-5 shows POT3). The high peaks prolonged equilibration times during which readings were unreliable; they could also damage the pressure sensor. The temperature response times (time to reach an equilibrium pressure within 1% after a temperature step) are given in Table 2-4. The equilibrium pressure was defined as the average pressure of the last 100 observations, including the range of noise of those observations (the maximum observed noise range of all POTs was  $4.2 \times 10^{-3}$  MPa,  $5.52 \times 10^{-4}$  MPa lower than the given manufacturer's range). The POTs we tested had temperature response times (Table 2-4) that were mostly shorter than the 0.33 d reported by Bocking and Fredlund (1979).

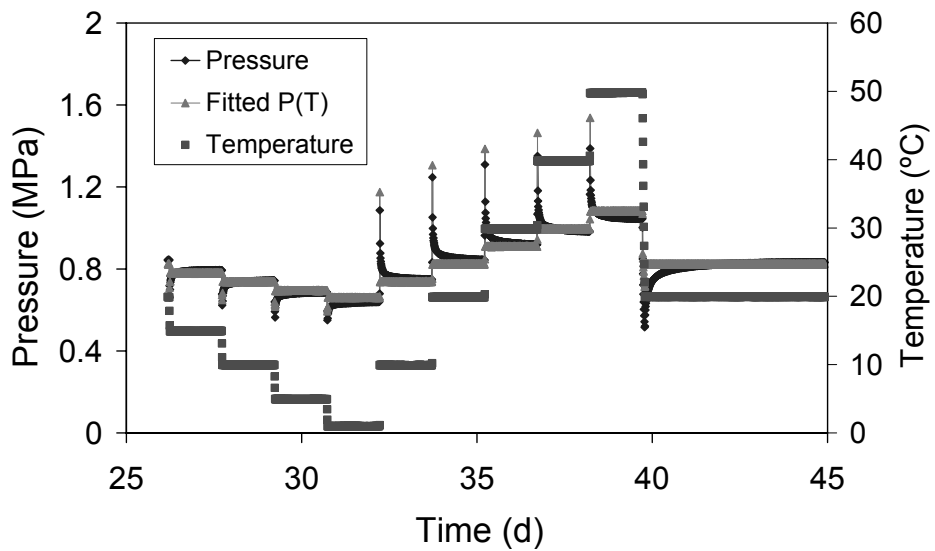


Figure 2-5. Pressure response of polymer tensiometer (POT) 3 (Table 2-2) to abrupt temperature changes using a water bath. Experiment started after an initial period (See Fig. 2-2).

Table 2-4. Averaged temperature response times of the polymer tensiometers (POT) listed in Table 2-2 to sudden temperature changes.

POT	Polymer	Chamber depth (cm)	Temperature response time (hours) averaged over the number of experiments [ <i>N</i> ] per temperature change			
			-10 °C	-5 °C	+10 °C	+5 °C
1	PAM FLUKA	1.0	-	0.816 [1]	-	0.816 [1]
2	PVP40000	1.0	-	1.22 [3]	10.7 [4]	-
3	Praestol	1.0	-	8.23 [3]	11.4 [4]	-
4	Praestol	0.20	4.18 [1]	3.74 [5]	3.26 [2]	-
5	Praestol	0.050	-	0.240 [6]	0.336 [2]	0.288 [2]

The temperature response times of the POTs were found to depend on polymer type and polymer chamber height, but again not on the magnitude of the pressure. The height of the polymer chamber affected the response time, possibly through its influence on the travel distance of water through the polymer solution or the compressibility of the polymer solution. Biesheuvel et al. (1999) tried to model the response time by assuming that it was determined entirely by the sensitivity ( $\omega$  (Pa m<sup>-3</sup>)) of the pressure transducer and the conductivity ( $K_c$  (m<sup>3</sup> s<sup>-1</sup> Pa<sup>-1</sup>)) of the ceramic. Their model hence implies that the size of the polymer chamber has no effect, which is contrary to our data. Furthermore, we calculated values of the product  $\omega K_c$  from  $\omega$  values given by the manufacturer and measured  $K_c$  values as reported by Biesheuvel et al. (1999). The  $\omega K_c$  values thus obtained differed several orders of magnitude from the  $\omega K_c$  values (s<sup>-1</sup>) fitted by Biesheuvel et al. (1999) to their experimental temperature response data. This indicates that the temperature response time of their instrument, which is quite similar to our large-chamber POTs, was much larger than what could be attributed to  $\omega$  and  $K_c$ .

The validity of Biesheuvel et al.'s (1999) assumption of an incompressible fluid can be tested if we assume that the compressibility of the polymer solution is similar to that of pure water. At 25 °C, a pressure increase of 1.0 MPa leads to a  $4.6 \times 10^{-11}$  m<sup>3</sup> volume reduction of water for a 0.10 cm<sup>3</sup> polymer chamber (the

smallest chamber in Table 2) (Lide 2005). Biesheuvel et al. (1999) reported sensitivities between  $1.0 \times 10^{-12} \text{ Pa m}^{-3}$  for traditional pressure transducers, to  $3.0 \times 10^{-17} \text{ Pa m}^{-3}$  for a newer transducer, leading to volume changes of  $1.0 \times 10^{-6} \text{ m}^3$  and  $3.3 \times 10^{-12} \text{ m}^3$ , respectively. This suggests that even for the smallest polymer chamber, the assumption of an incompressible fluid is invalid for the new pressure transducer. We thus conclude that the assumptions of insensitivity to chamber size and having an incompressible fluid in Biesheuvel et al.'s (1999) model are of limited practical use.

The equilibrium pressures of the block-wave experiments were used to determine the pressure-temperature relationships for all POTs. To more effectively compare the relationships, we scaled the pressure with  $(P_T - P_0)/P_0$  and the temperatures with  $(T - T_0)/T_0$ , where  $P_T$  (MPa) is the pressure at temperature  $T$  ( $^{\circ}\text{C}$ ), and  $P_0$  (MPa) is the reference pressure at reference temperature  $T_0$  ( $^{\circ}\text{C}$ ). Table 2-5 gives values of  $P_0$  and  $T_0$  for each POT. The various linear expansion coefficients of the materials, and the nonlinear temperature dependency of the osmotic potential of the polymer solution used in the instrument resulted in slightly curved pressure-temperature relationships as shown in Fig. 2-6.

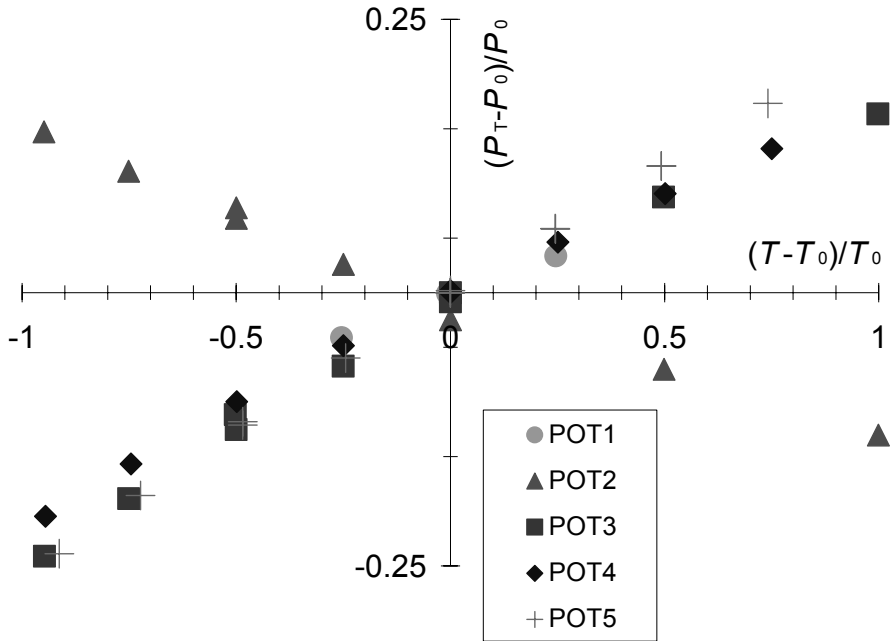


Figure 2-6. Scaled pressure ( $P$ ) – temperature ( $T$ ) relationships for the polymer tensiometers (POT) (Table 2-2) when placed in water.

The pressure-temperature relationships could be fitted well with a 2<sup>nd</sup> degree polynomial of the form

$$\frac{P_T - P_0}{P_0} = C_1 \left( \frac{T - T_0}{T_0} \right)^2 + C_2 \left( \frac{T - T_0}{T_0} \right) + C_3 \quad (2-1)$$

where  $C_1$ ,  $C_2$ , and  $C_3$  are fitting parameters. The various polymer concentrations produced different values of the fitting parameters (Table 2-5). The polymers we used all had a positive temperature-pressure dependency, except PVP 40000 which showed a decrease in pressure with increasing temperature.

The unscaled version of Eq. 2-1, which describes the static temperature behavior of a POT, was extended with a simple dynamic term to describe and predict the pressure behavior in Fig. 2-5.



$$P_T = C_1(T - T_0)^2 + C_2(T - T_0) + C_3 + A \frac{dT}{dt} \quad (2-2)$$

where  $A$  (MPa d °C<sup>-1</sup>) is a fitting parameter. A fit of Eq. (2-2) to the data (with  $A = 0.003$  MPa d °C<sup>-1</sup>) shows that the abrupt pressure peaks in Fig. 2-5 are linked to temporal changes in the temperature.

Table 2-5. Parameters of the temperature-pressure relationship (Eq. (2-1)) for polymer tensiometers (POT) 1-5 listed in Table 2-2.

POT	T <sub>0</sub> (°C)	P <sub>0</sub> (MPa)	C <sub>1</sub>	C <sub>2</sub>	C <sub>3</sub>	R <sup>2</sup>
1	20.0	1.85	-0.0528	0.1490	0.00009	1
2	19.9	1.35	0.0216	-0.1444	-0.0085	0.9954
3	19.9	0.87	-0.0351	0.2114	-0.0072	0.9988
4	19.9	1.75	-0.0231	0.1938	0.0007	0.9999
5	19.9	2.19	-0.0187	0.2438	0.0009	0.9999

A sinusoidal temperature wave is more representative of field conditions than a sudden rise or drop in temperature. Figure 2-7 shows that no anomalous peaks were observed for the imposed sinusoidal waves for POT3. Instead, the measured temperature inside the pressure sensor lagged behind the pressure response. The temperature sensor inside the POT showed a delay of 2 to 4 min compared with the observed temperature of the water reservoir (as measured with another thermometer), which did not explain the lag of approximately 80 min in Fig. 2-7. Again, this seems to be related to the temperature gradient over time; Eq. (2-2) fits well to the pressure observations (with  $A = 0.006$  MPa d °C<sup>-1</sup>). The reversal of the thermal expansion for water around 4 °C had no visible effect on the response of POT3. POT2, POT4, and POT5 showed similar results (POT1 and POT6 were not exposed to a sinusoidal temperature wave).

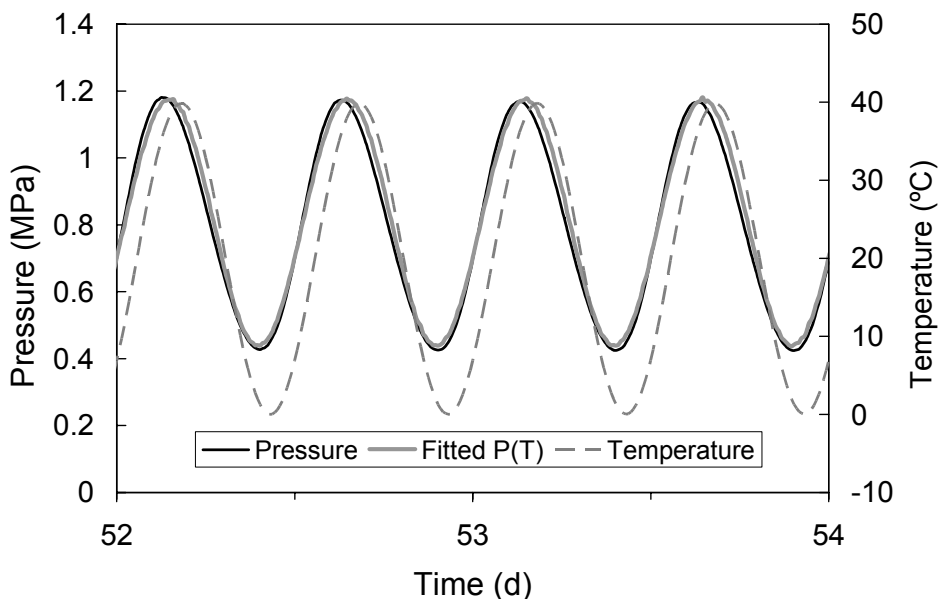


Figure 2-7. Pressure response of polymer tensiometer (POT) 3 (Table 2; placed in water) to a sinus temperature wave. Experiment started after long-term experiment (See Fig. 2-2).

## 2.5 Long-term behavior and rewetting

To establish the long-term behavior of the pressure inside the POTs and to determine the effect of the temperature experiments on long-term behavior, the temperature was fixed at 20.0 °C for extended periods of time before, between, and after applying the two types of temperature variations (Figs. 2-3 and 2-4). The observed gradually decreasing osmotic pressures were fitted with the equation:

$$\pi = b \exp - (t/\tau)^c \quad (2-3)$$

where  $b$  (MPa),  $\tau$  (d), and  $c$  (-) are adjustable parameters. Pressures before the peaks in Figs. 2-3 and 2-4 were not used for fitting. Table 2-6 shows the pressure decay, the fitted parameter values and the coefficient of determination ( $R^2$ ) for all

POTs. Large values for  $\tau$  imply a slow pressure decay. The pressure decay after 100 days for POT3 and POT4 was equal to or slightly less than those reported by Peck and Rabbidge (1969). However, the pressure decay we observed gradually became less (exponential decay), while Peck and Rabbidge (1969) observed a more linear relationship with time for the pressure decay.

The temperature response experiments that were imposed in between the long-term experiments seemed for most POTs to have no effect on the pressure decay, thus suggesting that the parameters in Eq. (2-3) are independent of temperature. The PVP 40000 inside POT2 showed a pressure collapse (Fig. 2-4) after a large pressure increase during the temperature experiments, which could not be explained by long-term pressure decay. We observed after a large pressure increase similar pressure collapses during the temperature experiments in several POTs containing PVP 40000 (data not further shown here). PVP 40000 hence seems to be a less suitable polymer for use in POTs.

The parameters of Eq. (2-1) and (2-3) for long-term operation can be determined during initial testing prior to field installation. This allows the POT field readings to be properly corrected during the entire operational period. To do so, one must first calculate the osmotic potential of the POT at the desired time for the selected (arbitrary) reference temperature from Eq. (2-3) (Table 2-6). The actual osmotic potential for the ambient temperature is then derived using the pressure-temperature relationship given by Eq. (2-1) (Table 2-5) of the sensor of interest.

Table 2-6. Parameters for the long-term pressure decay according to Eq. (2-3) for the polymer tensiometers (POT) listed in Table 2-2.

POT	Pressure decay shortly after pressure peak (day 11 to 12) (kPa d <sup>-1</sup> )	Pressure decay after 100 days (kPa d <sup>-1</sup> )	<i>b</i> (MPa)	$\tau$ (d)	<i>c</i> (-)	<i>R</i> <sup>2</sup> (-)
1	2.57	-	1.872	$9.48 \times 10^2$	0.9166	0.9991
2	8.73	0.726	6.265	$1.54 \times 10^{-4}$	0.0553	0.9906
3	1.03	0.405	0.8853	$5.62 \times 10^3$	0.6138	0.9798
4	1.89	0.337	1.796	$1.36 \times 10^5$	0.3572	0.9893
5	4.41	-	2.320	$1.26 \times 10^5$	0.2540	0.9887
6	7.41	-	2.350	$1.90 \times 10^4$	0.1978	0.9916

A key advantage of POTs over conventional tensiometers after drying out is presumably their ability to refill spontaneously with water. We therefore exposed POT2 and POT4 (Table 2-2) to air at a relative humidity of 60% (having an equivalent  $\psi_m$  of -67.66 MPa) for 72 hrs, and subsequently submerged them in water (20.0 °C).

We tested this ability by removing POT3 from the water reservoir at day 58 and immersing it again at day 61 (Fig. 2-2). Figure 2-8 shows the pressure response. The pressure responded within minutes, which is considerably faster than the response time observed by Peck and Rabbidge (1969). When placed in water, the POT rapidly rewetted and recovered within 9 d to its original osmotic pressure (corrected for the long-term trend). The overshoot observed during initial wetting (Fig. 2-3) did not occur, possibly because the polymer retained sufficient water to prevent significant air entry into the polymer chamber. Another possibility may be that the dried polymer compacted too much for air to be entrapped between polymer grains, thus allowing the air to be easily expelled during rewetting. POT2 gave similar results, which are not further shown here.

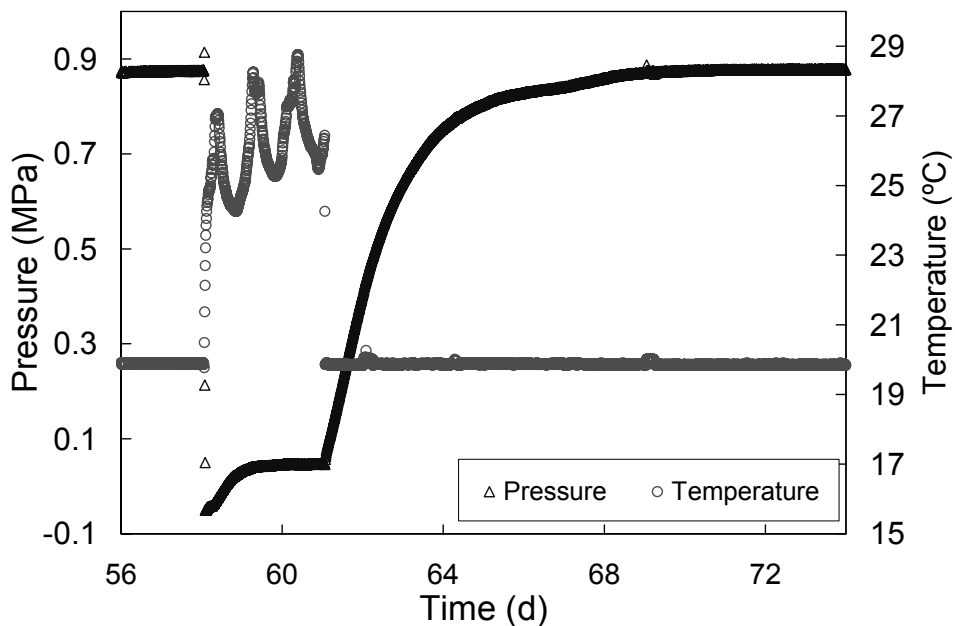


Figure 2-8. Self-restoring capacity of POT3 (Table 2). The tensiometer was temporarily removed from the water reservoir between days 58 and 61 (See Fig. 2-2 for overview experiments).

## 2.6 Repacked Soil Experiment

To test the POTs in a drying soil, we constructed an evaporation container (length 40 cm, width 30 cm, height 40 cm) with a perforated bottom, and with vapor outlet ports that connected to wall-to-wall perforated PVC tubes (outer diameters of 20 mm). The ports considerably shortened the pathways of water vapor to the atmosphere, thus allowing soil to dry out rapidly, even at larger depths. We packed Wichmond sandy loam (14% clay, 31% silt, 55% sand) uniformly in the container, and then installed various sensors (POT4, a Time Domain Reflectometry Probe (TDR), and a Conventional Tensiometer (CT)).

At the start of the experiments, the soil was saturated with non-chlorinated tap water, and then allowed to drain and evaporate. Tests indicated that the low salinity of the soil solution did not significantly affect the readings of POT4. During the

drying phase, gravimetric moisture contents ( $\theta_{\text{grav}}$ ) were determined of 20 cm<sup>3</sup> cylindrical soil samples for the purpose of calibrating the TDR sensor and determining the soil moisture retention curve ( $\theta(\psi_m)$ ).

During the evaporation experiment with repacked soil, the atmospheric demand for the first 140 to 150 d remained fairly low, resulting in slow drying. The humidity then decreased, leading to a higher evaporation rate and hence increased soil drying. All sensors in the soil container responded consistently (Fig. 2-9). Data from POT4 were corrected for the ambient temperature variations and the long-term pressure decay, and converted to  $\psi_m$ . The TDR data were converted to  $\psi_m$  using a soil-specific calibration curve and the measured  $\theta_{\text{grav}}(\psi_m)$ . Data from the 2 CTs were averaged.

The measurement range of the POT was clearly much larger than that of the CT, and exceeded the wilting point. At the conclusion of the experiments (183 d, 385 d since the initial start), POT4 reached its limit and dried out. Together with its ability to rewet spontaneously, this experiment demonstrates that a POT is able to function in a soil environment during an entire growing season. Relatively small deviations between POT4 and the CT and TDR results in the wet range between 50 and 150 days were probably caused by limited contact between the POT's flat ceramic and the soil. In the dry range, the TDR-derived  $\psi_m$  deviated from the POT observations. The TDR benchmark in this range was likely less reliable since TDR readings at  $\theta$  below about 0.10 are less accurate than those of a wetter soil.

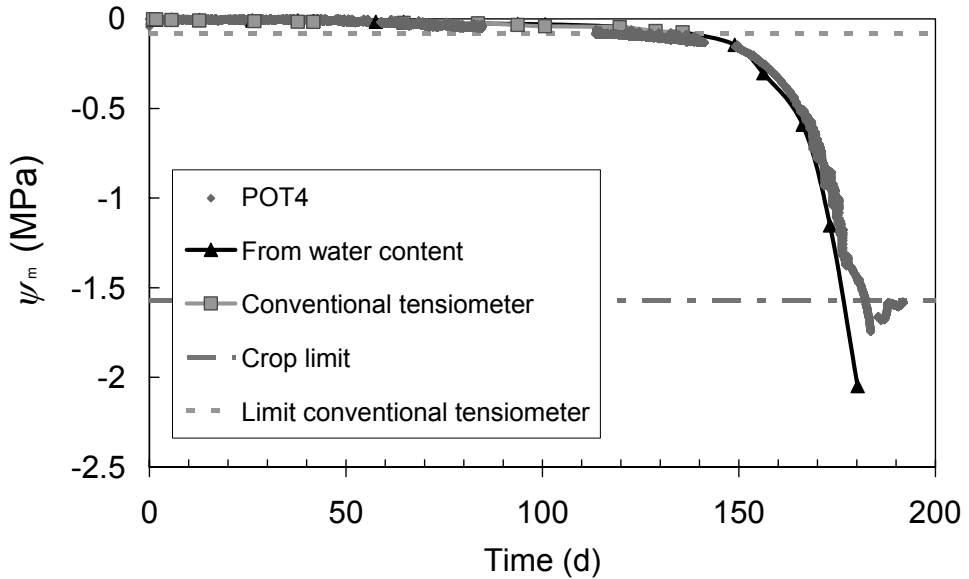


Figure 2-9. The matric potential  $\psi_m$  recorded by different instruments placed in soil, including a polymer tensiometer (POT). Day 0 in the figure corresponds with day 202 in Fig. 2-2. Table 2-2 lists key features of POT4.

## 2.7 Conclusions

In summary, we demonstrated the ability of a recently designed polymer tensiometer to measure matric potentials beyond wilting point and to function properly for time periods comparable to a growing season. Temperature effects and long-term pressure decay can be adequately quantified and corrected. Temperature response times were affected by polymer chamber height. Polymer tensiometers with small polymer chambers were found to perform best.

The polymer tensiometer appears very attractive for field applications because of their much wider measurement range and fast pressure response. While less of a problem for field applications, in the design of laboratory experiments the pressure response to abrupt temperature changes needs consideration. Future research should address the response of the POT-signal to temperature and temperature

gradients, the shape of the ceramic tip to ensure better contact with the soil, and the long-term sustainability of polymers in POTs installed in soils.



# Polymer tensiometers with ceramic cones: performance in drying soils

---

This chapter is a modified version of the manuscript: Van der Ploeg, M.J., H.P.A. Gooren, G. Bakker, C.W. Hoogendam, C. Huiskes, L.K. Koopal, H. Kruidhof and G.H. de Rooij, Polymer tensiometers with ceramic cones: performance in drying soils and comparison with water-filled tensiometers and time domain reflectometry.

### 3.1 Introduction

Measurement of the soil water matric potential ( $\psi_m$ ) is important to characterize and monitor processes in vadose zone hydrology, such as plant growth, crop production, aquifer recharge, and leaching below buried waste disposal sites (Young and Sisson 2002). Tensiometers are widely used instruments to monitor  $\psi_m$ , and have been used for almost 100 years (Or 2001, Young and Sisson 2002). All tensiometers consist of three elements: a ceramic that is in contact with the soil, a water reservoir in equilibrium with the soil water, and a pressure measurement device. Unfortunately, water-filled tensiometers are only able to measure  $\psi_m$  above approximately  $-0.09$  MPa. Soil physical experimental research is hampered by this very limited measurement range.

Reece (1996) stated that field psychrometers have a measurement range between  $-0.5$  and  $-5$  MPa when used with sensitive instrumentation, and without temperature gradients, but did not give additional quantitative data. Agus and Schanz (2005) on the other hand, note that thermocouple psychrometers have a slow response and are subject to significant measurement errors above  $-1.0$  MPa. Measurements of  $\psi_m$  between  $-0.09$  and  $-0.5$  MPa can be done by filter paper, electrical resistance, inference from soil moisture content ( $\theta$ ) and soil moisture retention curve  $\alpha(\psi_m)$ , and heat dissipation methods (e.g. Noborio et al. 1999, Andraski and Scanlon 2002, Agus and Schanz 2005). These methods are not derived from thermodynamic principles, but rely on calibrating sensor properties against known  $\psi_m$  (Campbell and Gee 1986). Difficulties arise from the non-uniqueness in the relationship between  $\psi_m$  and measured properties, as the measured properties also depend on other variables (for example temperature) (Campbell 1988).

Attempts have been made to circumvent cavitation of tensiometers and to extend their measurement range. Tamari et al. (1993) used microtensiometers that were able to measure until approximately  $-0.14$  MPa for short time periods only. Nucleation particles were removed by purging the tensiometers extensively with demineralized water, which created the possibility of having the liquid in a metastable state. To remove dissolved air from the tensiometer's water reservoir Miller and Salehzadeh (1993) used a stripper, and were thus able to reach  $-0.18$

MPa. For geotechnical applications Ridley and Burland (1993) constructed a tensiometer that measured  $\psi_m$  down to  $-1.5$  MPa, but the instrument only worked for a few hours or less. This tensiometer, which was also studied by Tarantino and Mongiovì (2001) required a 24 hour pre-hydration phase in a high pressure chamber at 4.0 MPa, to dissolve air bubbles, and stopped working as soon as cavitation occurred. The tensiometer can only be used in the laboratory due to the elaborate preparation prior to use.

Peck and Rabbidge (1966, 1969) were the first to use a polymer solution instead of water. The osmotic potential of a hydrophilic polymer causes a build-up of pressure when the polymer is exposed to free water through a membrane permeable to water but not to the polymer. Using the subsequent drop in pressure as a measure for the actual  $\psi_m$  in the soil, Peck and Rabbidge (1969) were able to measure down to  $-1.5$  MPa. Their instrument, later studied by Bocking and Fredlund (1979), suffered from gradual loss of pressure, unknown zero drift, temperature effects and slow equilibration times.

Progress on polymer filled tensiometers was not made until a ceramic was used that greatly reduced polymer leakage (Biesheuvel et al. 1999). In Chapter 2 a polymer filled tensiometer that worked properly beyond wilting point was presented, and an empirical relation was developed to predict the remaining loss in pressure caused by diffusion of some smaller-sized polymers through the membrane (Caulfield et al. 2003). It was shown as well that by reducing the volume of the polymer solution, the polymer tensiometer's (POT) response time decreased. In Chapter 2 flat ceramics were used, which provided a challenge to ensure good contact between the soil and a POT.

We developed POTs that included ceramic cones instead of flat ceramics. The cones have an air entry value below  $-1.75$  MPa, and remain equally conductive until the theoretical wilting point of  $-1.6$  MPa. The function of the cones is to transfer the  $\psi_m$  from the soil water to the polymer solution with minimum water displacement. We evaluated their performance in soil by comparing the recorded  $\psi_m$  with those derived from time domain reflectometry (TDR) readings of soil moisture content ( $\theta_{\text{TDR}}$ ) that were converted to  $\psi_m$  using the soil moisture retention curve ( $\theta_{\text{grav}}(\psi_m)$ ). TDR has gained widespread acceptance as a standard method to

measure  $\theta_{\text{TDR}}$  (e.g. Ferré and Topp 2002), and has served as a method to develop sensors that infer  $\psi_m$  instantly (e.g. Or and Wraith 1999).

The objective of this chapter is to present POT designs that minimize the volume of the polymer solution while maximizing the ceramic area in contact with the polymer solution, and that solve contact problems between the ceramic and the soil. We thoroughly tested the designs in two soil types, and compared the observations with TDR and water-filled tensiometer measurements. Furthermore, the possibility of combining POT and TDR data to derive *in situ* moisture retention curves ( $\theta_{\text{TDR}}(\psi_m)$ ) was investigated.

### 3.2 Design and operational procedures

We used a design (Table 3-1) that incorporated a solid cylindrical ceramic instead of a flat ceramic (Fig. 3-1, and Fig. 3-2) (Peck and Rabbidge 1966, 1969, Biesheuvel et al. 1999, Bakker et al. 2007), to ensure good contact with the soil. The  $2\ \mu\text{m}$   $\gamma\text{-Al}_2\text{O}_3$  membrane that prevents large polymer leakage (Alami-Younssi et al. 1995, Bakker et al. 2007, De Vos and Verweij 1998) was applied to the base of the ceramic cones. The construction details were described in Chapter 2, with the exception that their 0.2 mm synthetic ring was replaced by a rubber O-ring at the side of the pressure transducer. This modification eliminated undesired forces to the top of the transducer, which may lead to deformation and malfunctioning of the transducer. We used four designs, in which the surface area of the ceramic in contact with the soil and the surface area in contact with the polymer chamber were varied, i.e. by adjusting the length and diameter of the ceramic. This resulted in different polymer chamber heights (Table 3-1). The various POT designs (identified by a number in the first column of Table 3-1) had repercussions for the level of skill required to manufacture the POT, and also affected its behavior. The polymer chamber height (Table 3-1) ranged from 2.5 to 1.1 mm (2 to 4 times smaller than described by Bakker et al. (2007)). We used seven POTs filled with Praestol 2500 and one with Dextran 500 (see Table 3-2 for specific properties).

To allow the polymer to saturate, the POTs were placed in a temperature controlled water bath filled with demineralized water for at least 28 days at  $25\ \text{°C} \pm 0.01\ \text{°C}$ . Long-term behavior and pressure-temperature relationships were determined before using the POTs in soil. From the measurements to determine the

pressure-temperature relationships we could also determine temperature response times of the various POT designs (Bakker et al. 2007, Chapter 2). Pressure change caused by external pressure variations were instantaneous regardless of POT design, and are therefore not further discussed.

Table 3-1. Properties of polymer tensiometers (POTs) used in the evaporation boxes (EB).

POT design	EB	Placement in EB <sup>†</sup>	Polymer type	Chamber depth (10 <sup>-3</sup> m)	Polymer amount (g)	Ceramic area in contact with polymer solution (10 <sup>-3</sup> m <sup>2</sup> )	Ceramic surface in contact with soil (10 <sup>-3</sup> m <sup>2</sup> )
1A	1	BR	Praestol 2500	2.5	0.275	0.167	1.45
1B	2	BL	Dextran 500	2.5	0.229	0.167	1.45
2	1	BL	Praestol 2500	1.2	0.087	0.224	1.76
3A	1	TR	Praestol 2500	1.1	0.124	0.224	1.76
3B	1,2	TL	Praestol 2500	1.1	0.100	0.224	1.76
4A	2	TR	Praestol 2500	1.1	0.067	0.260	1.74
4B	2	BR	Praestol 2500	1.1	0.090	0.260	1.74

<sup>†</sup> Top left (TL), Top right (TR), Bottom left (BL), Bottom right (BR).

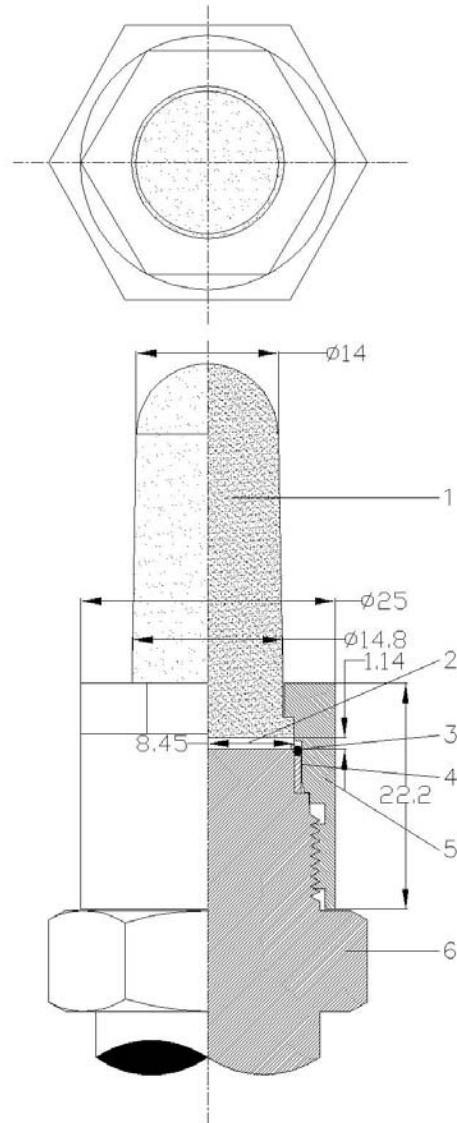


Figure 3-1. Polymer tensiometer (POT) design with cone-shaped ceramic containing (1) an  $\alpha\text{-Al}_2\text{O}_3$  support layer with a  $\gamma\text{-Al}_2\text{O}_3$  membrane at the base of the cone, (2) polymer chamber, (3) rubber O-ring, (4) stainless steel ring, (5) stainless steel mounting ring, and (6) a pressure transducer. Various arrows indicate lengths in mm of components of the POT ( $\varnothing$  is diameter).



Figure 3-2. Polymer tensiometer with cone-shaped ceramic.

Table 3-2. Properties of the polymers used in the polymer tensiometers.

Polymer (Trade name)	Polymer type	Average molar mass ( $\text{kg mol}^{-1}$ )	Percentage of anionic groups	Phase separation when dissolved in water at
Praestol 2500	Polyacrylamide	2500	1 <sup>†</sup>	< -35 °C <sup>‡</sup>
Dextran 500	Polysaccharide	500	0	< 0 °C, > 50 °C

<sup>†</sup>Davidson (1980), <sup>‡</sup>Molyneux (1983).

### 3.3 Temperature response times

Temperature response times for the various POT designs are given in Table 3-3. The temperature response times include the time it took the water bath to warm in case of a temperature rise, and to cool in case of a temperature drop. For 5 °C increments, and depending on the temperature in the laboratory, a temperature drop could take up to 0.408 hours and a temperature rise up to 0.166 hours. For 2.5 °C increments we could decrease cooling time to 0.166 hours, and heating time to 0.084 hours.

Table 3-3. Temperature response times for the various POT designs.

POT design	Temperature response time in hours averaged across the number of experiments [ <i>N</i> ] per temperature change <sup>†</sup>			
	5 °C drop	2.5 °C drop	5 °C rise	2.5 °C rise
1A	2.76 [6]	-	2.54 [6]	-
1B	-	0.576 [2]	-	1.13 [2]
2	0.576 [6]	-	0.336 [6]	-
3A	0.816 [6]	-	0.672 [6]	-
3B	0.816 [6]	0.792 [2]	0.480 [6]	0.480 [2]
4A	-	0.240 [2]	-	0.168 [2]
4B	-	0.336 [2]	-	0.288 [2]

<sup>†</sup>See Chapter 2 for details.

Smaller polymer chamber heights resulted in shorter response times. An exception is POT1B that had a comparable response time with POT3B at a temperature drop of 2.5 °C, despite its larger polymer chamber height. In POT1B the response time for the 2.5 °C drop was shorter than for the 2.5 °C rise, whereas all other POTs showed the opposite. This deviating behavior can probably be attributed to the Dextran used in this POT.

POT design 3 and 4 (Table 3-1) show that a larger ceramic area in contact with the polymer solution shortened the temperature response time. Finally, the amount of polymer inside the polymer chamber had an effect on the temperature response times. This effect could be observed in POT2, which has a larger polymer



chamber height than POT3A and POT3B, but contained less amount of polymer, and subsequently showed shorter response times. Similarly POT 4A had shorter response times than POT4B, even though the chamber depth and the ceramic area in contact with the polymer solution were equal.

### 3.4 Evaporation experiments

To determine  $\psi_m$  with POTs, the starting pressure in water of each individual POT is required as a reference. For the evaporation experiment this reference pressure was determined by averaging pressure measurements over 24 h before the instruments were taken out of the water bath, and installed in soil. We ignored the hydrostatic pressure component, since the immersion depth ( $< 0.2$  m) produced a pressure three orders of magnitude smaller than the osmotic pressure.

We filled two evaporation boxes (EB) of 400 by 300 mm and 400 mm height (Fig. 3-3), one with sand (97.6% sand, 1.6% silt, 0.8% clay; EB1), and the other with loam (42.8% sand, 38.8% silt, 18.4% clay; EB2). Both materials were sieved at 2 mm, and uniformly pre-wetted. We added soil in 5 cm layers, tamped them, and raked the upper 2 cm before adding a new layer. The containers were equipped with a perforated bottom that was covered by a steel grid and a cloth, and with wall-to-wall perforated PVC tubes (outer diameter of 20 mm), also covered with cloth. The perforations facilitated fast and uniform drying of the soil. Air humidity in the laboratory was kept low by using an air dryer.

Each EB was equipped with 4 POTs (See Table 3-1 for specifics), 4 TDR-probes (Minitrase, Soilmoisture Equipment) and 4 conventional, water-filled tensiometers (CTs) that were installed while filling the boxes (Fig. 3-3). We used 3-rod TDRs with 8 cm long, 0.32 cm diameter rods spaced at 1.4 cm, which yields an approximate measurement volume of  $250 \text{ cm}^3$  (Ferré et al. 1998, Huisman et al. 2001). The POTs and TDRs were placed opposite to each other; the CTs were placed in between. The CTs contained a gas stripper that was connected to a vacuum pump to prevent formation of air bubbles inside the instrument (Miller and Salehzadeh 1993). EB1 (sand) was gradually saturated from the bottom by placing the box in a larger, water tight encasing, and adding non-chlorinated tap water at  $1 \text{ cm h}^{-1}$  (with a maximum of  $8 \text{ cm d}^{-1}$ ) for seven days, then leaving the set-up water-logged for two days before opening an outlet in the outer casing to drain the sand.

EB2 (loam) was similarly saturated at a rate of  $2 \text{ cm h}^{-1}$  (with a maximum of  $12 \text{ cm d}^{-1}$ ) for four days, and drained six days later. The influence of salts of the tap water and in the original soil solution on the osmotic potential inside the POTs was assumed to be negligible. Soil samples were taken during the experiment to verify the relation between the bulk electrical conductivity and the soil moisture content ( $\theta$ ) (see Fig. 3-3) for locations. A soil sample was obtained by inserting a syringe open at both sides, and collecting the soil inside the syringe. The syringe was then closed by rubber corks at each side of the syringe.

After some time the drying process slowed down in EB1. We therefore placed a small ventilator in front of the box facing the outlets of the PVC tubes 42 days after drying commenced. A similar ventilator was used for EB2 during the entire experiment. To establish a soil specific relation between  $\theta$  and measured dielectric permittivity of the TDRs, soil samples of  $20 \text{ cm}^3$  were taken during the experiment. To verify rewetting of the POTs at the end of the experiment, EB1 was moistened from below again for 7 days, and then gradually saturated in 3 days. EB2 was not rewetted to prevent density changes due to soil swelling. Instead, POTs were taken out of the soil, and placed back into the temperature controlled water bath. POT responses were recorded before, during and after the transfer from the soil to the water bath. After the evaporation experiments, pressure-temperature relations were again determined for all POTs, to check for changes in the chemical properties of the polymer solutions.

We obtained  $100 \text{ cm}^3$  soil cores ( $N=27$ ) from both boxes to determine  $\theta_{\text{grav}}(\psi_{\text{m}})$ -curve and the bulk density. For  $\psi_{\text{m}}$  between  $-2 \times 10^{-4}$  and  $-1 \times 10^{-2}$  MPa, we placed the soil cores in a hanging water column set-up (Romano et al. 2002), and related  $\theta$  to  $\psi_{\text{m}}$  in the center of the sample (sample height 5 cm). For  $\psi_{\text{m}}$  below  $-1 \times 10^{-2}$  MPa we used the pressure plate method with 0.5 cm high samples (Campbell 1988, Dane and Hopmans 2002).

To determine *in situ* retention curves, each POT was paired with an opposite TDR (see Fig. 3-3). Data were paired according to measurement time. Differences between the internal clocks of the POTs and TDRs were negligible. We assumed that instrument location in the tank and the different measurement volumes of both instruments did not affect the shape of the retention curve. To fit the gravimetric measurements from soil cores, and the *in situ* measured retention data we used the frequently used equation of Van Genuchten (1980):

$$\Theta = \frac{\theta - \theta_r}{\theta_s - \theta_r} = [1 + (-\alpha h_m)^n]^{-m} \quad (3-1)$$

Where  $\Theta$  is the normalized volumetric moisture content,  $\theta$  is the volumetric moisture content,  $\theta_r$  is the residual moisture content,  $\theta_s$  is the saturated moisture content,  $\alpha$  ( $L^{-1}$ ) is a parameter to scale the matric head  $h_m$  (L), and both  $n$  and  $m$  are independent, dimensionless parameters.

Because we initially saturated the soil, the resulting moisture retention curve is the main drainage curve (Dane and Hopmans 2002). We fitted a retention curve to the soil core data. This retention curve was subsequently used to convert  $\theta_{TDR}$ -observations into  $\psi_m$  to have as a comparison to POT readings.

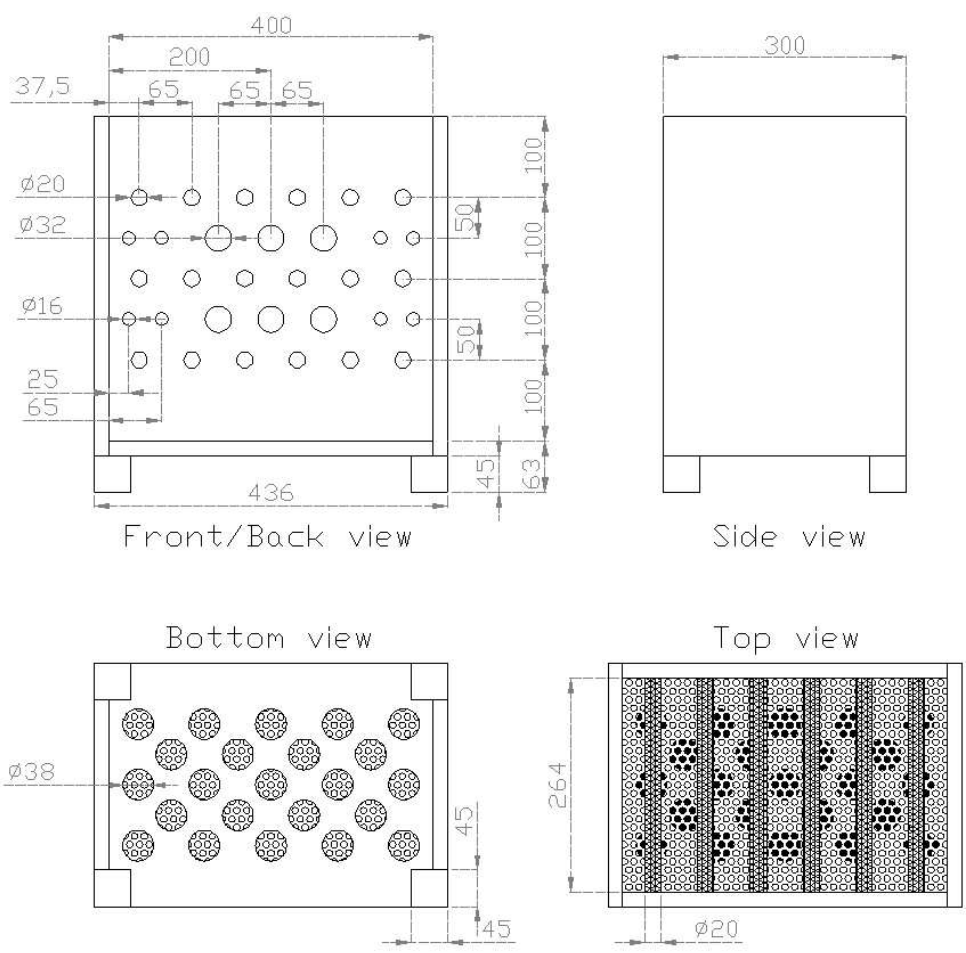


Figure 3-3. Design of the box used for the evaporation experiment. Ports of 20 mm diameter held wall to wall perforated tubes that were covered with cloth. Polymer tensiometers (POTs) were placed through the 32 mm front ports, top-left, top-right, bottom left, bottom right. Time domain reflectometry wave guides (TDR probes) were placed at back ports of 32 mm, one opposite of each POT. Conventional tensiometers (CTs) were placed at the front and back top middle and bottom middle 32 mm ports. Ports of 16 mm facilitated soil sampling to verify the bulk electrical conductivity-volumetric soil moisture relationship during the experiment. All measures are in mm.

### 3.4.1 Soil drying process

The initial  $\theta_{\text{TDR}}$  in EB2 (loam) was higher compared to EB1 (sand), which is probably an effect of soil repacking (dry bulk density of EB1  $1504 \text{ kg m}^{-3}$  ( $N=16$ ); of EB2  $1366 \text{ kg m}^{-3}$  ( $N=18$ )). Average reduction in  $\theta_{\text{TDR}}$  per day was 0.0067 for EB1 and 0.012 for EB2; the latter was probably higher due to the use of the ventilator throughout the experiment. Average soil temperatures were also slightly higher in EB2 ( $25.9 \text{ }^\circ\text{C}$ ) than in EB1 ( $24.7 \text{ }^\circ\text{C}$ ). Figure 3-4 shows the development of  $\psi_m$  and  $\theta_{\text{TDR}}$  in time of EB1 and EB2.

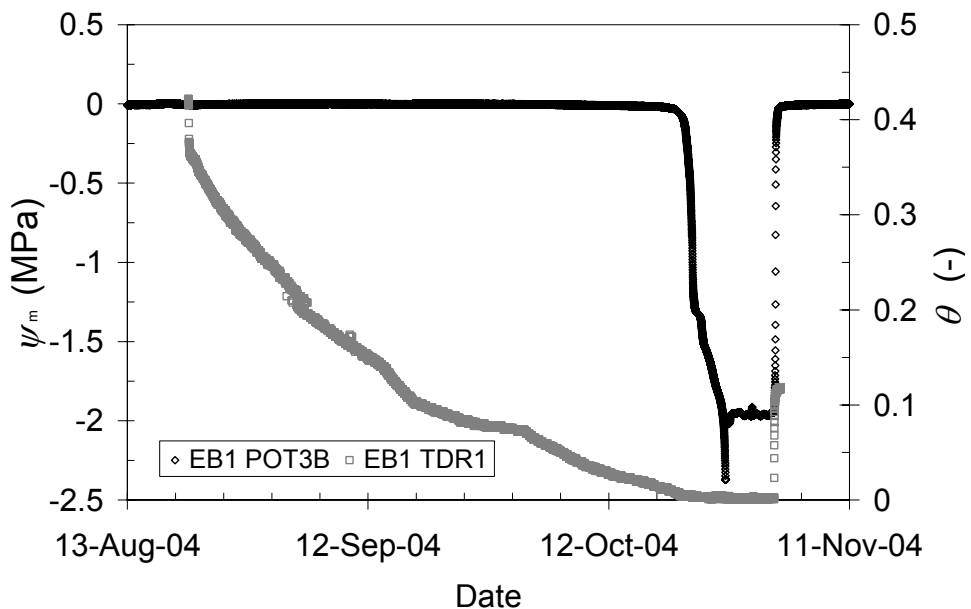


Figure 3-4. Development of the matric potential  $\psi_m$  of polymer tensiometer 3B (POT3B) and volumetric moisture content  $\theta$  (TDR1) in time for evaporation box EB1 (continued on next page).

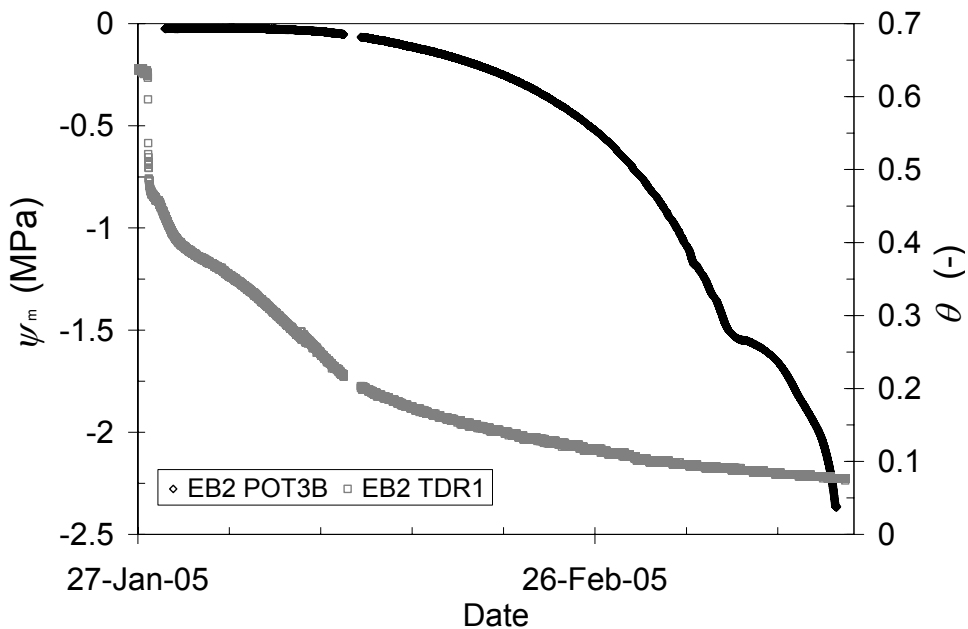


Figure 3.4 (continued from previous page) for EB2.

POT3B in EB1 showed a sudden drop in pressure after 21 October 2004, where the same POT3B showed a much more gradual drop in EB2. These pressure responses are consistent with the typical retention curves of sand (EB1) and loam (EB2). The TDR measurements showed a fast  $\theta_{TDR}$  decrease by drainage of the saturated soil, and a gradual decrease of  $\theta_{TDR}$  as a result of evaporation. In EB1 the placement of the small ventilator at October 1, 2004 can be seen in the slope of  $\theta_{TDR}$  around that date. We do not know the reason of the slightly erratic behavior around September 8, 2004.

### 3.4.2 Comparison of polymer tensiometers, time domain reflectometry probes and conventional tensiometers

Moisture content measurements ( $\theta_{TDR}$ ) were converted to  $\psi_m$  by means of the independently determined moisture retention curve  $\theta_{grav}(\psi_m)$  (gravimetric measurements on soil cores). Figure 3-5 shows the comparison for EB1 of POT

measured potentials with converted  $\theta_{\text{TDR}}$  measurements from the TDR opposite of each POT, and with potential measurements from the CTs in close vicinity of the POTs (See Fig. 3-3). Differences between sensors were small until October 7, 2004. Then, the converted potentials from TDR 1 and 2 started to deviate from the POT and CT measured potentials, while TDR 3 and 4 still followed the trend of the other instruments. CT1 cavitated on October 19, 2004 at  $-0.025$  MPa and CT3 on October 21, 2004 at  $-0.082$  MPa. All POTs continued to function beyond the theoretical wilting point of  $-1.6$  MPa. The horizontal stretch immediately after cavitation represents atmospheric pressure within the polymer chamber (zero relative pressure). The negative  $\psi_m$  recorded just before cavitation reflect subatmospheric pressures. The  $\gamma\text{-Al}_2\text{O}_3$  membrane will remain saturated until 112 MPa, thus blocking air from entering the polymer chamber. Water can still leave the polymer chamber though, and as a result the volume of the polymer solution can become less than the chamber volume, producing negative pressure readings.

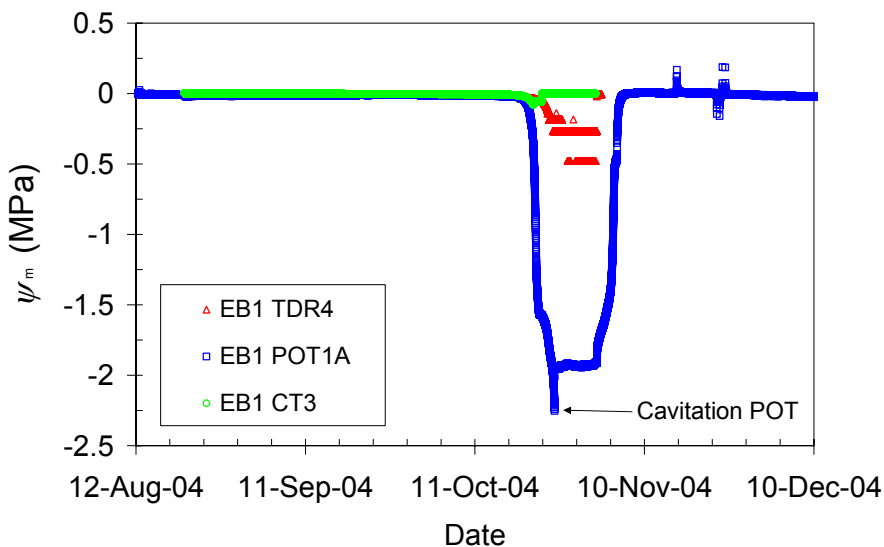


Figure 3-5A. Development of the matric potential  $\psi_m$  in time measured by polymer tensiometers (POT), time domain reflectometry probes (TDR) and water-filled tensiometers (CT) in evaporation container 1 (EB1) that was filled with sand. Each sub-figure shows a POT-TDR pair installed opposite to one another, and the nearest CT. (continued on next page)

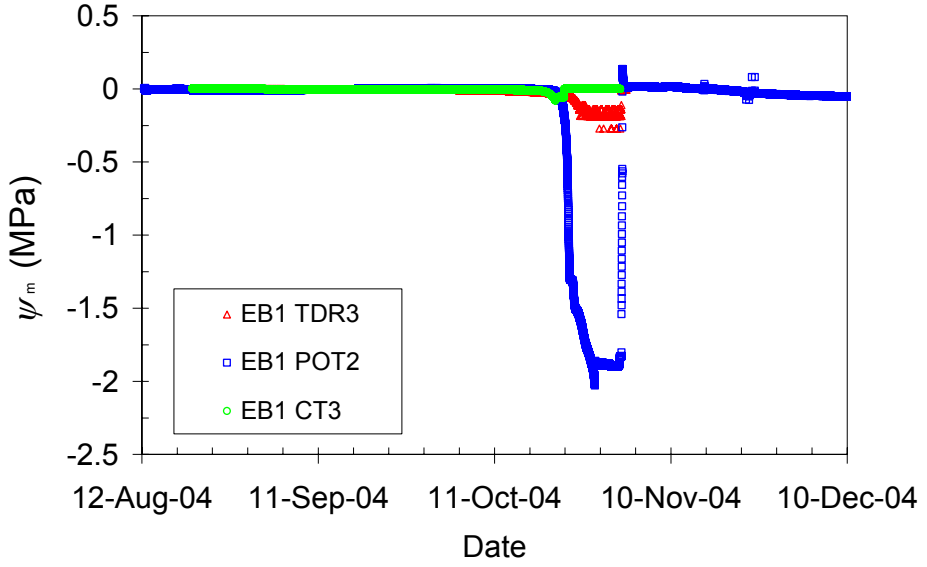


Figure 3-5B. (continued from previous page)

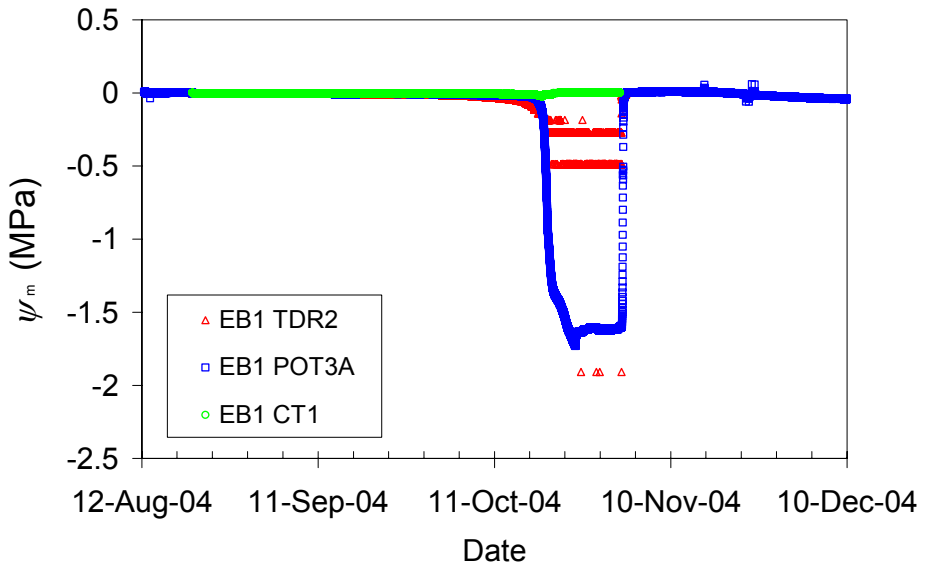


Figure 3-5C. (continued on next page)



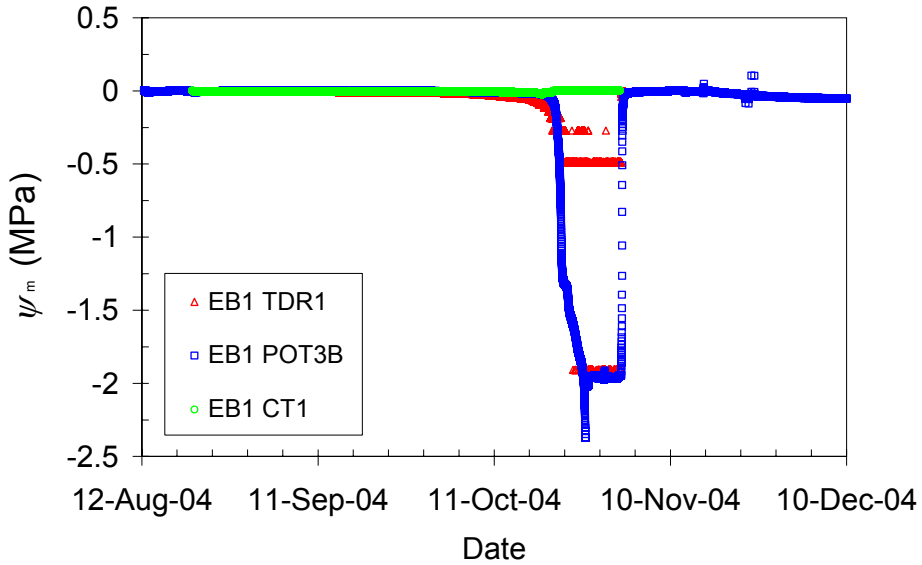


Figure 3.5D. (continued from previous page)

Table 3-4. Rewetting response times for the various POT designs.

POT design	Rewetting response times in days <sup>†</sup>	
	In evaporation box 1	In a water bath
1A	3.98	-
1B	-	0.668
2	0.503	-
3A	0.615	-
3B	0.600	0.140
4A	-	0.203
4B	-	0.564

<sup>†</sup>Response time defined as the period between the onset of rewetting and the time at which the observed pressure change equaled the measurement noise.

At November 1, 2004 when the evaporation container was moistened from below, all POTs regained their original pressure within 0.7 days, except POT4B that needed almost 4 days (Table 3-4). At November 15, 2004, small peaks in the measurements reflect replacement of the POTs of EB1 in a water bath with demineralized water. From November 22-24, 2004 we determined the temperature response of the POTs to compare to the temperature response before the evaporation experiment. No significant changes were found.

In EB1, the TDRs all started to show very noisy converted  $\psi_m$  after October 20, 2004, when the soil had dried considerably. This was due to the very low  $\theta_{TDR}$  (Fig. 3-6). Even limited noise in  $\theta_{TDR}$ -values is magnified in the derived  $\psi_m$ -values in the steep dry end of the moisture retention relationship.

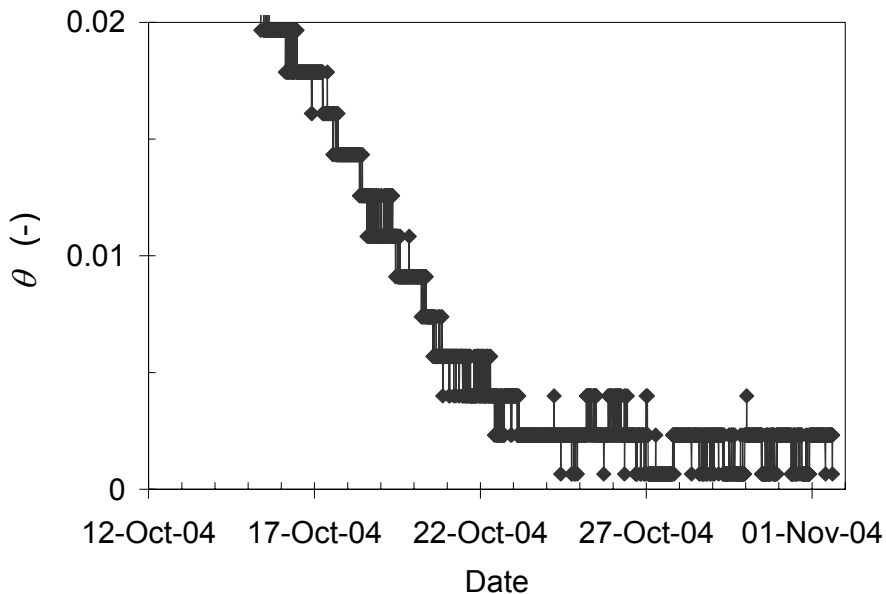


Figure 3-6. Volumetric moisture content ( $\theta$ ) measurements in dry soil by one of the time domain reflectometers (TDR1) installed in evaporation container 1 (EB1).

For EB2, the comparison between POT, TDR and CT (Fig. 3-7) shows the same trends as in EB1; in the beginning all measurements were close, converted potentials of the TDRs started to deviate around February 7, 2004, and CT and

POT data were in good agreement until the CTs cavitated; CT1 on February 13, 2005 at  $-0.083$  MPa, and CT4 on February 15, 2005 at  $-0.050$  MPa. All POTs functioned beyond wilting point. After the experiment, when we placed the POTs in the temperature controlled water bath, all POTs regained pressure within 0.7 days (Table 3-4). Comparison of the rewetting times of POT3B in the soil and the water bath indicated a faster pressure recovery in the water bath. The slower recovery in the soil probably stems from the wetting front that traveled upwards through the soil, and the available water flux at the interface between soil and ceramic. Temperature response of the POTs in EB2 were not significantly different before and after the evaporation experiment.

The TDR converted  $\psi_m$  showed some noise, but this did not explain the observed difference between the TDR and POT measurements, that was more pronounced in EB2 compared to EB1. These differences will be explained by comparing the moisture retention curves from *in situ* observation, soil core data, and the Van Genuchten fits.

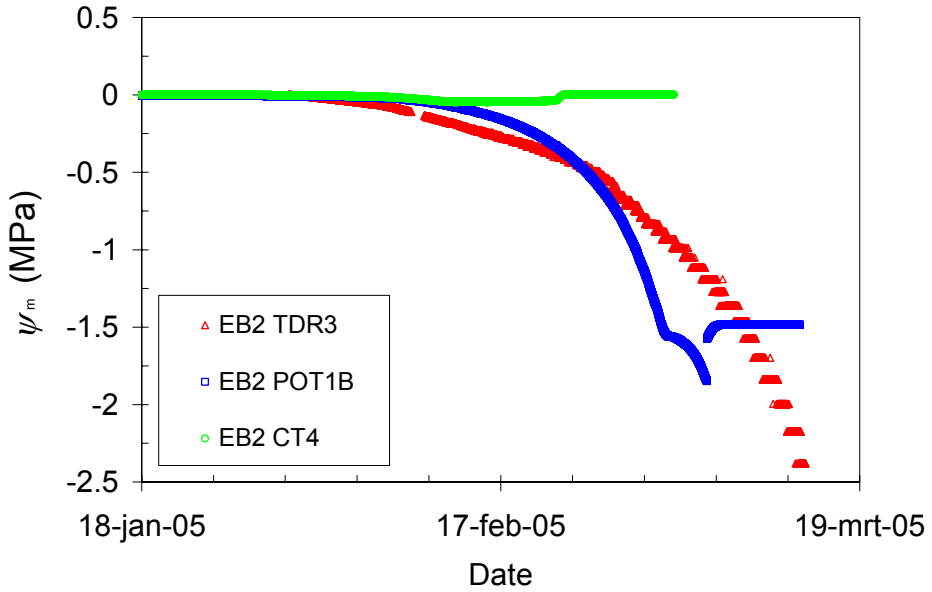


Figure 3-7A. Development of the matric potential  $\psi_m$  in time measured by polymer tensiometers (POT), time domain reflectometry probes (TDR) and water-filled tensiometers (CT) in evaporation container 2 (EB2) that was filled with loam. Each sub-figure shows a POT-TDR pair installed opposite to one another, and the nearest CT (continued on next page).

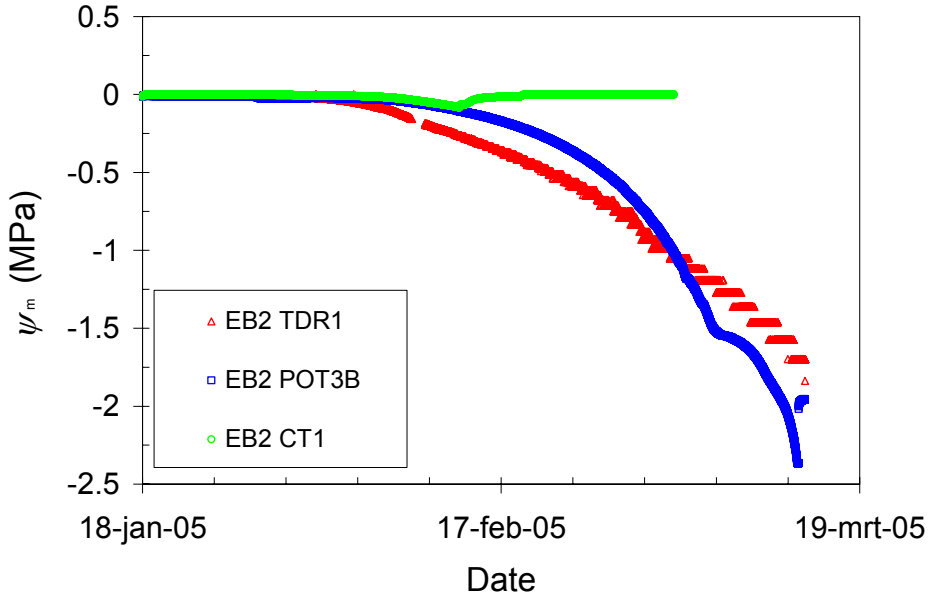


Figure 3-7B. (continued from previous page)

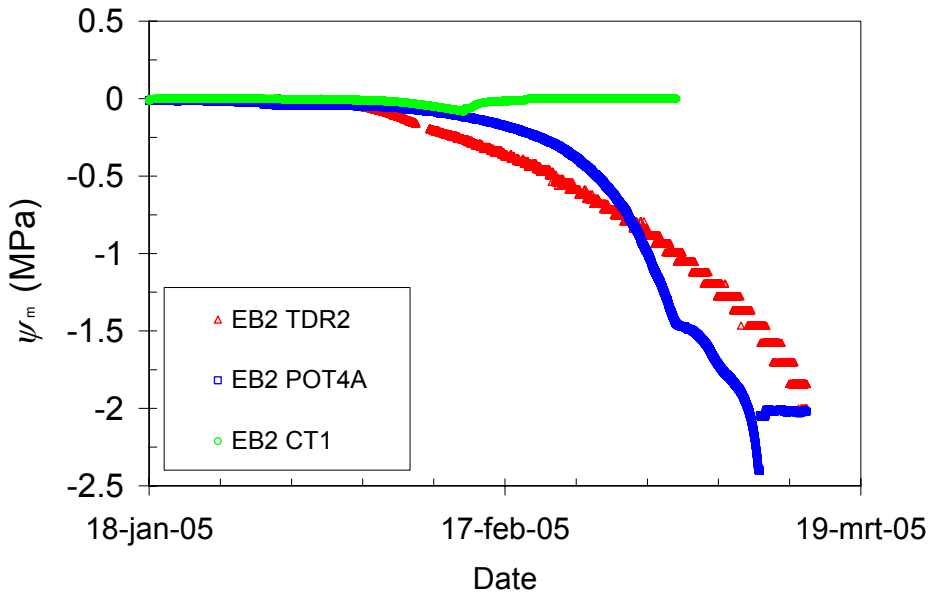


Figure 3-7C. (continued on next page)

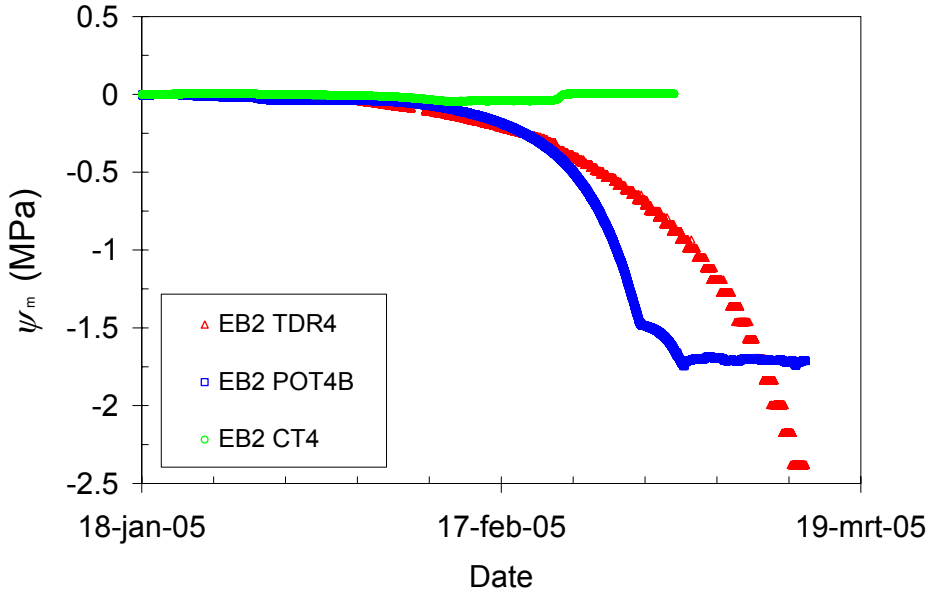


Figure 3-7D. (continued from previous page)

### 3.4.3 Comparison of moisture retention curves

We plotted retention curves of  $\theta_{\text{TDR}}$  and the POT-measured  $\psi_m$  together with soil core data and fitted retention curves (Figure 3-8 and 3-9). We were mostly interested in the dry end of the moisture retention curve, and therefore plotted on a linear scale instead of the more conventional log scale. For the *in situ* curve, data were selected with a volumetric moisture interval of 0.05, and a potential interval of 0.5 MPa. Additionally for EB1, a number of strategic points were selected to better describe the sharp bend in the transition from the wet to the dry end of the retention curve. For EB2 the moisture retention curve was smooth and such additional points were unnecessary. During fitting, the residual moisture content was fixed at 0 in most cases to prevent the occurrence of negative volumetric moisture contents in the dry end of the curve. Fitted parameter values and  $R^2$  for each data set are given in Table 3-5. For most *in situ* data, the retention curve showed a good fit, with  $R^2$  above 0.75. For combination POT2 TDR3 the fit had a

$R^2$  of about 0.3; this was due to the slightly deviating pressure values ( $<0.01$  MPa) of POT2 between a  $\theta_{TDR}$  of 0.3 to 0.4.

From Figs. 3-8 and 3-9 it can be seen that *in situ* and soil core data deviate slightly from each other, probably as a result of different measurement techniques. Madsen et al. (1986) and Peck and Rabbidge (1969) observed discrepancies between pressure plate and other methods, although these authors mostly observed moisture contents that were higher in case of the pressure plate method, while we sometimes observed lower moisture contents as well. Nevertheless, despite the differences in measurement volumes and instrument location of POTs and TDRs, the *in situ* retention curves are comparable with the retention curves determined on soil core data. With the observed and fitted retention data we can explain the observed differences between TDR converted potentials and the POT measured potentials (Figs. 3-5 and 3-7).

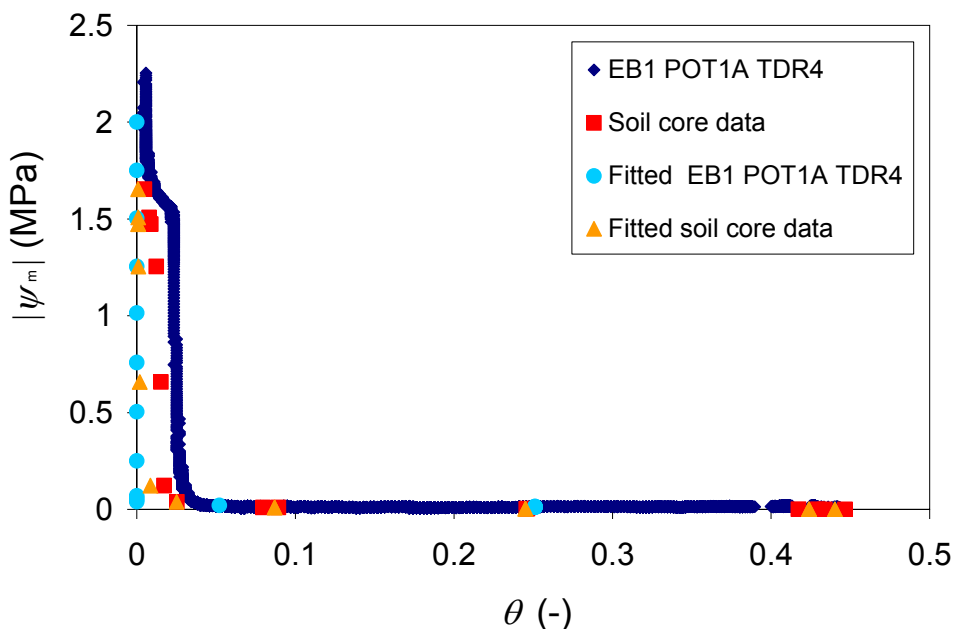
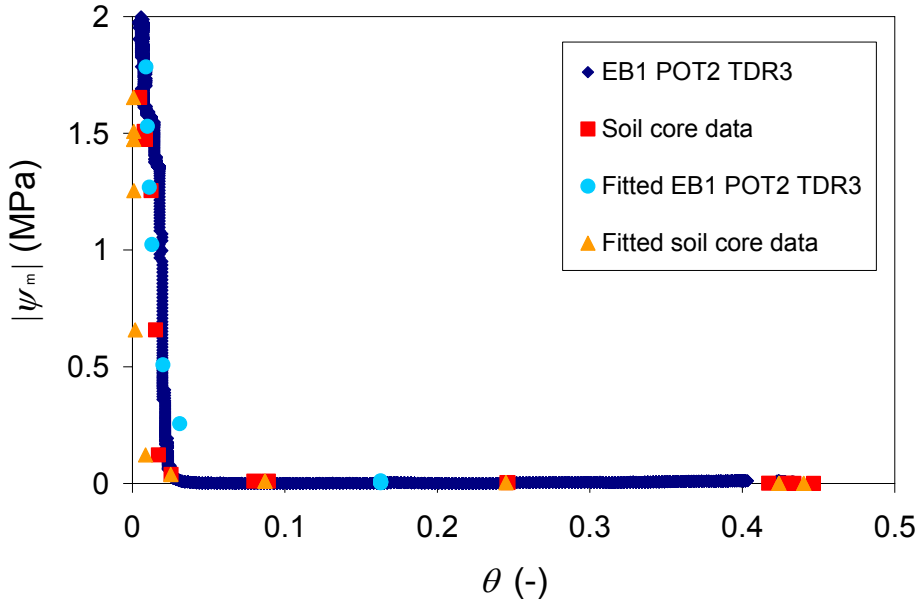


Figure 3-8A. Moisture retention curves of EB1 for the paired polymer tensiometers (POTs) and time domain reflectometers (TDR) together with gravimetric data from soil cores, and Van Genuchten fitted retention curves (Eq. (3-1)). Matric potential values ( $\psi_m$  (MPa)) are absolute. (continued on next page)



3-8B. (continued from previous page)

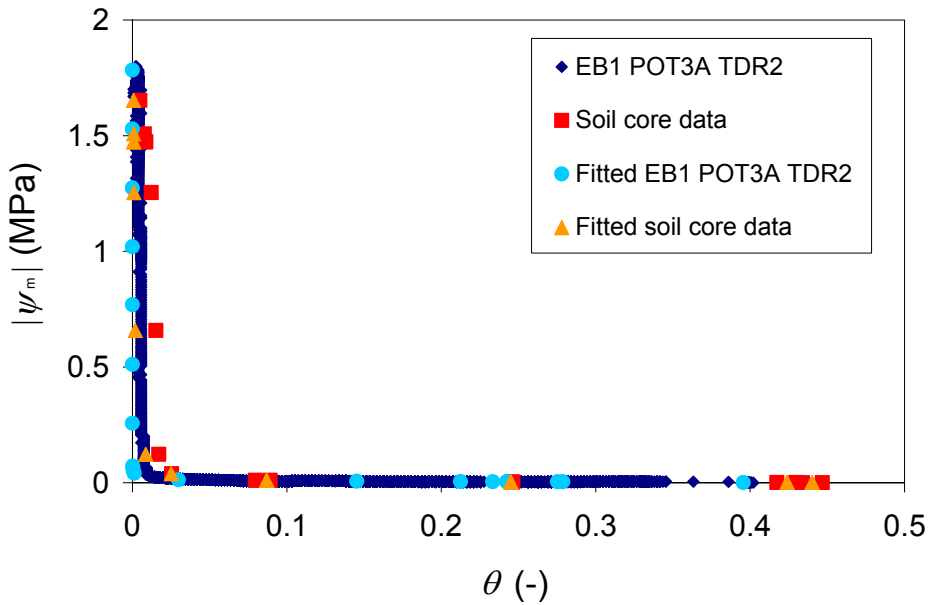


Figure 3-8C. (continued on next page)



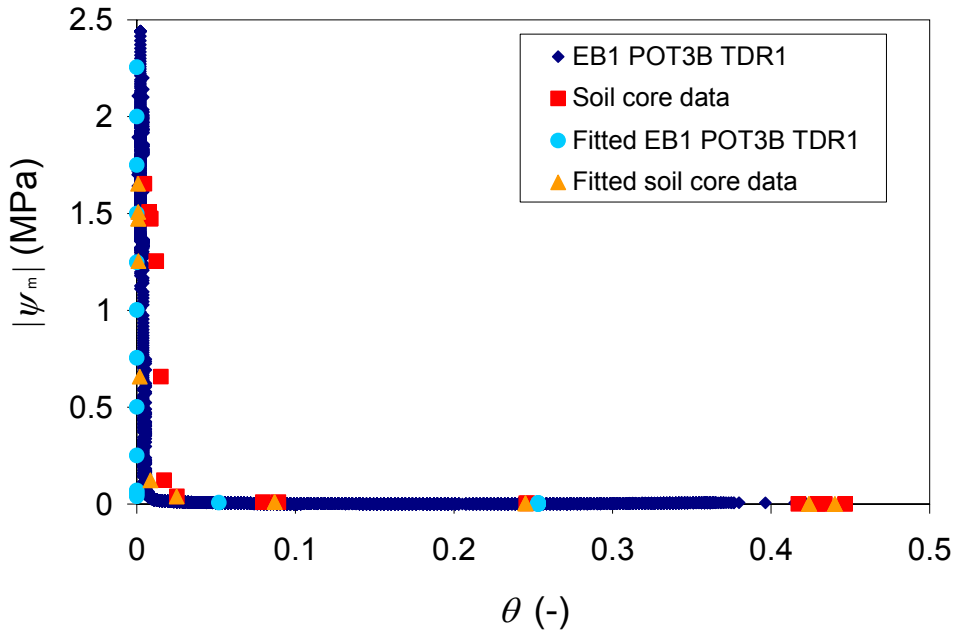


Figure 3-8D. (continued from previous page)

In Fig. 3-8A and B, the soil core data and the fit on soil core data show slightly lower pressure values than the *in situ* observations when the moisture content is between 0 and 0.05, while in Fig. 3-8C and D, the soil core data and fit show slightly higher values than the *in situ* observations in the same range. This explains the deviations of the TDR converted potentials from POT measured potentials in Fig. 3-5, where TDR3 and 4 seem to have slightly less negative potentials from October 7, 2004, while TDR1 and 2 show the opposite. In Fig. 3-8 it can be seen that for pressure values higher than 0.01 MPa, fitted values are always positioned left from observed values, indicating that the fitted values will result in less negative pressure values at equal moisture contents. Due to the limited accuracy in dry soils, this cannot be seen in Fig. 3-5.

For EB2, the deviations between *in situ* observations, soil core data and fits are more pronounced, and occur over the entire range of measured potentials (see Fig 3-9).

Table 3-5. Parameter values for moisture retention curves fitted by Eq. (3-1).

EB	Provided data	$\theta_s$	$\theta_r$	$\alpha$	$m$	$n$	$R^2$
1	Data from soil cores	0.44021	0.00	0.05735	0.27124	3.4232	0.9298
	POT1A	0.25111	0.00 <sup>†</sup>	0.00542	0.34072	66.40	0.7410
	TDR4						
	POT2	0.16292	0.00 <sup>†</sup>	0.00538	0.05245	12.16	0.3003
	TDR3						
	POT3A	0.25306	0.00	0.01617	0.12297	211.385	0.7919
	TDR2						
	POT3B	0.39595	0.00	0.02188	0.76923	3.4720	0.9034
	TDR1						
2	Data from soil cores	0.42628	0.00	0.00192	0.48602	1.005	0.99278
	POT1B	0.4759	0.00 <sup>†</sup>	0.01515	0.01777	17.5954	0.9241
	TDR3						
	POT3B	0.4491	0.00 <sup>†</sup>	0.00952	0.04364	8.1052	0.9660
	TDR1						
	POT4A	0.4492	0.00 <sup>†</sup>	0.00412	0.03578	12.056	0.9192
	TDR2						
	POT4B	0.44919	0.00 <sup>†</sup>	0.00412	0.03578	12.056	0.9192
	TDR4						

<sup>†</sup>Prefixed value.

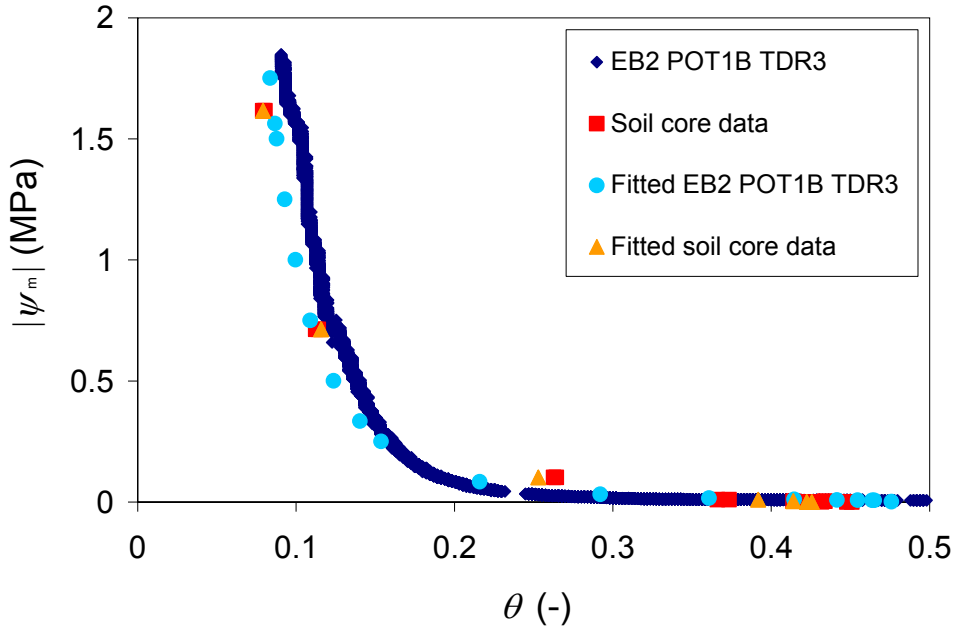


Figure 3-9A. Moisture retention curves of EB2 for the paired polymer tensiometers (POTs) and time domain reflectometers (TDR) together with gravimetric data from soil cores, and Van Genuchten fitted retention curves (Eq. (3-1)). Matric potential values ( $\psi_m$  (MPa)) are absolute. (continued on next page)

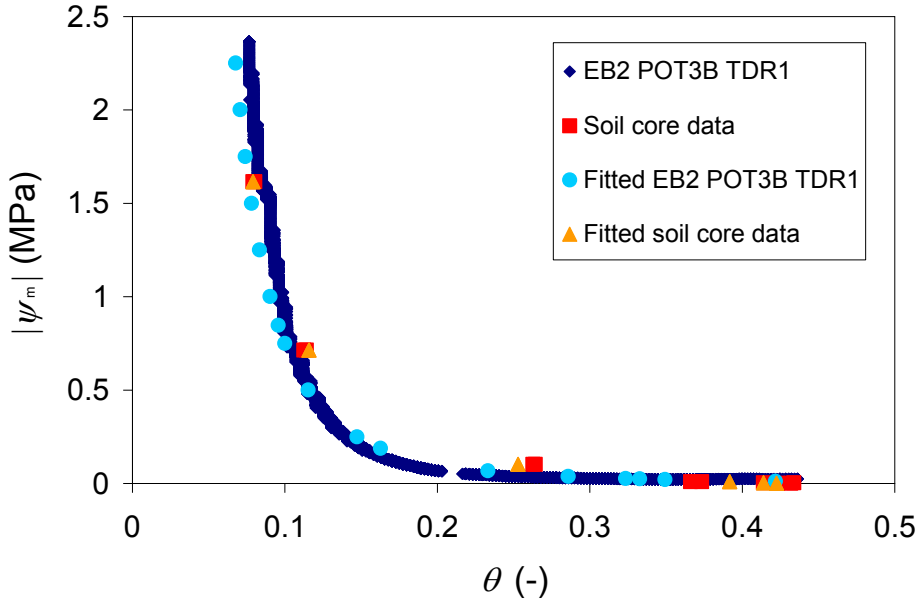


Figure 3-9B. (continued from previous page)

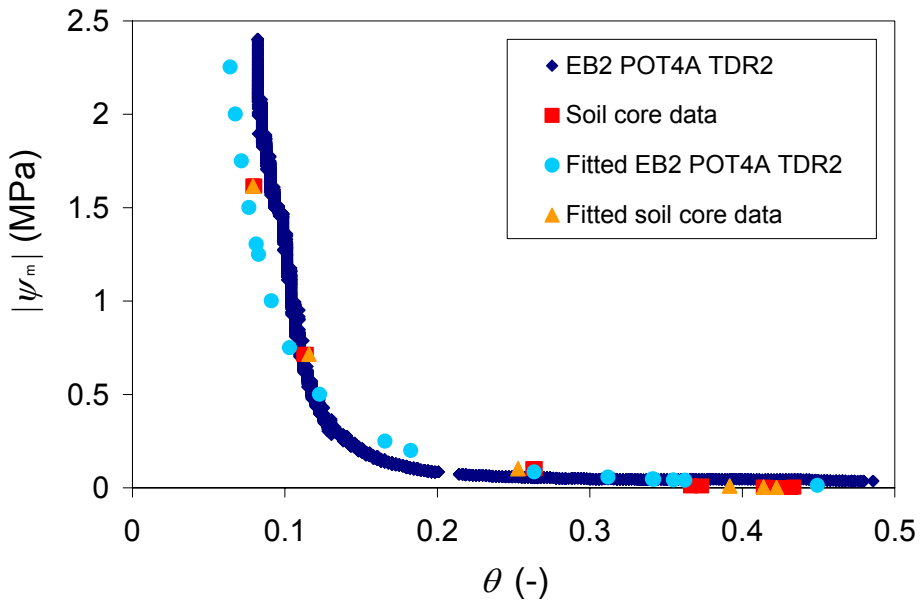


Figure 3-9C. (continued on next page)

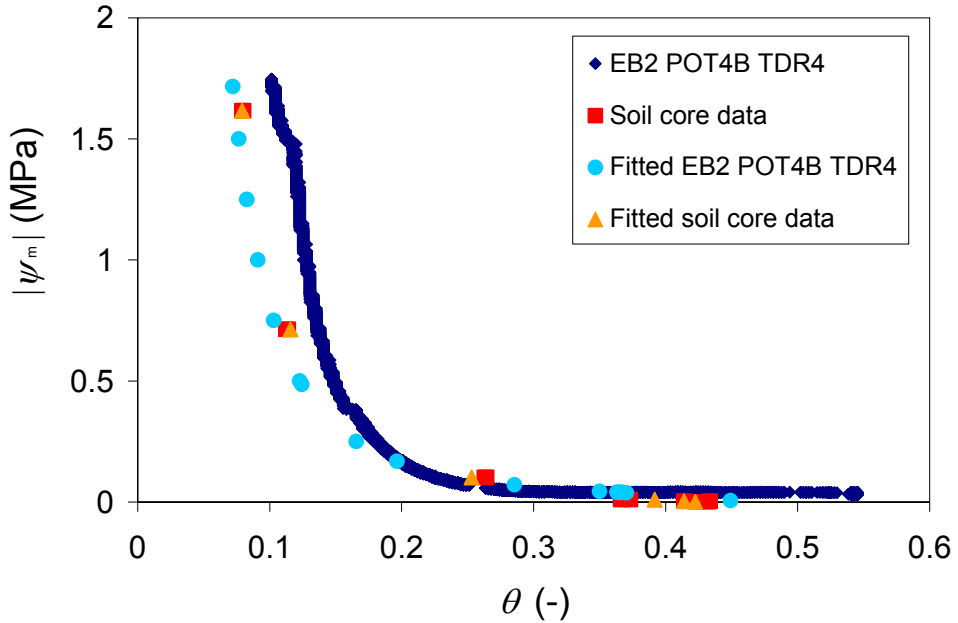


Figure 3-9D. (continued from previous page)

In Fig 3-9B, the soil core data and fitted values indicate higher absolute pressures than the *in situ* observations at a moisture content of around 0.25, while the fitted soil core observation at 1.6 MPa coincides with the *in situ* observations. This is resembled in Fig. 3-7B, where the TDR converted potentials are lower than the POT and CT observations from Feb 7 to Feb 27, 2005, while later on the POT and TDR converted potentials lie much closer. In Fig. 3-9A and C, the fitted soil core observation at 1.6 MPa deviates as well, and similarly the TDR converted potentials show larger deviations in Fig. 3-7A and C. In Fig. 3-9D, the fitted soil core observation at a moisture content of about 0.25 does coincide with the *in situ* observations, but at 1.6 MPa the deviation from the *in situ* observations is even more pronounced than in Fig 3-9A, B and C, and this can also be observed in the TDR converted potentials in Fig. 3-7D.

In the dry range, the fitted *in situ* data for both EBs always predicted lower  $\psi_m$  than were observed at any given moisture content. The underprediction indicates that retention curve fits have to be interpreted carefully in the dry range of the

moisture retention curve, and in combination with the limited accuracy of TDR in dry soils highlight the risk of using TDR converted potentials in that range.

### 3.5 Conclusions

The temperature response times of the various POT designs indicate an effect of polymer chamber size, and ceramic area in contact with the polymer solution. Designs that minimized polymer chamber height, while maximizing the ceramic area in contact with polymer solution had the shortest response times. For all POT designs response times to regain pressure by rewetting were remarkably shorter than reported in Chapter 2. It should be noted that the reported response times are an extreme scenario: from completely dry polymer to fully saturated. In practice, pressure recovery will generally be much faster.

POTs with ceramic cones have an enhanced soil contact compared to POTs with flat ceramics; we never observed poor soil contact. We compared four designs by testing them in soil, and the results showed similar responses. A preferred design therefore mostly depends on the maximization of the ceramic membrane's surface in contact with the polymer solution, and the polymer chamber's depth (Bakker et al. 2007).

*In situ* moisture retention curves were comparable to retention curves from soil cores, and could be fitted with the Van Genuchten curve. Although *in situ* moisture retention curves will never exceed the upper measurement limit of POTs, pairing POT and TDR data will give a unique opportunity to study the dynamics of moisture retention curves in field soils.

A detailed analysis of POT-measured matric potentials, TDR-measured moisture contents, and the fitted retention curve revealed the risks associated with converting soil moisture readings in dry soils to matric potentials.

## Chapter 4

---

# Performance of polymer tensiometers in root water uptake studies in dry soil

---

This Chapter is a modified version of: Van der Ploeg, M.J., H.P.A. Gooren, G. Bakker and G.H. de Rooij. 2008. Matric potentials measurements by polymer tensiometers in cropped lysimeters under water-stressed conditions. *Vadose Zone Journal* 7: 1048-1054.

## 4.1 Introduction

In many regions of the world plant growth and productivity are limited by water deficits. Droughts have become more frequent and intense, and as a result the area of land characterized as ‘very dry’ has more than doubled since the 1970s (Dai et al. 2004, Huntington 2006). Although 70-85% of the world’s consumable water is currently allotted to agriculture, increasing urban demands for potable water due to population growth will continue to compete with agricultural water use from now on (Somerville and Briscoe 2001, Foley et al. 2005). The need to understand plant responses to water deficits has never been more acute. The driving force for root water uptake is the water potential gradient between soil and root. Unsaturated water flow in the root zone often occurs at soil water matric potentials ( $\psi_m$ ) that are below the range of water-filled tensiometers (to approximately  $-0.09$  MPa; Young and Sisson 2002). As a consequence, little is known about the distribution of root water uptake over the root zone under dry conditions. Hopmans and Bristow (2002) and Feddes and Raats (2004) noted that the lack of knowledge about root water uptake under stressed conditions has unavoidably lead to the rather schematical representation of the root zone in unsaturated models.

Long-term water stress alters the physiological functioning of the entire plant (Kramer, 1983, Smith and Griffiths, 1993), but little is known about the short-term dynamics of root water uptake under water-stressed conditions. New techniques such as X-ray tomography, NMR, and 2D light transmission imaging have improved our understanding of plant responses to dry conditions (Tollner et al. 1994, Van der Weerd et al. 2001, Garrigues et al. 2006), but these techniques are complicated and not suitable for field use. Fortunately, the recent development of a polymer tensiometer (POT) (Bakker et al. 2007) that measures  $\psi_m$  down to  $-1.6$  MPa creates new possibilities for studying the dynamics of  $\psi_m$  in the vicinity of roots, in the laboratory as well as in the field.

Total soil water potential  $\psi_{tot}$  is a direct indication of the amount of energy required by plants to take up water. A plausible hypothesis is that a plant distributes the water uptake over its root network in a way that minimizes the expenditure of energy at any given moment (Dirksen et al. 1994, Adiku et al. 2000). This would be consistent with the observations of Bohm et al. (1977) that



root water uptake and root density correlate poorly. However, direct observation of low  $\psi_m$  within a plant's root zone may provide knowledge of the plant's ability to satisfy its water needs (and of its strategy to maximize this ability).

The main objective of this Chapter is to evaluate the performance of POTs in the root zone during an entire cropping cycle, including the POT's ability to register  $\psi_m$  over the full range encountered in a cropped soil. A second objective is to investigate the added value of  $\psi_m$  measurements for root water uptake studies in water-stressed conditions. The dynamics of  $\psi_m$  and soil moisture content ( $\theta_{\text{TDR}}$ ) were investigated under varying levels of water stress in three lysimeters cropped with maize (*Zea Mays L.*).

## 4.2 Setup of the lysimeter experiment

Plant water stress will increase with decreasing  $\psi_m$ , until  $\psi_m$  reaches a level where root water uptake is no longer possible. For agricultural crops this level is around  $-1.6$  MPa (Koorevaar et al. 1983). However, the  $\psi_m$ -range within which different crops begin to be affected by water stress is less well known.

Taylor and Ashcroft (1972) provided data of  $\psi_m$  (including data for maize) at which 'water should be applied for maximum yields of various crops grown in deep, well-drained soil that is fertilized and otherwise managed for maximum production'. Kroes and van Dam (2003) use these  $\psi_m$ -values in combination with the water stress reduction function of Feddes et al. (1978). Based on the Feddes reduction function and the data of Taylor and Ashcroft (1972) we defined 3 treatments; no-stress (minimum  $\psi_m = -0.15$  MPa), intermediate stress (minimum  $\psi_m = -0.45$  MPa) and severe stress (minimum  $\psi_m = -0.80$  MPa); with minimum  $\psi_m$  being the most negative matric potential (measured by any of the POTs) that was allowed during the specific treatments.

We constructed 3 lysimeters of 0.70 m long by 0.50 m width and 1.70 m high (Fig. 4-1). Each lysimeter consisted of 3 vertical segments of 0.50 m depth for easier backfilling. Below the lowest compartment, a drainage compartment of 0.20 m depth was filled with gravel to support the weight of the soil. Each lysimeter was placed on a stainless steel frame to allow weighing on a movable scale (1500 kg

range, 0.2 kg resolution). We filled the lysimeters with a prewetted loamy soil (10.9% clay, 58.2% silt, 31.9% sand) in 0.05 m layers, packing the layer by tamping with constant force, and raking the upper 0.02 m before applying a new layer. We installed three instrumental layers at 0.2, 0.6, and 1.1 m depth during filling. Each layer contained three POTs (Bakker et al. 2007; measurement range 0 to  $-1.6$  MPa, accuracy  $2.38 \times 10^{-3}$  MPa), three time domain reflectometry (TDR) probes (three wire, 0.1 m length, 0.0175 m wire spacing, observed  $\theta_{\text{TDR}}$  resolution of 0.001 (-)), and three conventional tensiometers (CT). We outfitted the POTs with solid ceramic cones (See Chapter 3). Each POT was calibrated for long-term pressure decay and temperature influence according to Bakker et al. (2007) (See Chapter 2). Preliminary testing showed that the distance between each POT and TDR-probe was sufficient to prevent measurement interference (see also Baker and Lascano 1989, Zegelin et al. 1989). Because root profiles of maize may be greatly altered by temporary drought stress (Box et al. 1989), we monitored root growth during the experiment by installing horizontal acrylic rhizotubes every 0.1 m depth, except at 0.5 and 1.0 m due to the construction of the boxes. The acrylic material itself does not have an effect on root growth (Brown and Upchurch 1987, Johnson et al. 2001). Root images were captured using a cold-light boroscope with a diameter of 6.35 mm (Heine Optotechnik GmbH) and a digital camera (Nikon Coolpix 4500). The final images were  $320 \times 240$  pixels and captured a curved rhizotube area of  $1 \text{ cm}^2$ . During the experiment, root presence was detected by visual inspection of the images.

All sides of the lysimeters were insulated by a layer of 0.1 m polystyrene to reduce temperature influence on root growth (McMichael and Burke 1996). The lysimeters were uniformly irrigated by emptying syringes with equal amounts of water in each of the cells of a metal grid firmly placed on the soil surface. Because nutrient analysis indicated that the soil contained enough nutrients for plant growth during the experiment, non-chlorinated tap water was used for irrigation instead of nutrient solution. Each lysimeter had an artificial growing light, and reflective material to enhance plant growth in the lysimeter. The reflective material restricted light interference from the other lysimeters, ensuring each lysimeter received an equal amount of light. Prior to sowing, the soil in the lysimeters was left to consolidate for a month, and irrigated to maintain realistic moisture profiles.

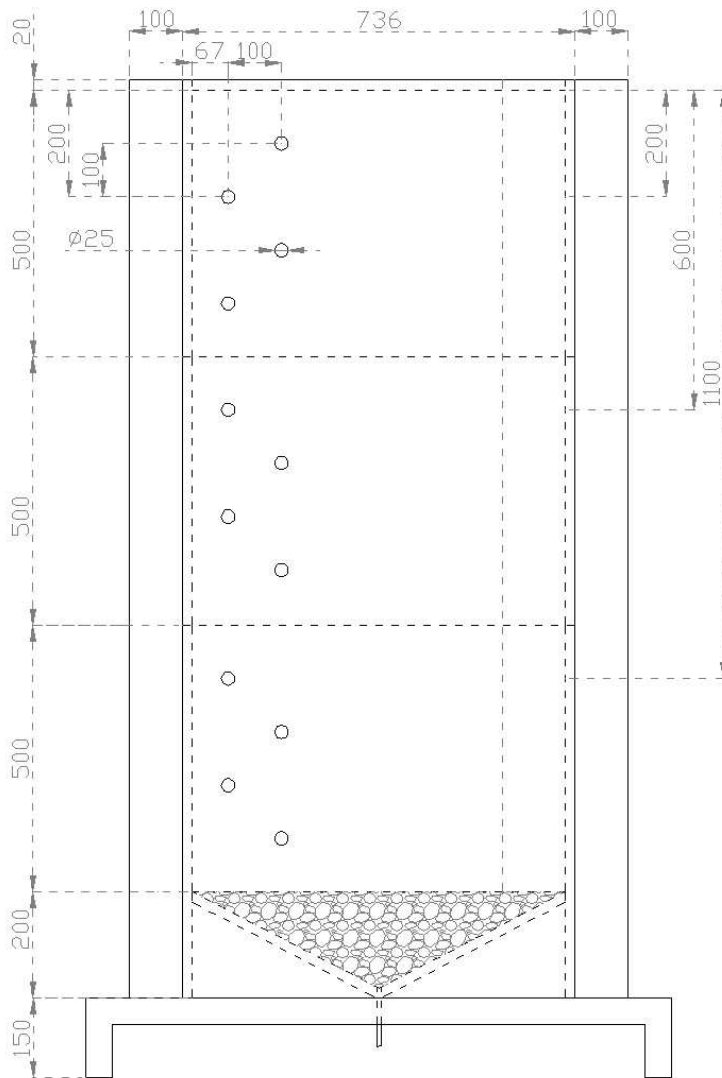


Figure 4-1A. Schematic diagram (front view) of the lysimeters, consisting of 3 compartments that facilitated backfilling. The lowest compartment incorporated a drainage compartment. The lysimeters were insulated with 100 mm thick polystyrene insulation. The lysimeters were placed on a stainless steel frame with a height of 150 mm. Ports (25 mm) at 67 and 167 mm from the side indicate the rhizotubes that were installed. The instrumentation levels are at 200, 600 and 1100 mm. All measures are in mm. (continued on next page)

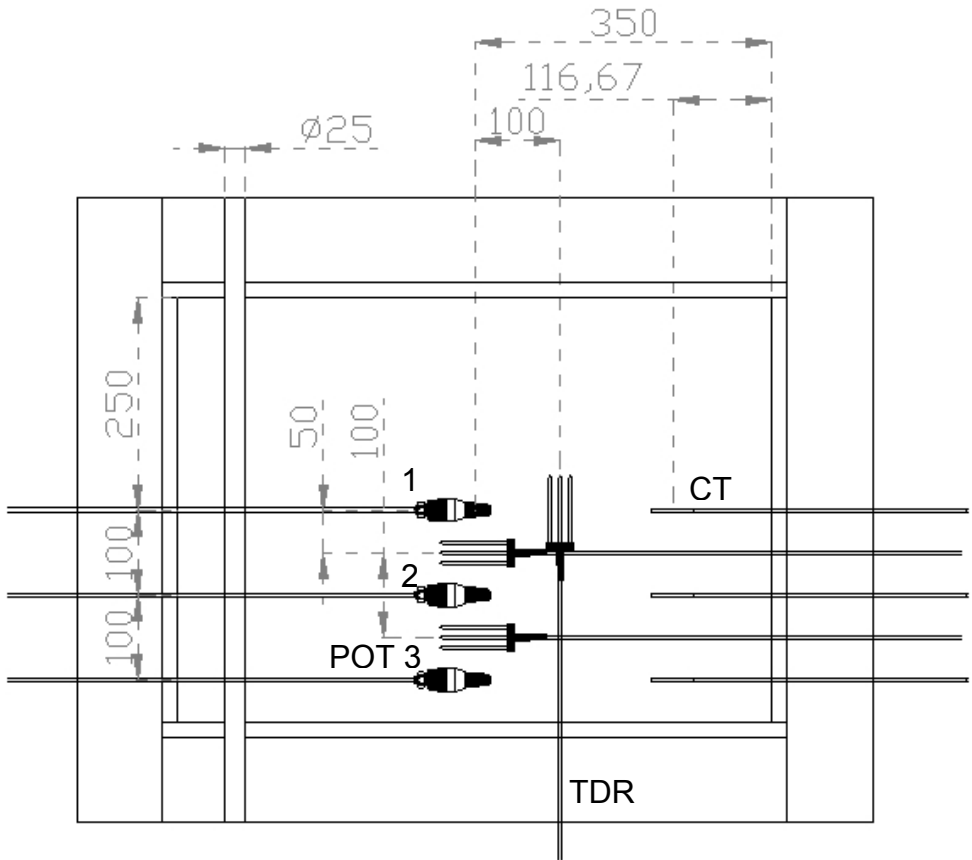


Figure 4-1B. (continued from previous page) Top view of the instrumental layout at 200, 400 and 1100 mm, with three polymer tensiometers (POT), three time domain reflectometry probes (TDR) probe, three conventional tensiometers (CT), and a rhizotube (diameter  $\varnothing = 25$  mm). Note the L-shaped layout of the TDR probes. All measures in mm. (continued on next page)

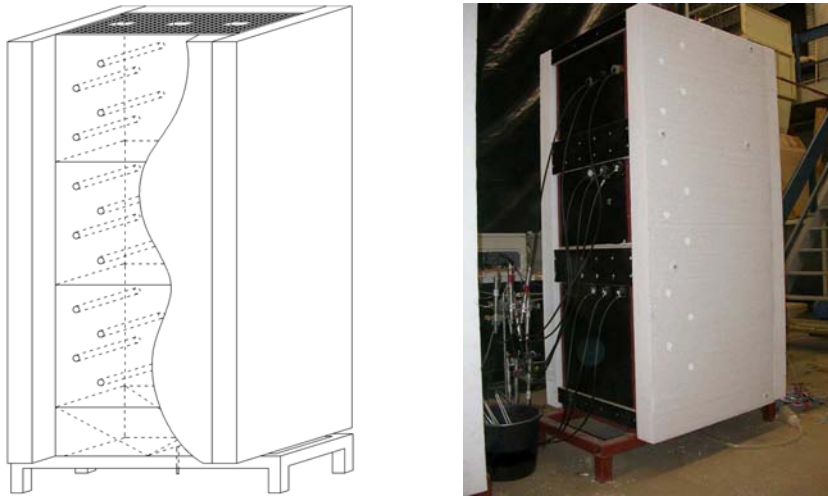


Figure 4-1C. (continued from previous page) 3D view of the lysimeter, including insulation and stainless steel frame.

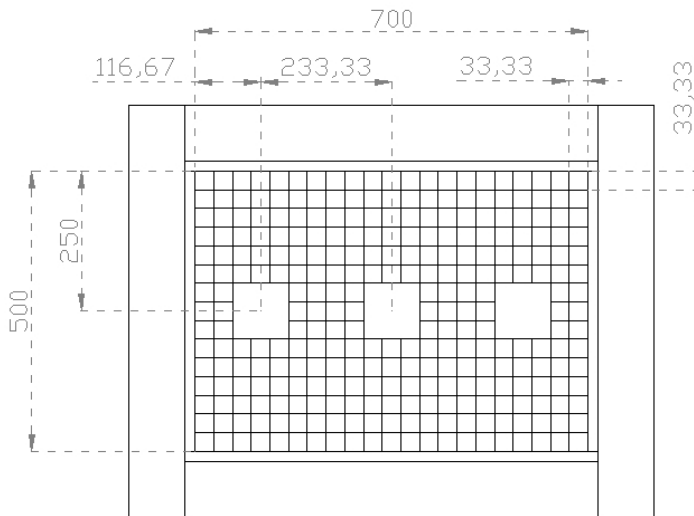


Figure 4-1D. Top view of the lysimeter, with all measures in mm. On top of the soil a grid was placed to ensure uniform irrigation. The maize seeds were sown 50 mm deep at  $(x, y) = (250, 117)$ ,  $(250, 350)$ , and  $(250, 583)$  (with  $(0, 0)$  denoting the back-left corner; x running from back to front, y from left to right). By doing so, all seeds had equal areas of soil ( $0.1166 \text{ m}^2$ ).

On September 5<sup>th</sup>, 2005 maize (*Zea Mays L.*) was sown in every lysimeter at the horizontal coordinates  $(x, y) = (0.25 \text{ m}, 0.117 \text{ m}), (0.25 \text{ m}, 0.35 \text{ m}), (0.25 \text{ m}, 0.583 \text{ m})$ , (with  $(0, 0)$  denoting the back-left corner;  $x$  running from back to front,  $y$  from left to right) to ensure equal volumes of soil were available for each maize plant. The plants were optimally irrigated (Fig. 4-2) during the initial growth stage that lasts approximately 20 days for maize (Allen et al. 1998). After 25 days we terminated irrigation on two lysimeters, until the prescribed water stress level was attained at one of the shallow POTs.

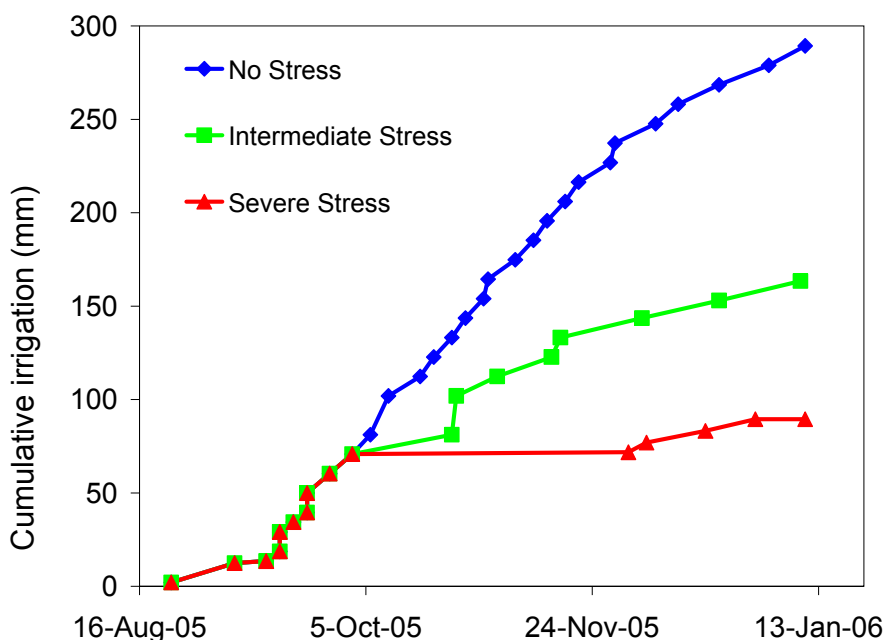


Figure 4-2. Cumulative irrigation for the no-stress, intermediate stress and severe stress treatment.

Minimum  $\psi_m$  was reached on October 24, 2005 for the intermediate stress, and on December 2, 2005 for the severe stress treatments. The stress level was subsequently maintained by using small, frequent irrigations. The remaining lysimeter was irrigated throughout the experiment to maintain the minimum  $\psi_m$  as the no-stress treatment. Temperature and relative humidity (RH) were recorded with a thermo-hygrometer (Oregon Scientific, accuracy 0.1 °C and 1% RH) above

one lysimeter for the first 25 days during which the irrigation was the same for all treatments, and thereafter above every lysimeter on alternating days to record possible changing conditions between the lysimeters. The thermo-hygrometer was placed on the polystyrene insulation, close to the soil surface, but not hindering evaporation. The RH data were converted to vapor pressure deficit (e.g. Allen et al. 1998). The experiment lasted 4 months until all plants completed their growth cycle. At this point, undisturbed soil samples were taken to determine soil hydraulic properties (98 cm<sup>3</sup> sample rings) using the soil core method (Blake and Hartge 1986). Samples taken close to the TDR probes were used for gravimetric moisture content ( $\theta_{\text{grav}}$ ) determination at 200, 600, 1200, 3200, and 10000 Pa (averaged over the 5 cm high sample) on a suction table (Romano et al. 2002). Disturbed samples were used in a pressure plate extractor setup (Dane and Hopmans 2002) to determine the soil moisture retention curve at 0.1 and 1.6 MPa. Root length density ( $L_r$ ) samples were obtained using an auger with plunger and a sample volume of 385 cm<sup>3</sup> (e.g. Oliveira et al. 2000). To remove the soil from the RLD samples, they were hand washed according to Oliveira et al. (2000), stored in a 10% ethanol solution for a maximum of 3 weeks, scanned at 400 dpi, and analyzed with the computer program WinRHIZO (Himmelbauer et al. 2004). We determined a cumulative  $L_{r,z}$  (cm cm<sup>-2</sup>), which is the length of root present under a unit area of soil surface to a specified depth (Atkinson 2000):

$$L_{r,z} = \int_{z_1}^{z_2} L_r dz \quad (4-1)$$

### 4.3 Experimental conditions

Immediately after filling, the mass of the lysimeters differed by less than 3.2 kg (see Table 4-1), indicating a uniform packing process. On the other hand, the soil bulk density profile determined after the experiment showed some variation within and between lysimeter soil profiles (Fig 4-3). Possible reasons for this variability are unavoidable heterogeneity in packing or initial moisture content, shrinking or swelling under the different moisture regimes, and the non-uniform occurrence of roots in the soil profile. The coefficient of variation (CV) is 0.03911 ( $N=14$ ) for the wet, 0.04203 ( $N=15$ ) for the intermediate, and 0.05525 ( $N=15$ ) for

the dry treatments. According to Hillel (1998) bulk density distributions with a CV smaller than 0.15 can be considered highly uniform, and we consider our observed density variations as minor. However, even small variability in density may affect moisture distribution.

Lysimeter soil surface temperatures varied between 18.5 and 32.8 °C, and the vapor pressure deficit between 0.89 and 3.17 kPa. Table 4-1 shows that the total irrigation and the evapotranspiration decrease with increasing stress levels (See Fig 4-2. as well) Total drainage differed only slightly among the lysimeters (Table 4-1), but drainage ceased in all lysimeters after day 25 for the remainder of the experiment in all treatments.

Table 4-1. Target matric potentials ( $\psi_m$ ), lysimeter mass, and water balance terms for the different water stress treatments outlined in the main text.

Water stress level	Target minimum	Initial mass (kg)	I <sup>†</sup> (mm)	D <sup>‡</sup> (mm)	Final mass (kg)	ET <sup>§</sup> (mm)
	$\psi_m$ at 0.2 m depth (MPa)					
No	-0.15	897.8	289.3	0.23	883.8	328
Intermediate	-0.45	894.6	163.4	0.78	855.8	274
Severe	-0.80	896.6	89.5	0.14	844.8	237

<sup>†</sup>Irrigation, <sup>‡</sup>Drainage, <sup>§</sup>Evapotranspiration.



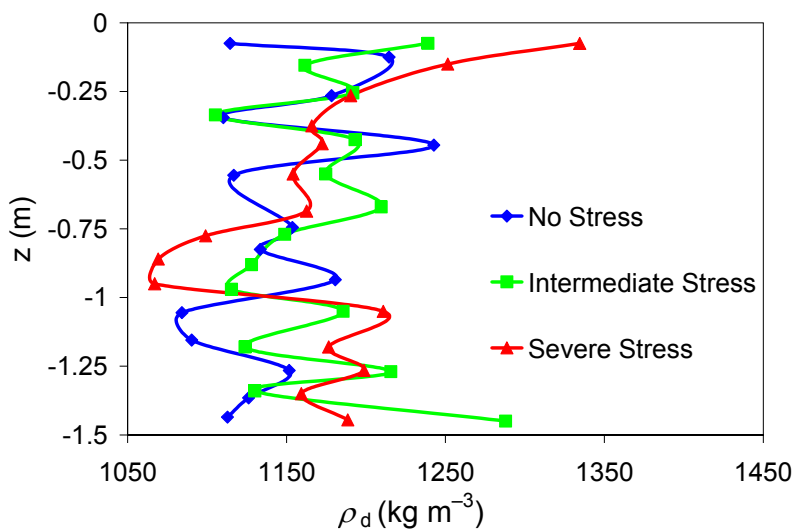


Figure 4-3. Distribution of soil dry bulk density with depth for the 3 lysimeters under the no-stress, intermediate stress and severe stress treatment, as determined after completion of the experiment.

#### 4.4 Comparison of polymer tensiometers and time domain reflectometry probes

Figure 4-4 shows distributions of matric potentials (left) and soil moisture (right) down the profile for all lysimeters at three dates. The contour plots were constructed from the 9 POT and 9 TDR observations in each lysimeter (see Fig. 4-4A). In the lysimeters, the TDRs were not located in one vertical plane, but in an L-shaped layout (top view; Fig. 4-1). For clarity we ‘unfolded’ the L-shape and plotted it in 2D, with the bend indicated by a dashed line at  $x = 0.25$  m. The  $z$ -line (vertical coordinate; zero at the soil surface, positive upwards) at  $x = 0.2$  m in the figure is located at  $(x, y) = (0.35 \text{ m}, 0.25 \text{ m})$  in reality. The central maize plant in each lysimeters was sown at  $(x, y, z) = (0.25 \text{ m}, 0.35 \text{ m}, -0.05 \text{ m})$ .

On September 8<sup>th</sup>, 2005 (Fig. 4-4B) all lysimeters were still receiving equal amounts of irrigation (see Fig. 4-2). The  $\psi_m$ -profiles were therefore still in the wet range and rather featureless. The profiles were wetter in the top of the lysimeter because of irrigation, and drier at the bottom as a result of the low moisture content

at packing and the seepage face boundary condition. The minor differences in  $\theta_{\text{TDR}}$  among the lysimeters can be explained by small differences in soil density, which affects the  $\theta_{\text{TDR}}$ -distribution, but not the  $\psi_{\text{m}}$ . No roots were observed in the rhizotubes to this date. We therefore consider the observed moisture and potential profiles to be strictly abiotically controlled by soil hydraulic properties, and the initial and boundary conditions.

By October 23<sup>rd</sup>, 2005 (Fig. 4-4C), the intermediate stress and severe stress lysimeters had not been irrigated for four weeks. The  $\psi_{\text{m}}$ -profile of the no stress treatment remained in the wet range. In contrast,  $\psi_{\text{m}}$ -values in the intermediate stress and severe stress treatment were between  $-0.3$  and  $-0.5$  MPa in the upper profile, with similar  $\psi_{\text{m}}$ -values below  $0.7$  m depth. The  $\theta_{\text{TDR}}$ -values in the no stress treatment was still greater than  $0.1$  ( $\text{m}^3 \text{m}^{-3}$ ) in most of the profile as a result of continued irrigation. The soil profiles in the other two treatments were completely (intermediate stress) or largely (severe stress) below a  $\theta_{\text{TDR}}$ -value  $0.1$  ( $\text{m}^3 \text{m}^{-3}$ ). Rhizotube observations at this time showed that roots had grown to  $-1.1$  m depth in the no stress, to  $-0.8$  m in the intermediate stress, and to  $-0.9$  m severe stress treatment.

On December 8th, 2005 (Fig. 4-4D),  $\psi_{\text{m}}$  in the no stress treatment remained essentially unchanged, but the other treatments indicated continued drying throughout the entire lysimeter. At this date, the severe stress lysimeter had a significantly lower  $\psi_{\text{m}}$  than the intermediate stress lysimeter at all depths. Consistent with the  $\psi_{\text{m}}$ -data,  $\theta_{\text{TDR}}$  in the severe stress lysimeter were somewhat lower than in the intermediate stress lysimeter, whose moisture distribution had hardly changed since October 23<sup>rd</sup>, because it was maintained at its target  $\psi_{\text{m}}$ . All lysimeters had received irrigation a few days before, which resulted in slightly higher  $\psi_{\text{m}}$ -values in the upper part of the intermediate stress profile, compared to October 23<sup>rd</sup>.

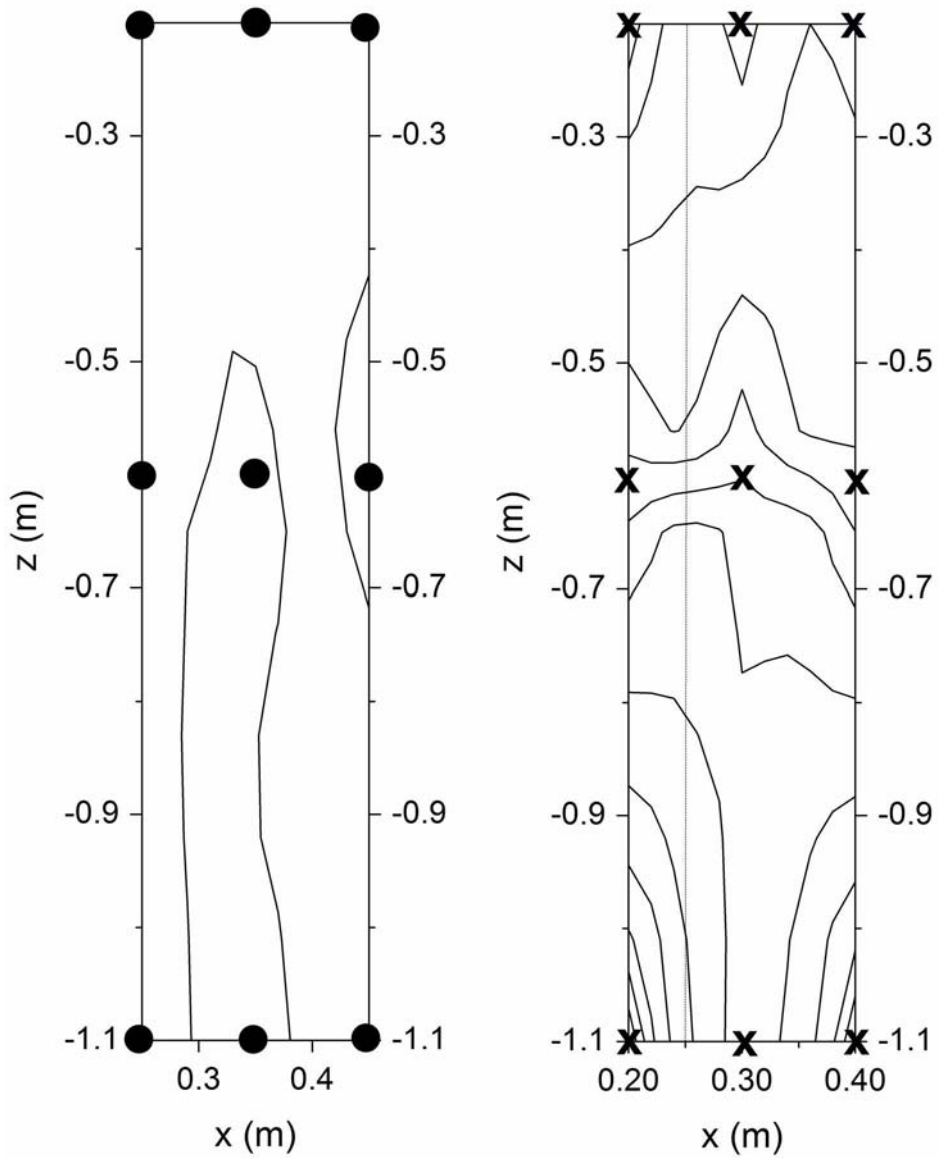


Figure 4-4A. Location of the polymer tensiometers (POT) (left panel, O) and time-domain reflectometry (TDR) probes (right panel, X). For the TDR, the horizontal coordinate is transformed to plot an L-shaped trajectory in 2D.

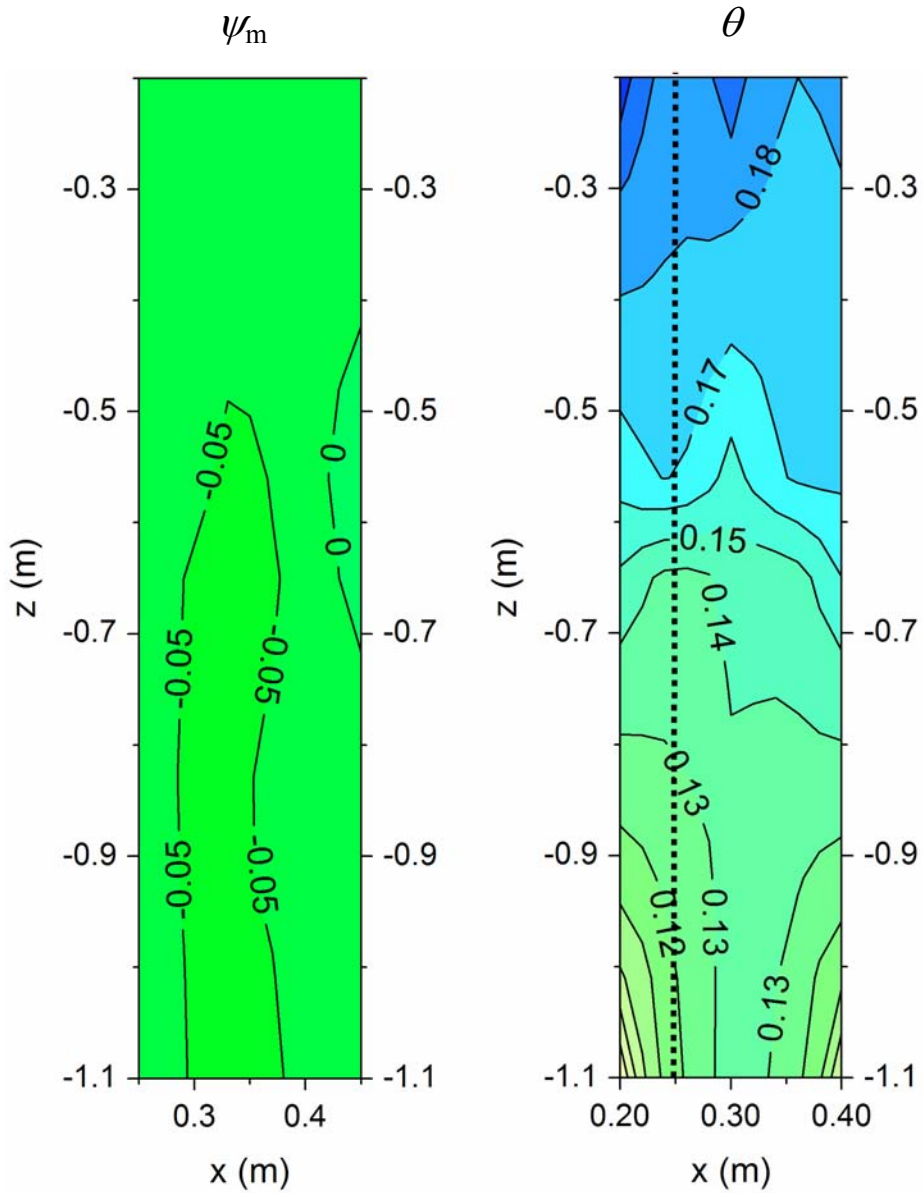


Figure 4-4B. 8 Sep 2005 No Stress  
 Matric potential ( $\psi_m$ ) and volumetric moisture content ( $\theta$ ) distribution. For the  $\theta$ -distribution, the horizontal coordinate is transformed to plot an L-shaped trajectory in 2D. (continued on next page)

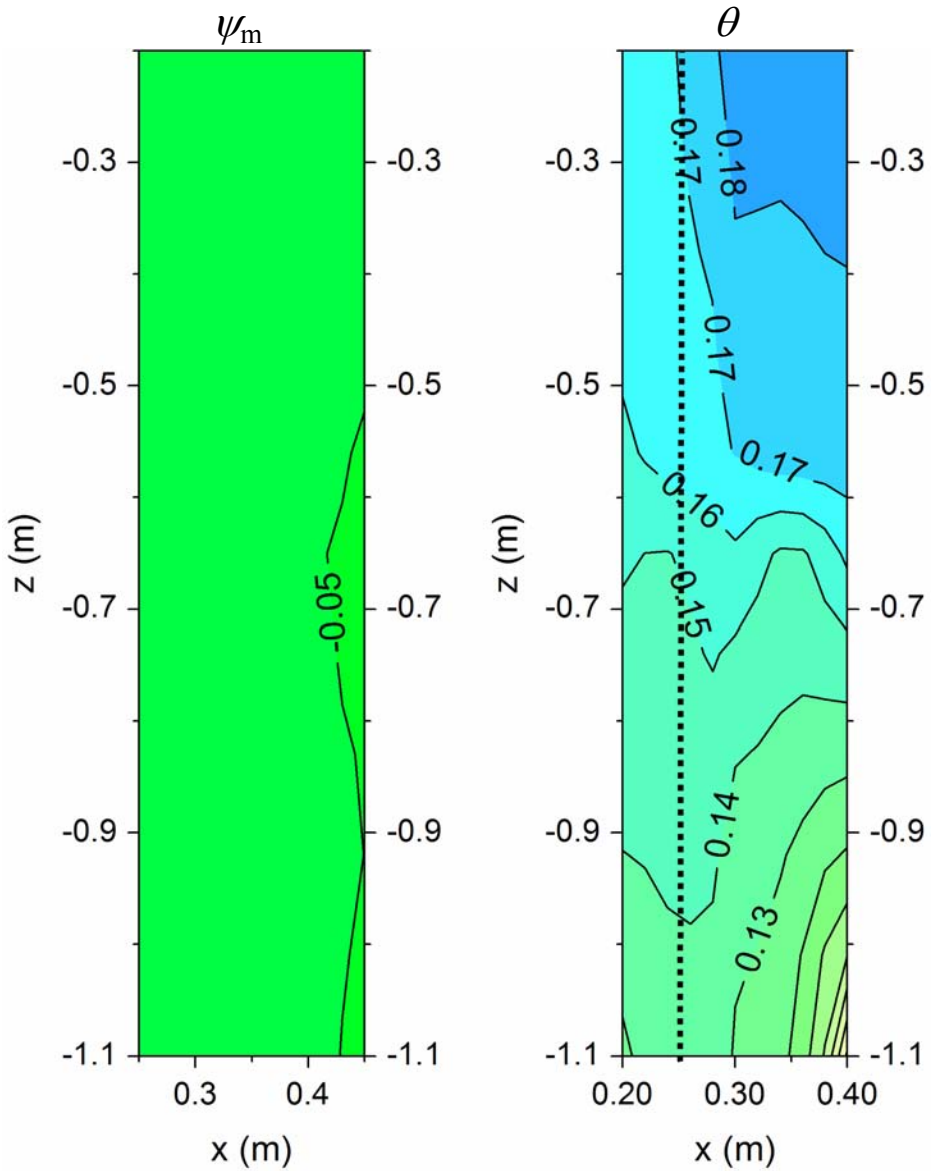


Figure 4-4B. (continued from previous page) 8 Sep 2005 Intermediate Stress. Matric potential ( $\psi_m$ ) and volumetric moisture content ( $\theta$ ) distribution. For the  $\theta$ -distribution, the horizontal coordinate is transformed to plot an L-shaped trajectory in 2D. (continued on next page)

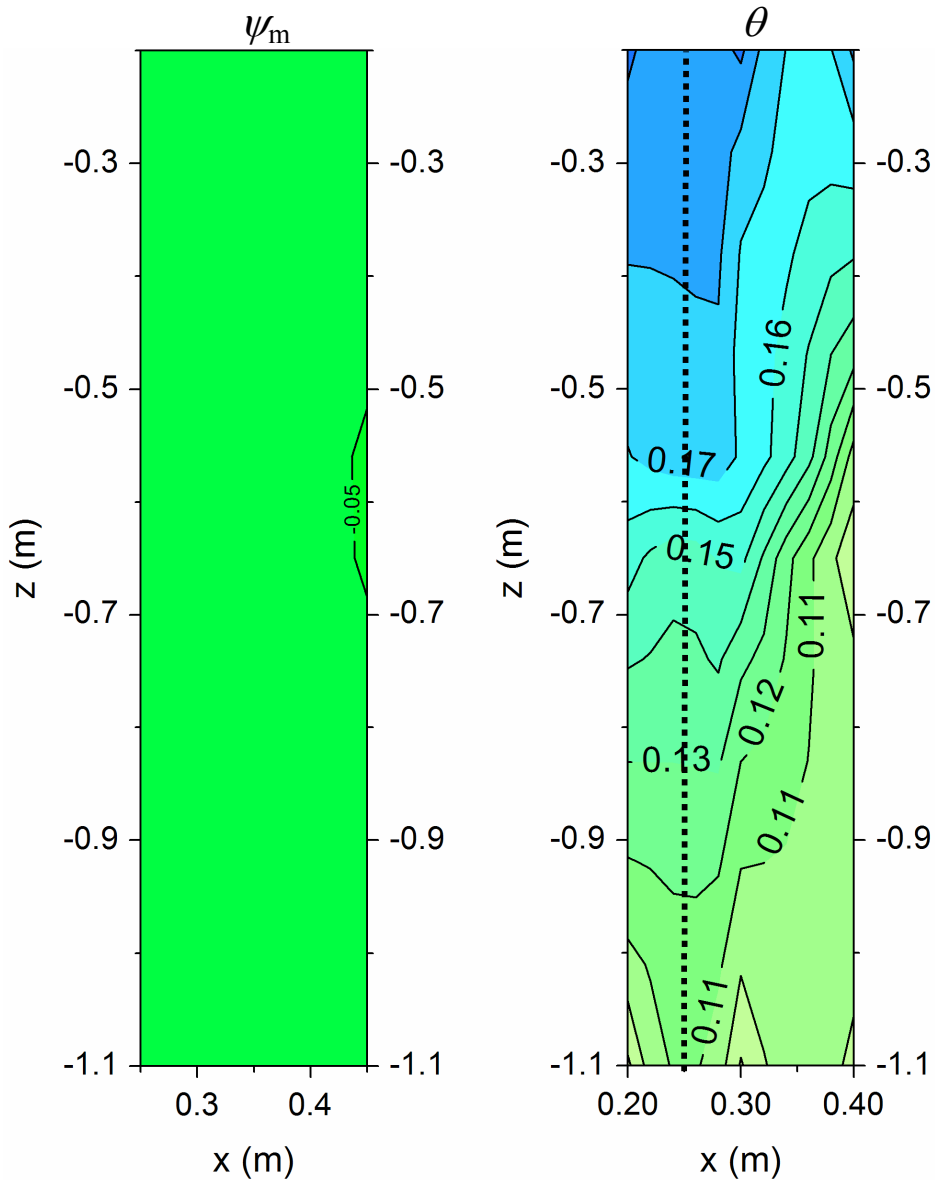


Figure 4-4B.(continued from previous page) 8 Sept 2005 Severe Stress.  
 Matric potential ( $\psi_m$ ) and volumetric moisture content ( $\theta$ ) distribution. For the  $\theta$ -distribution, the horizontal coordinate is transformed to plot an L-shaped trajectory in 2D.

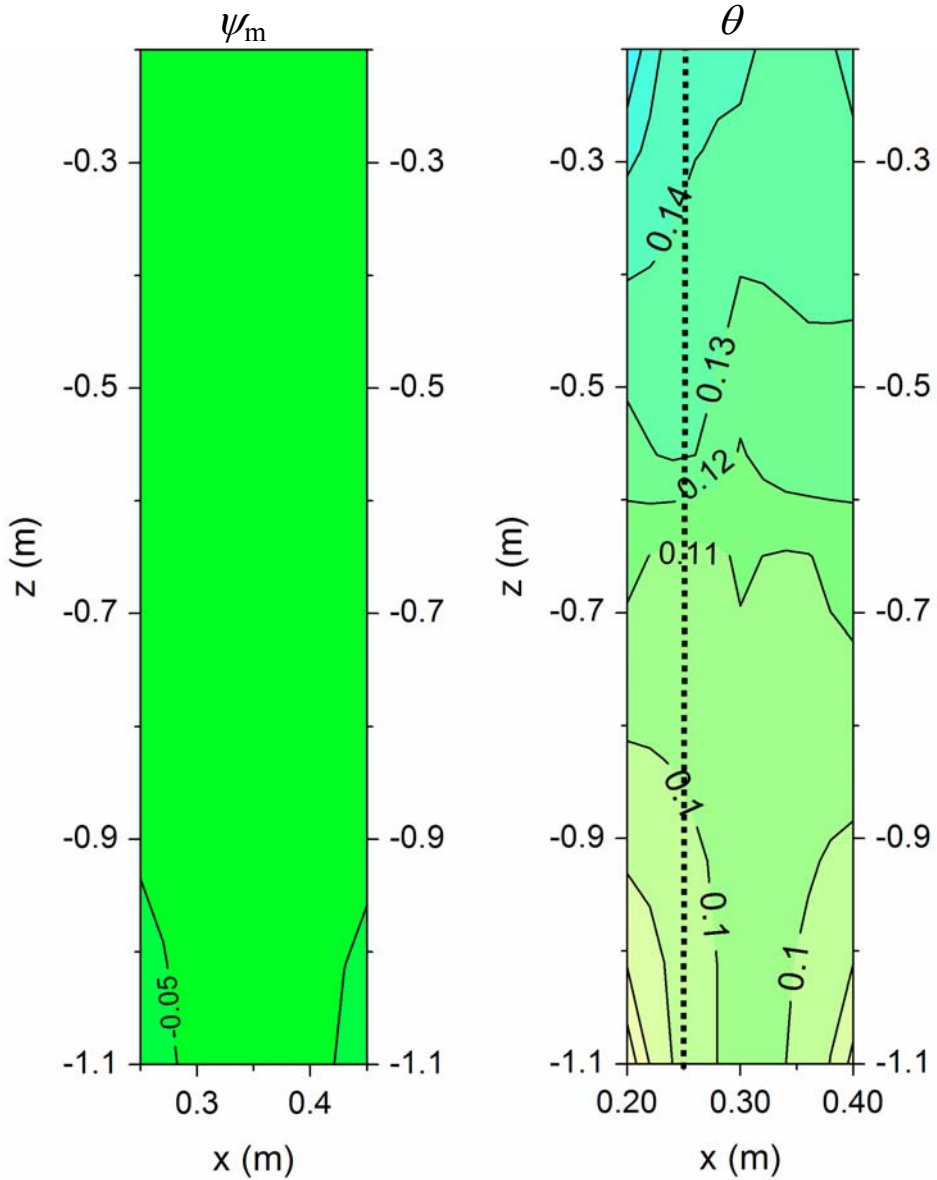


Figure 4-4C. 23 Oct 2005 No Stress.

Matric potential ( $\psi_m$ ) and volumetric moisture content ( $\theta$ ) distribution. For the  $\theta$ -distribution, the horizontal coordinate is transformed to plot an L-shaped trajectory in 2D (continued on next page).

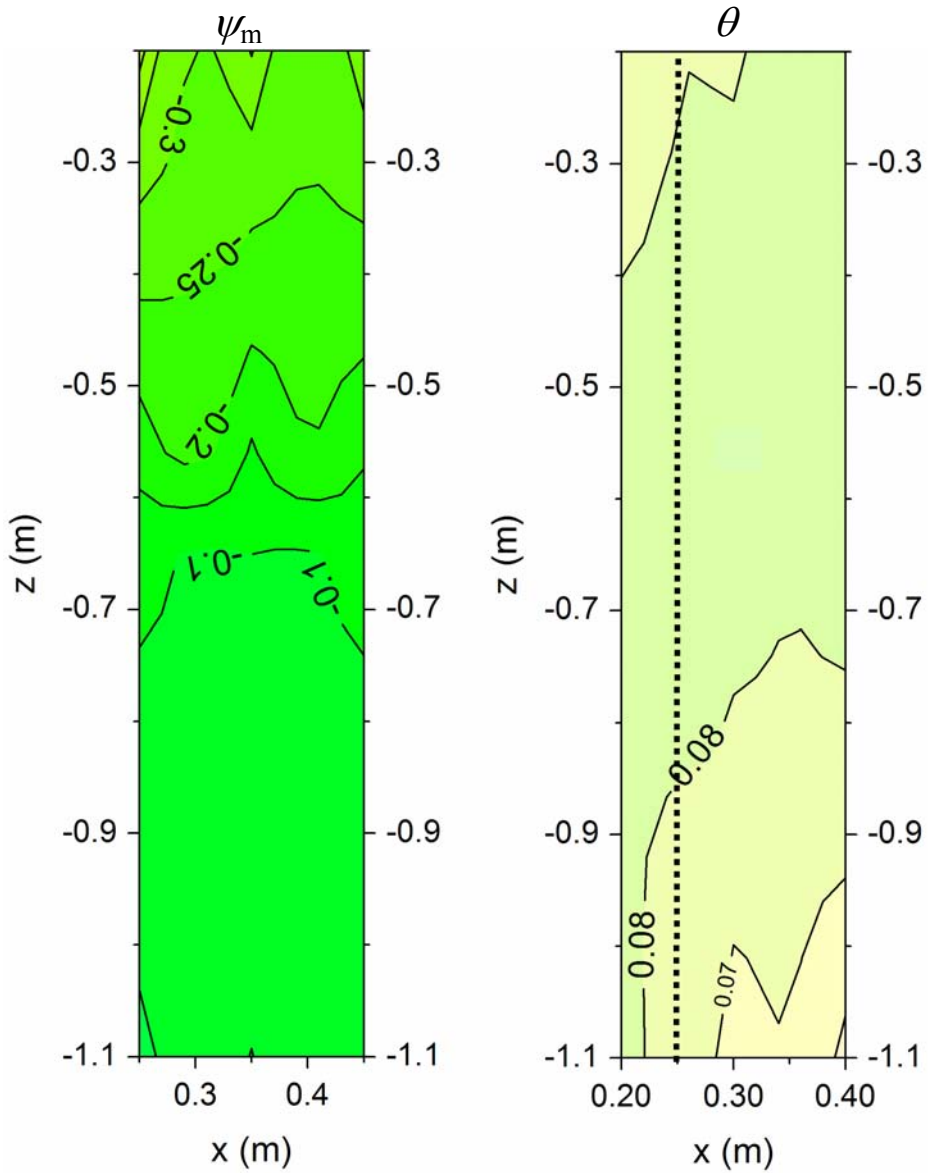


Figure 4-4C (continued from previous page) 23 Oct. 2005 Intermediate Stress. Matric potential ( $\psi_m$ ) and volumetric moisture content ( $\theta$ ) distribution. For the  $\theta$ -distribution, the horizontal coordinate is transformed to plot an L-shaped trajectory in 2D (continued on next page).



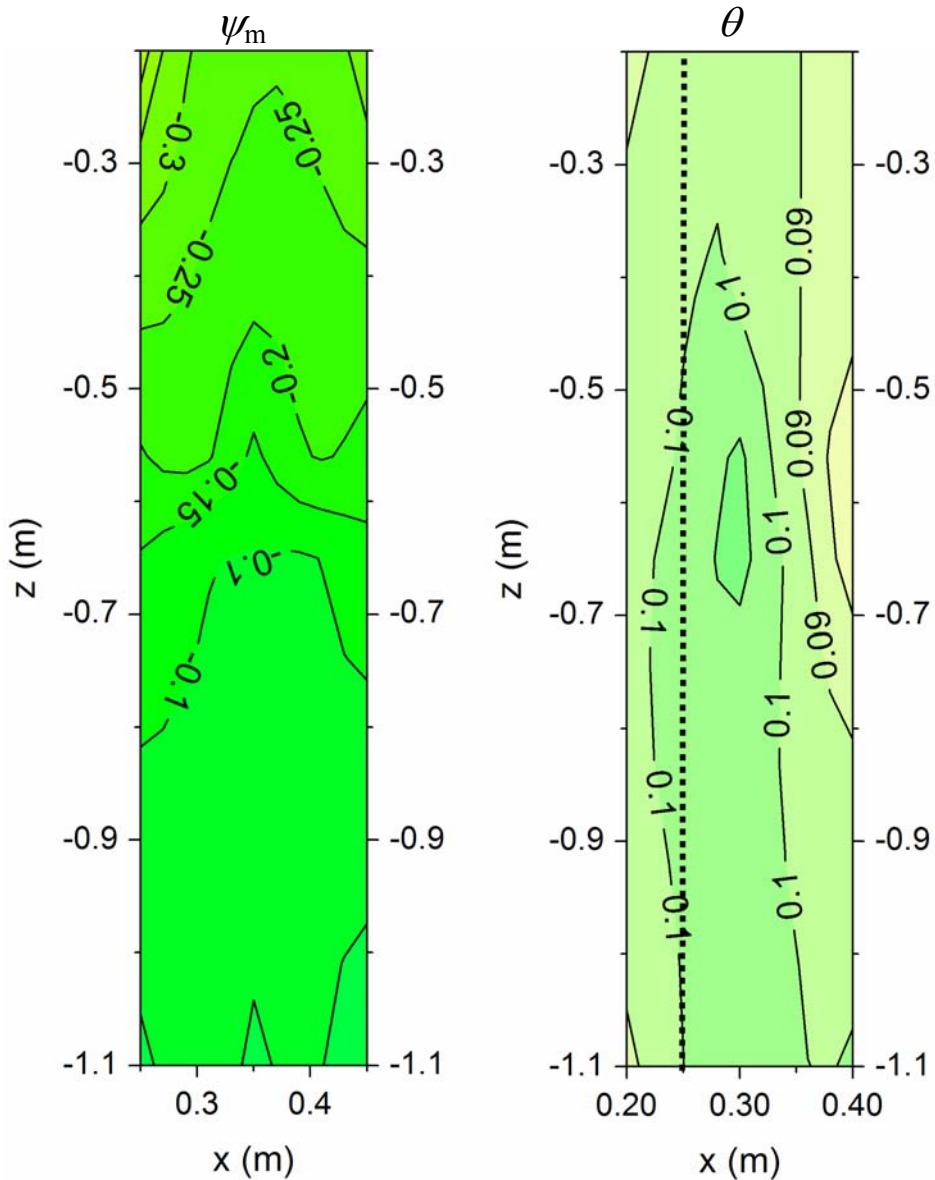


Figure 4-4C. (continued from previous page) 23 Oct. 2005 Severe Stress. Matric potential ( $\psi_m$ ) and volumetric moisture content ( $\theta$ ) distribution. For the  $\theta$ -distribution, the horizontal coordinate is transformed to plot an L-shaped trajectory in 2D.

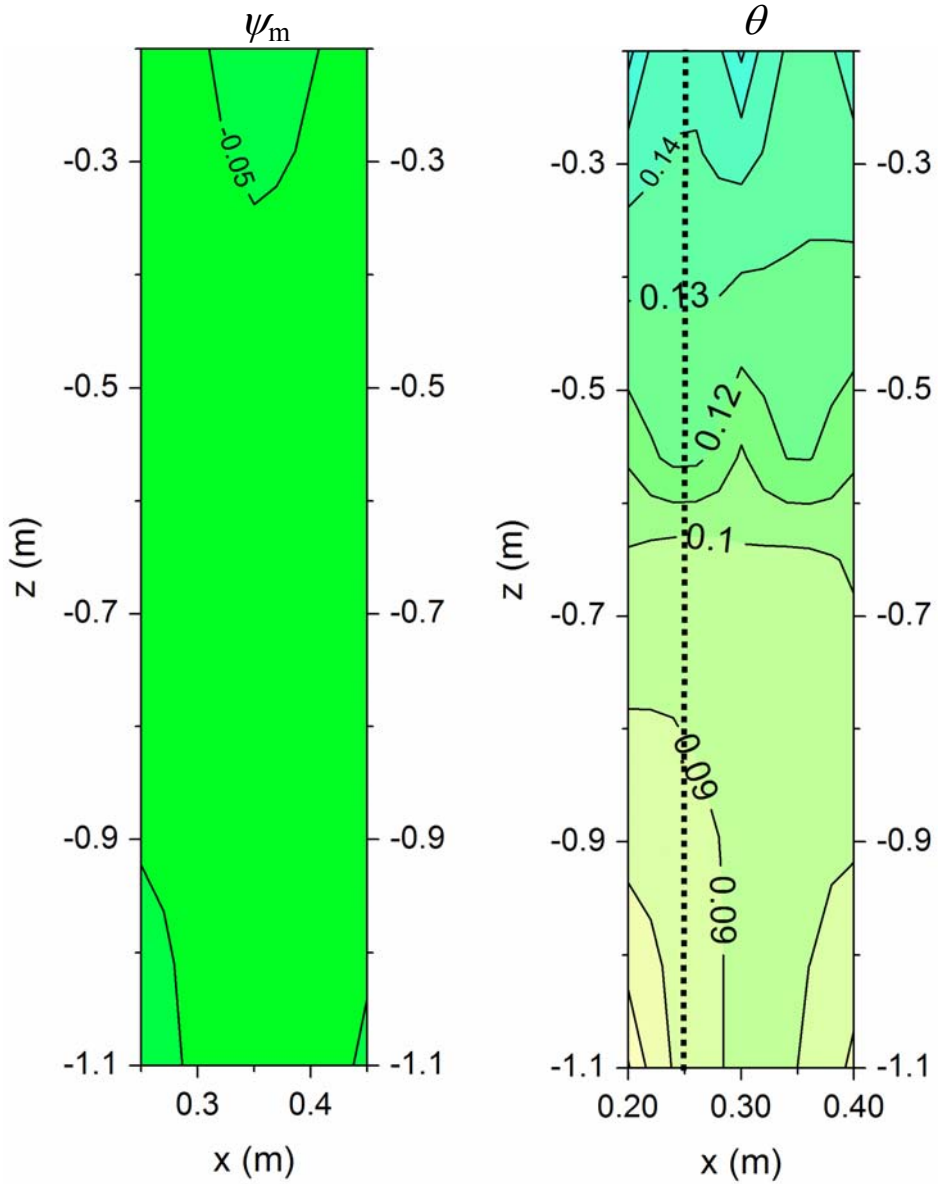


Figure 4-4D 8 Dec. 2005 No Stress.

Matric potential ( $\psi_m$ ) and volumetric moisture content ( $\theta$ ) distribution. For the  $\theta$ -distribution, the horizontal coordinate is transformed to plot an L-shaped trajectory in 2D (continued on next page).

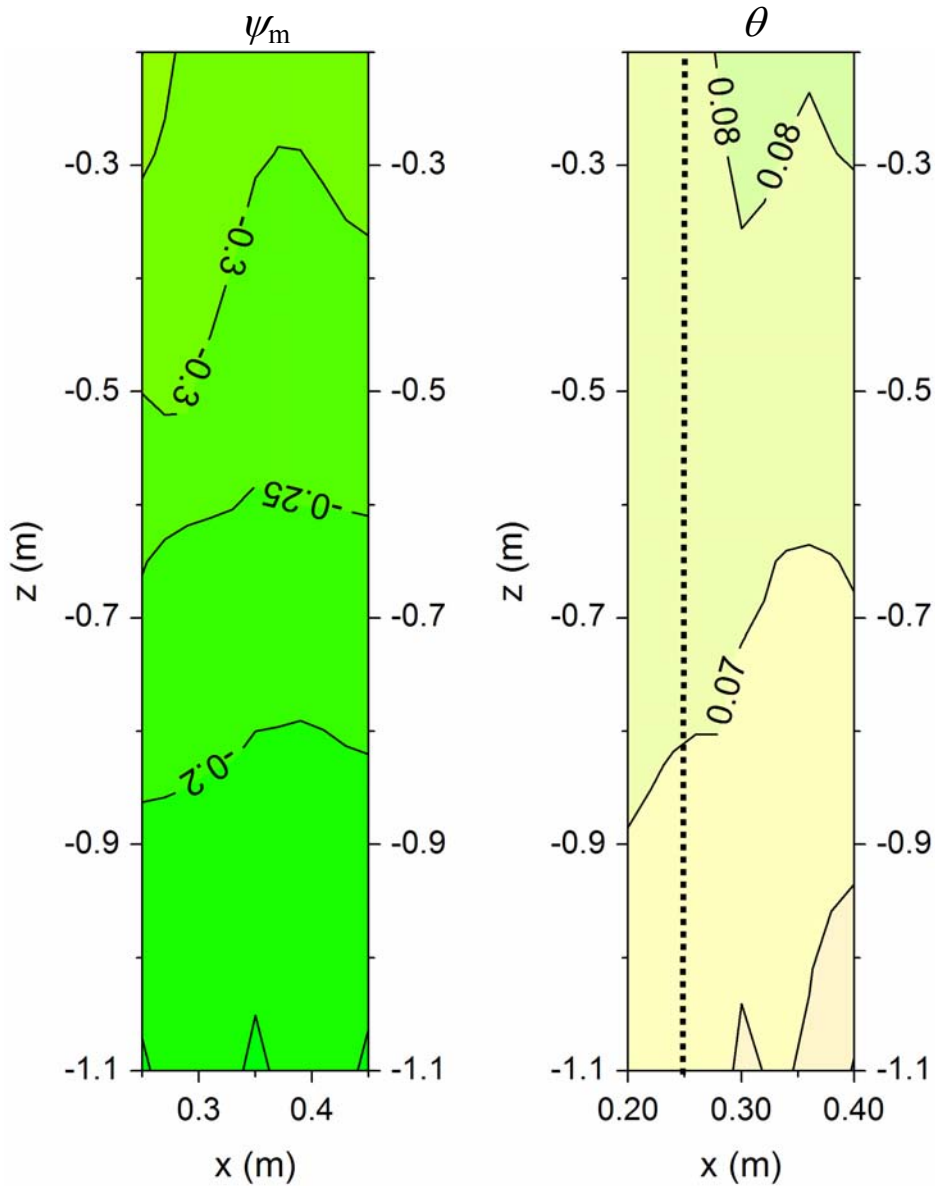


Figure 4-4D. (continued from previous page) 8 Dec 2005 Intermediate Stress. Matric potential ( $\psi_m$ ) and volumetric moisture content ( $\theta$ ) distribution. For the  $\theta$ -distribution, the horizontal coordinate is transformed to plot an L-shaped trajectory in 2D (continued on next page).



With both the intermediate stress and severe stress lysimeter firmly in the dry range,  $\theta_{\text{TDR}}$  differed much less than  $\psi_m$  (compare  $\theta_{\text{TDR}}$  and  $\psi_m$ -values in the intermediate stress and severe stress treatment in Fig. 4-4D). The limited change in moisture can be explained by the shape of the moisture retention curve (Fig. 4-5). The observed  $\psi_m$  and  $\theta_{\text{TDR}}$  data from Fig. 4-4 were paired, coupling each POT to the nearest TDR probe, which resulted in 27 moisture retention data points ( $\theta_{\text{TDR}}(\psi_m)$ ). These *in situ*  $\theta_{\text{TDR}}(\psi_m)$  data were plotted together with the gravimetrically determined data from undisturbed samples and pressure plate extractor measurements. Almost all of the *in situ*  $\theta_{\text{TDR}}(\psi_m)$  data have moisture contents below 0.2. Moreover, the two stress treatments have their target potential in the steep end of the retention curve, where the moisture content

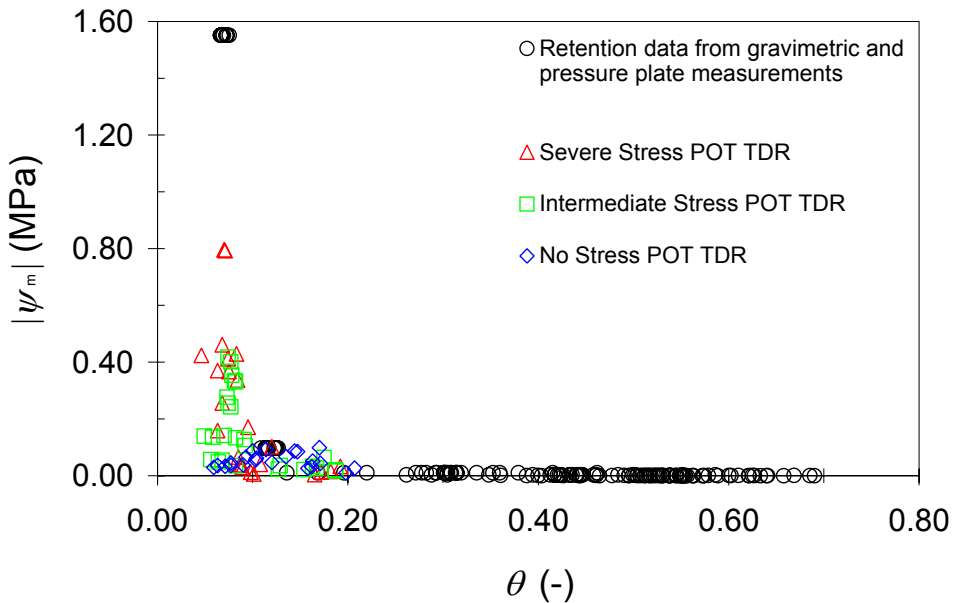


Figure 4-5. The laboratory soil moisture retention data for the loamy soil (10.9% clay, 58.2% silt 31.9% sand) used in the lysimeters, together with paired polymer tensiometer (POT) and time domain reflectometry (TDR) probe data under the no-stress, intermediate stress, and severe stress treatment. Matric potential values  $\psi_m$  (MPa) are absolute.

is below 0.1, and thus the  $\theta_{\text{TDR}}$  data can provide little information due to the limited applicability of TDR in this dry range. Apart from representing the effect of different soil moisture regimes, the combined POT and TDR measurements also reflect the hysteretic nature of the soil moisture characteristic.

The gravimetric data in Fig. 4-5 clearly show the effect of small structure differences (a result from the packing, swelling and shrinking properties of the soil and root presence) on the moisture content. In wet soils ( $\psi_m > -1.0 \times 10^{-2}$  MPa), where structure affects the moisture content, the CV of the moisture content ranges from 0.11 to 0.22 ( $N=26$ ). In contrast, in the dry end ( $\psi_m < -0.1$  MPa), the CV ranges from 0.050 to 0.045 ( $N=10$ ), reflecting the dominating effect of soil texture in dry conditions.

The patterns depicted in Fig. 4-4 suggest that the horizontal distance to the stem has only a negligible effect on the effort required to extract water from the soil. Alternatively, one could argue that the bulk of the water was lost through the soil surface (evaporation). However, the evidence of drying at depth supports a significant role of the roots in removing water from the soil. Overall, the contour plots suggest a fairly uniform drying process laterally, with the non-uniformity mainly stemming from the spatial variation in initial wetting and soil properties. More importantly, Fig. 4-4 clearly shows that in the water-stressed cases after October 23, 2005 (intermediate stress and severe stress treatment) the  $\psi_m$ -gradient between 0.4 and 0.6 m depth is larger than the gradient between 0.2 and 0.4 m depth, and that  $\psi_m$  is larger (less negative) at depth. The upward Darcian flux density is therefore larger between 0.4 and 0.6 m depth than at 0.2 and 0.4 m depth, thus indicating water must have been removed between those depths. This is only possible by root water uptake. As the plants matured and the soil dried, water extraction progressed to larger depths, until, in the end, water at all depths could be potentially targeted by the roots.

Rhizotube observations showed root growth throughout the profile of all lysimeters. The  $\psi_m$  and  $\theta_{\text{TDR}}$  profiles varied greatly at the end of the experiment (see also Table 4-1 for water storage differences at the end of the experiment). The  $L_{r,z}$  that was determined from soil sampling did not show large variations (Fig. 4-6), with intermediate stress about  $6 \text{ cm cm}^{-2}$  less than the nearly similar values of no stress ( $97.4 \text{ cm cm}^{-2}$  at  $-1.4 \text{ m}$ ) and severe stress ( $103.6 \text{ cm cm}^{-2}$  at  $-1.5 \text{ m}$ ).

Limiting  $\psi_m$  values were reached some time after ceasing irrigation, thereby suggesting a reason for the similarities in  $L_{r,z}$  irrespective of treatment. Stress levels however, gradually increased during the experiment, and were reached well before the end of the growth cycle. Moreover, comparing treatments, the differences in  $L_{r,z}$  are more pronounced between the intermediate stress and the other treatments, although the stress levels of the intermediate stress and severe stress treatment were comparable during the first month after ceasing irrigation.

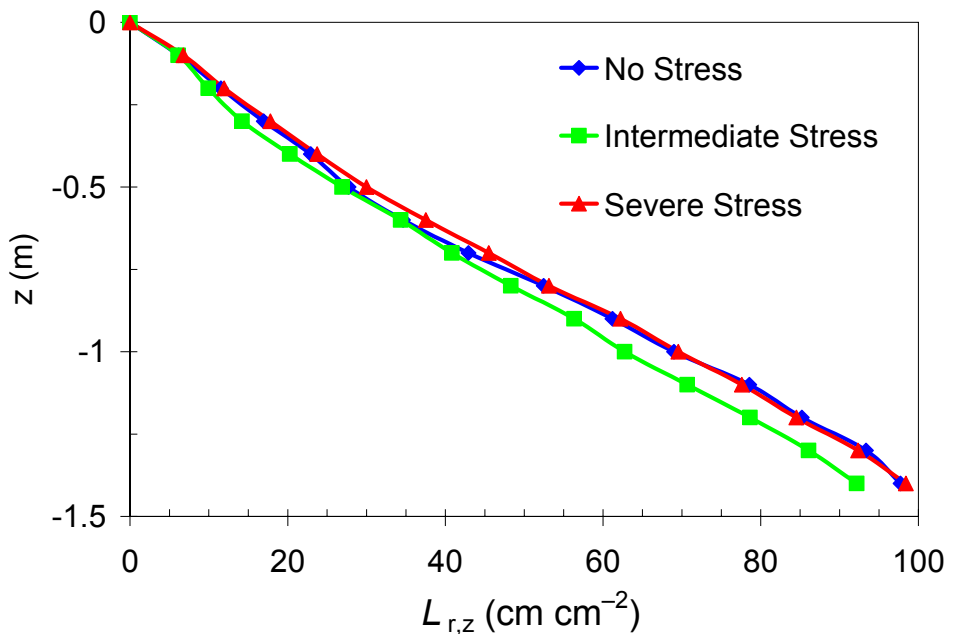


Figure 4-6. Cumulative Root length density ( $L_{r,z}$ ) of the lysimeters under the no-stress, intermediate stress and severe stress treatments.  $L_{r,z}$  is the length of root under a unit area of soil surface to a specified depth.

Coelho and Or (1999) suggest the measured  $L_r$  to be a measure of potential water uptake areas, as was observed in kiwifruit by Green and Clothier (1995). This seems to imply a limited effect of actual water stress on the root distribution and density. The root system may adapt to the soil water regime by developing fine roots and root hairs (which cannot be measured in  $L_r$  determinations) at preferred locations or depths to locally increase the water uptake efficiency. Increased root

water uptake efficiency of deep roots in combination with the capacity of maize to slowly grow roots in dry soil (Sharp and Davies 1985) may have contributed to the observed similarities in  $L_{r,z}$ .

## 4.5 Conclusions

This study evaluated the performance of POTs in cropped soil, and explored the potential for using POTs in lysimeters under varying levels of water stress. The POTs successfully monitored the soil water matric potentials of the two water stressed treatments, thus providing a means to better define levels of local water stress. The moisture retention curve showed that volumetric moisture contents for this particular loam soil were below 0.1 when water stress reached the defined stress levels. For these low moisture contents, TDR measurements may be of little use. Cumulative RLD data showed an inconclusive effect of the water stress levels; increased water uptake efficiency from deep roots in combination with slow but continuing root growth in drier soil may explain the observed similarities.

We conclude from the soil matric potential profiles given in Fig. 4-4 that under water-stressed conditions after October 23, 2005, root water uptake occurred between 0.3 and 0.5 m depth. The maize plants were able to extract water under very dry conditions, and continued to extract water from those dry regions. Such observations indicate that POTs have the potential to improve experimental analysis of root water uptake in dry soils, and thus they may help unraveling plant root water uptake strategies under various levels of water stress.

This knowledge can improve the representation of the root zone in unsaturated models, and ultimately be used to optimize irrigation regimes. Other potential applications lie in rain fed agriculture with generally much drier soils, and in range lands or other non-irrigated ecosystems.



## Chapter 5

---

# Water uptake strategies by maize plants under varying levels of water stress

---

This chapter is a modified version of the manuscript: Van der Ploeg, M.J., H.P.A. Gooren, G. Bakker and G.H. de Rooij. 2008. Water uptake strategies by maize plants under varying levels of water stress.

## 5.1 Introduction

Plants may experience water stress during several periods of their life cycle even outside the arid/semi-arid regions (Wilson et al. 2001, Grace 1999, Chaves et al. 2002). Plant responses to water scarcity are complex, and usually involve stress avoidance and tolerance strategies (Blackman and Davies 1985, Gollan et al. 1986, Mansfield and De Silva 1994). When soil water availability falls below a certain level, root water potentials can reach such low values that this triggers the synthesis of several plant growth regulators (plant hormones) including abscisic acid (Wright 1977, Bacon 2004). Abscisic acid can be associated with water use efficiency by plants (it was recently noticed that water use efficiency may correlate with lower yields, despite several breeding programs that focus on water use efficiency) (Bacon 2004).

Water stress inhibits the growth of shoots more than roots, and in drying soils roots respond by enhanced geotropism (Sharp and Davies 1985, Sharp and Davies, 1989). Several studies note the absence of a relation between root distribution and root water uptake patterns (Green and Clothier 1995, Coelho and Or 1999, Garrigues et al. 2006, Hainsworth and Aylmore 1989, Hamblin and Tennant 1987, Adiku et al. 2001) possibly because methods to quantify roots may not include the smallest fraction of roots (root hairs, which take up most of the water), the high turn-over rate of root hairs, and often roots are only measured at the end of the experiment. On the other hand, limited water availability may have a distinct influence on the root distribution (e.g. Box et al. 1989).

Modeling approaches to verify root water uptake processes complement experimental studies. Root water uptake has classically been modeled according to (i) the micro/mesoscopic approach (Gardner, 1960), which emphasizes the role of soil for the water transfer towards a single root, and (ii) the macroscopic approach (Molz, 1981), in which local details are neglected and uptake is represented by a more or less empirical sink term through which potential transpiration is distributed over the root zone. Recently, the need to describe root water and nutrient uptake with more spatial detail within the root zone has been recognized,

and this has led to models based on the architectural description of the root system (Doussan et al. 1998, Dunbabin et al. 2002, Pagès 2004, Garrigues et al. 2006).

To parameterize and validate such models for root water uptake processes, experimental devices are needed that provide information at compatible modeling scales (i.e. from the single root to root system scale). Observation of water uptake by roots is technically challenging. Methods include the combination of root hydraulic conductivity and root water potential measurements simultaneously (Zwieniecki and Boersma 1997), pressure chambers or pressure probes to measure xylem pressures (e.g. Donovan et al. 2001, Zimmerman et al. 2004, Brooks et al. 2004), nuclear magnetic resonance imaging (Scheenen et al. 2000), use of radioactive tracers (Polomski and Kuhn 2002), porometers to measure leaf transpiration, and heat pulse techniques to measure sap flow (Swanson 1975, Green et al. 2006).

Alternatively, root water uptake can be approached by measuring the soil water status (See also Chapter 1). This approach targets the effect of root water uptake on the soil solution phase. The difference between the root water potential and the soil water potential is a driving force for root water uptake. Consequently, a direct indication of the amount of energy required by plants to take up water can be obtained by measuring the soil water potential in the vicinity of roots. An hypothesis encountered in literature (Dirksen et al. 1994, Adiku et al. 2000) is that plants are able to distribute the water uptake over the root network to minimize the expenditure of energy at any given moment. Up to now a critical evaluation of this hypothesis is difficult due to instrument limitations.

Measurement of the soil water potential in moderately dry to dry soils was not possible until the development of a polymer tensiometer (POT) (Bakker et al. 2007 (Chapter 2), Van der Ploeg et al. 2008 (Chapter 4)). POTs can potentially measure soil matric potentials ( $\psi_m$ ) down to  $-1.6$  MPa, which is an almost 20-fold measurement range increase compared to previously existing tensiometers (Young and Sisson 2002). POTs are thus especially useful in dry soil, where other measurement devices, like frequently used soil moisture sensors, may become less sensitive (Van der Ploeg et al. 2008 (Chapter 4)).

A sufficient number of POT prototypes recently became available to carry out systematic experiments. We established different levels of water stress in three cropped lysimeters and deployed multiple POTs strategically placed in the root zone of individual plants. We investigated the dynamics of  $\psi_m$  and the spatial distribution of roots in each of them. This Chapter presents an exploratory analysis as a first step in unraveling plant root water uptake strategies in dry soil.

## 5.2 Experimental setup

We constructed three lysimeters of 0.70 m length by 0.50 m width and a height of 1.70 m (Fig. 4-1 in Chapter 4). The lysimeters were filled with a prewetted loamy soil (10.9% clay, 58.2% silt, 31.9% sand). We installed three instrumental layers at 0.2, 0.6, and 1.1 m depth during filling. Each contained three POTs (see Chapter 3); measurement range 0 to  $< -1.6$  MPa, accuracy  $2.38 \times 10^{-3}$  MPa). The POTs were calibrated for long-term pressure decay and temperature influence according to Bakker et al. (2007) (Chapter 2). Because root profiles of maize may be greatly altered by temporary drought stress (Box et al. 1989), we monitored root growth during the experiment by installing horizontal acrylic rhizotubes with a diameter of 2.5 cm every 0.1 m depth, except at 0.5 and 1.0 m due to the construction of the boxes. The acrylic material itself does not have an effect on root growth (Brown and Upchurch 1987, Johnson et al. 2001). Root movies were captured at four dates using a cold-light boroscope with a diameter of 6.35 mm (Heine Optotechnik GmbH) and a digital camera (Nikon Coolpix 4500). The boroscope looked upward, viewing a circular area of  $1 \text{ cm}^2$  of rhizotube surface. The final images were  $320 \times 240$  pixels. During the experiment, root presence was detected by visual inspection of the images. The image quality did not allow automated analysis, but visual analysis did not pose any problems. We chose to make root counts, because this parameter is less influenced by the conditions at the interface than root length and is independent of any property of the root after the root has touched the rhizotube (Smit et al. 2000). Root counts were made of slightly overlapping captured areas of slightly less than  $1 \text{ cm}^2$ . When

a root appeared on two overlapping images, it was only counted when it covered the area for more than the radius of the captured image. Substantial preferential root growth may be a problem (Ephrath et al. 1999), but was observed at the surface of only one rhizotube.

The lysimeters were insulated by a layer of 0.1 m polystyrene (on the sides of the lysimeter) to reduce temperature influence on root growth (McMichael and Burke 1996). The lysimeters were uniformly irrigated by emptying syringes with equal amounts of water in each of the cells of a metal grid firmly placed on the soil surface. Because nutrient analysis indicated that the soil contained enough nutrients for plant growth during the experiment, non-chlorinated tap water was used for irrigation instead of nutrient solution. Each lysimeter had an artificial growing light, and reflective material to enhance plant growth in the lysimeter. The reflective material restricted light interference from the other lysimeters, ensuring each lysimeter received an equal amount of light. Prior to sowing, the soil in the lysimeters was left to consolidate for a month, and irrigated to maintain realistic moisture profiles.

The lysimeters were subjected to three irrigation schemes to establish different levels of water stress. Plant water stress increases with decreasing  $\psi_m$ , and may eventually reach a level where root water uptake is no longer possible. For agricultural crops this level is usually taken at  $-1.6$  MPa (Koorevaar et al., 1983). However, values of  $\psi_m$  at which different crops begin to be affected by water stress is less well known, yet this is highly relevant for root water uptake behavior.

Taylor and Ashcroft (1972) provided data of  $\psi_m$  (including data for maize) at which ‘water should be applied for maximum yields of various crops grown in deep, well-drained soil that is fertilized and otherwise managed for maximum production’. Kroes and van Dam (2003) use these  $\psi_m$ -values in combination with the water stress reduction function of Feddes et al. (1978) to model water stress. Based on the Feddes reduction function and the data of Taylor and Ashcroft (1972) we defined three treatments; no stress (minimum  $\psi_m = -0.15$  MPa), intermediate stress (minimum  $\psi_m = -0.45$  MPa) and severe stress (minimum  $\psi_m = -0.80$  MPa);

with minimum  $\psi_m$  being the most negative matric potential (measured by any of the POTs) that was allowed during the specific treatments.

On September 5th, 2005 maize (*Zea Mays*, *L.*) was sown in every lysimeter (see Fig. 4-1) at the horizontal coordinates  $(x, y) = (0.25 \text{ m}, 0.117 \text{ m}), (0.25 \text{ m}, 0.35 \text{ m}), (0.25 \text{ m}, 0.583 \text{ m})$ , (with  $(0, 0)$  denoting the back-left corner;  $x$  running from back to front,  $y$  from left to right) to ensure equal volumes of soil were available for each maize plant. The plants were optimally irrigated during the initial growth stage of approximately 20 days (Allen et al. 1998). After 25 days we terminated irrigation on two lysimeters, until the prescribed water stress level was attained at one of the shallow POTs. Minimum  $\psi_m$  was reached on October 24, 2005 for the intermediate stress, and on December 2, 2005 for the severe stress treatment. The stress level was subsequently maintained by small, frequent irrigations. The no stress lysimeter was irrigated throughout the experiment to maintain its target minimum  $\psi_m$ .

The experiment lasted four months until all plants completed their growth cycle. At this point, undisturbed soil samples (98 cm<sup>3</sup> sample rings) were taken to determine soil hydraulic properties using the soil core method (Blake and Hartge 1986), see Chapter 4 for details. Unsaturated conductivities  $K_s(\psi_m)$  were determined on nine undisturbed samples of 667 cm<sup>3</sup> by the Wind method (Arya 2002) and the conductivity model of Mualem-Van Genuchten (Mualem 1976, Van Genuchten 1980). Root length density samples were obtained using an auger with plunger and a sample volume of 385 cm<sup>3</sup> (e.g. Oliveira et al. 2000). The samples were hand washed according to Oliveira et al. (2000) to remove the soil, stored in a 10% ethanol solution for a maximum of three weeks, spread out on a transparent rectangular scanning tray, scanned at 400 dpi, and analyzed with the computer program WinRHIZO (Himmelbauer et al. 2004). We determined the root length density ( $L_r$  (cm cm<sup>-3</sup>)), which is the length of root present in a unit volume of soil (Atkinson 2000).

## 5.3 Root water uptake strategies

### 5.3.1 Matric potential measurements by polymer tensiometers

Figure 5-1 shows the development of the  $\psi_m$  in time of the three lysimeters.

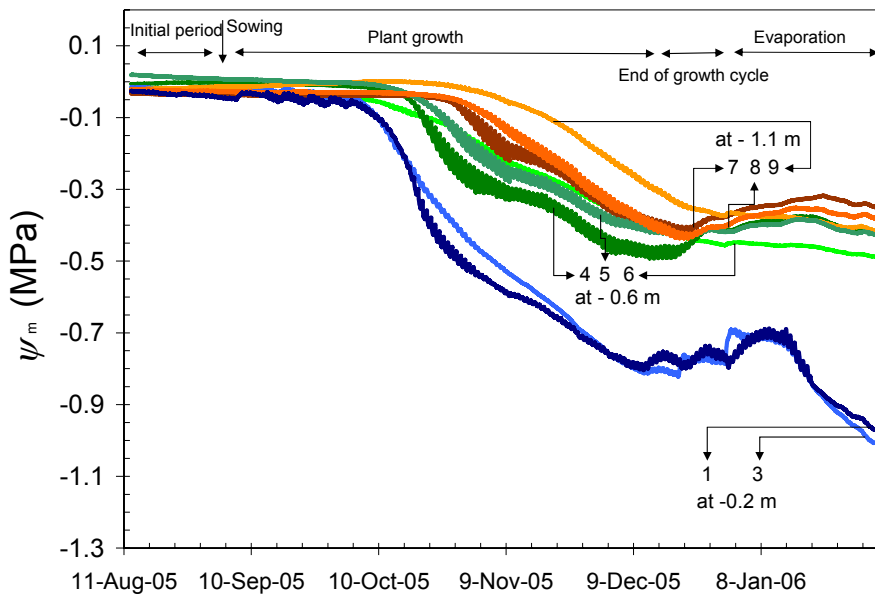


Figure 5-1A. Development of the matric potential  $\psi_m$  in time as measured by polymer tensiometers (POTs) in the lysimeter cropped with maize (*Zea Mays, L.*) subject to severe water stress. For placement of the POTs see Fig. 4-1 in Chapter 4. POT 2 was omitted as the pressure drop during the experiment was unacceptably large. (continued on next page)

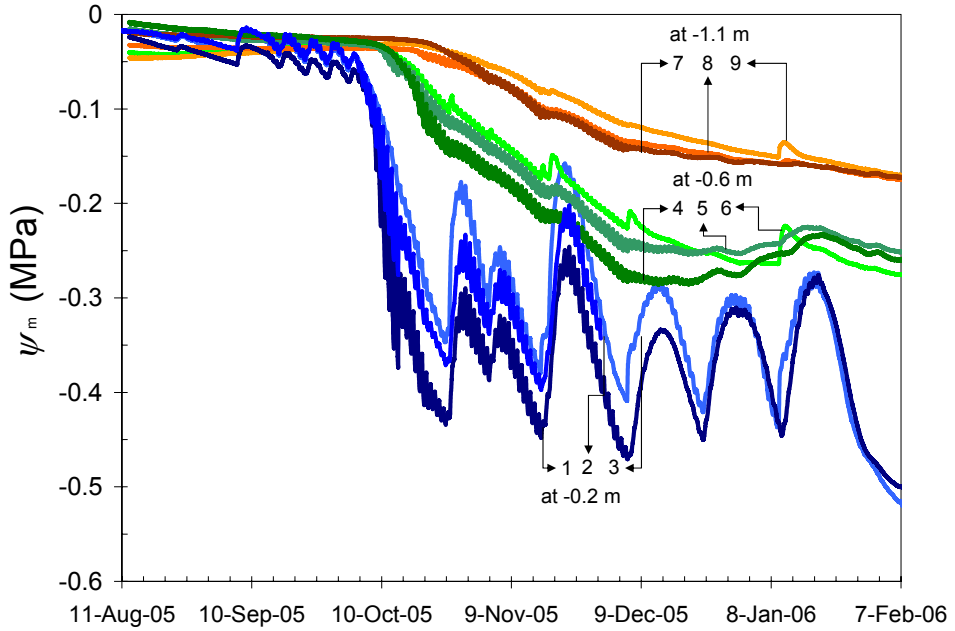


Figure 5-1B. (continued from previous page) Development of the matric potential  $\psi_m$  in time as measured by polymer tensiometers (POTs) in the lysimeter cropped with maize (*Zea Mays, L.*) subject to intermediate water stress. POT 2 series is incomplete due to a broken pressure transducer. For placement of the POTs see Fig. 4-1 in Chapter 4 (continued on next page).



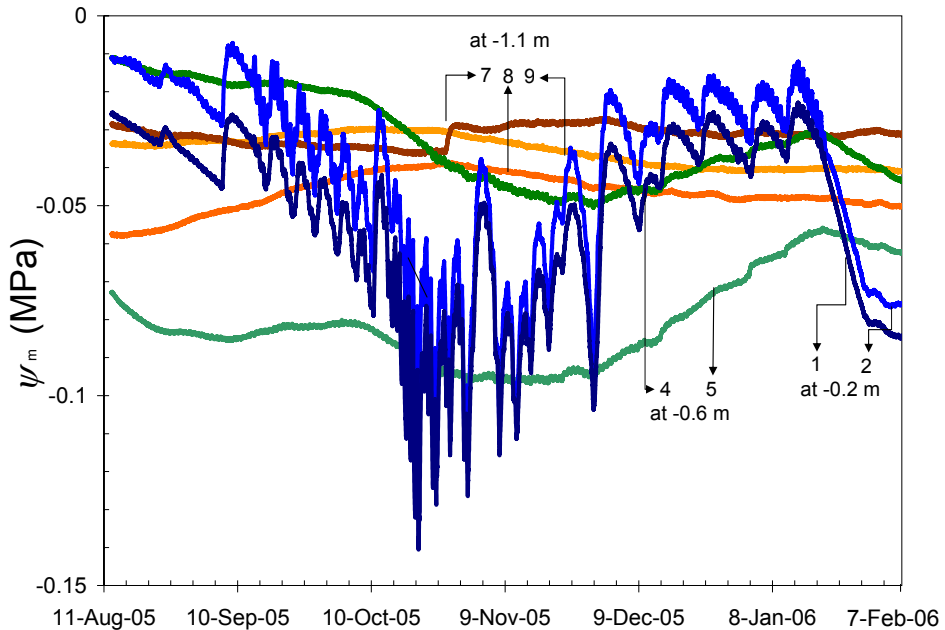


Figure 5-1C. (continued from previous page) Development of the matric potential  $\psi_m$  in time as measured by polymer tensiometers (POTs) in the lysimeter cropped with maize (*Zea Mays, L.*) subject to no water stress. POT 3 was omitted as the temperature gradient before and after the lysimeter experiment changed  $0.002 \text{ MPa}^\circ\text{C}^{-1}$ . The pressure transducer of POT 6 failed from Sep. 12, and is not further shown. For placement of the POTs see Fig. 4-1 in Chapter 4.

Figure 5-1A shows the initial period (terminated when the plants were sowed), the plant growth stage that gradually transgressed into the final phase of the growth cycle during which the plants died, and the evaporation phase towards the end of the experiment. These phases were discernible in all treatments, and had approximately equal lengths. The distribution of root water uptake was greatly affected by the water stress level. In the severe and intermediate stress treatment (Figs. 5-1A and 5-1B) the maize plants continued to take up water throughout the plant growth stage, even under very dry conditions.

The moisture retention relation of the lysimeter soil (see Fig. 4-5 in Chapter 4) shows that  $d\theta/d\psi_m$  drops dramatically when  $\psi_m$  falls below  $\sim -0.1$  MPa. In the severe stress treatment, values below  $-0.1$  MPa were reached at  $-0.2$  m on October 10, 2005 (Fig. 5-1A). From that time,  $\psi_m$  at  $-0.6$  m started to reduce and the diurnal cycle in  $\psi_m$  became more pronounced. Around October 21, 2005,  $\psi_m$  at  $-0.6$  m reached below  $-0.1$  MPa, and root water uptake began to affect the readings at  $-1.1$  m, as evidenced by the rapid reduction in  $\psi_m$  and the onset of diurnal cycles. At all depths,  $\psi_m$  continued to reduce but particularly the water uptake at  $-0.2$  m was probably quite limited. Possibly, the root system at  $-0.2$  m became less active: at the times the diurnal cycle became more pronounced at larger depths, its amplitude reduced at  $-0.2$  m. In the intermediate stress treatment a similar transition over depth of reduction in  $\psi_m$ , and changes in the diurnal cycle at different depths can be observed. Both treatments show that root water uptake moved downward nearly instantaneously when the steep dry end of the moisture retention curve was reached at a particular depth.

In the severe stress treatment, vertical gradients would have supported upward flow. The unsaturated conductivity  $K_s(\psi_m)$  however, is so low (See Table 5-1) that the resulting flux was insufficient to replenish the water that was extracted by roots. The vertical gradients persisted between  $-0.2$  and  $-0.6$  m during the evaporation stage, when the plants had died and root water uptake was zero. The observed wetting in December 2005 and January 2006 (even at larger depths) was therefore against the upward flow direction, and can only be explained by preferential flow resulting from irrigation events, possibly along the roots present in the profile, or along paths previously occupied by roots. In the evaporation stage, the top soil dried out further while  $\psi_m$  at  $-0.6$  and  $-1.1$  m dropped only slightly, indicating the low flux density over the vertical profile as a result of the low  $K_s(\psi_m)$ .

In the intermediate stress treatment (Fig. 5-1B), the POT readings at  $0.2$  m depth are strongly affected by irrigations. The vertical gradients indicated an upward flow direction, except for the period around November 9, 2005. At that time, POT readings at  $0.2$  m depth show a higher  $\psi_m$  than the POT readings at lower depths. The resulting gradient would therefore indicate downward flow at

that time, although the actual flux density would probably have been small as a result of the  $K_s(\psi_m)$  relation. At  $-0.6$  m, POT 6 (and on two occasions POT 9 at  $-1.1$  m) exhibited a spike in the readings shortly after irrigation events, which suggests the existence of a local preferential flow path (similarly as in the no stress treatment).

Table 5-1. Unsaturated conductivity values ( $K_s(\psi_m)$ ) at  $-0.01$  and  $-0.1$  MPa determined on nine samples with the Wind method (Arya, 2002) and the conductivity model of Mualem-Van Genuchten (Mualem 1976, Van Genuchten 1980).  $K_s(\psi) = \rho_w^{-1} g^{-1} K_s(h)$

$K_s(\psi)$ at $\psi = -0.01$ MPa ( $\text{m}^2 \text{Pa}^{-1} \text{d}^{-1}$ )	$K_s(\psi)$ at $\psi = -0.1$ MPa ( $\text{m}^2 \text{Pa}^{-1} \text{d}^{-1}$ )
$8.5 \times 10^{-8}$	$2.0 \times 10^{-10}$
$2.2 \times 10^{-7}$	$5.2 \times 10^{-11}$
$4.0 \times 10^{-8}$	$1.3 \times 10^{-12}$
$1.2 \times 10^{-7}$	$1.7 \times 10^{-10}$
$9.1 \times 10^{-8}$	$1.8 \times 10^{-10}$
$1.2 \times 10^{-7}$	$4.6 \times 10^{-12}$
$1.9 \times 10^{-9}$	$3.4 \times 10^{-13}$
$6.5 \times 10^{-9}$	$3.8 \times 10^{-13}$
$1.0 \times 10^{-9}$	$2.4 \times 10^{-16}$

In the no stress treatment (Fig. 5-1C),  $\psi_m$  at  $-0.2$  m was dominated by the frequent irrigations. At  $-0.6$  m POT 4 and 5 followed the overall trend at  $-0.2$  m without the oscillations. The POT readings at  $1.1$  m depth varied little over time. Episodes of downward and upward flow conditions occurred in the top of the profile. The diurnal cycles were virtually absent below  $-0.2$  m. The observed  $\psi_m$  at  $0.6$  and  $1.1$  m depth seem to be a result of  $\psi_m$ -gradients, which are larger at the beginning than at the end. The dryness of the soil, even in the non stressed

treatment, results in low unsaturated conductivity ( $K_s(\psi_m)$ ) values (see Table 5-1). Consequently the flux as a result of the occurring  $\psi_m$ -gradient will be small.

In summary, root water uptake was significant at all depths in the severe and intermediate stress treatment. The uptake at larger depths was triggered when the reduction of  $\psi_m$  no longer yielded substantial amount of extractable soil water. This is contrary to the minimum energy hypothesis that was formulated for non-stressed plants (Dirksen et al. 1994, Adiku et al. 2000). In this hypothesis the root water uptake is controlled by the unsaturated conductivity and the sum of the matric and gravitational potential. This spatial change in root water uptake seems to be related with the shape of the moisture retention curve, and occurs well before the wilting point ( $\sim -1.6$  MPa).

The diurnal cycles merit further attention. Such cycles have been observed in the soil, as well as in the leaf water potential for several species (Ameglio et al. 1990, Caldwell et al. 1998, Dawson 1993, Vetterlein et al. 1993). The cycles observed by us were triggered by growing lamps instead of sunlight (Fig. 5-2).

The discontinuities in their derivatives correspond exactly to the switch-on and switch-off times of the lamps (Fig. 5-2A), irrespective of the depth or the water stress level. The amplitude of the cycle depends both on depth and water stress level in a manner consistent with the overall water uptake distribution as qualitatively derived above from  $\psi_m$  observations in Fig. 5-1.

The five-day period in Fig. 5-2 represents the time at which the top soil in the severe-stress treatment was so dry that more water could be taken up at  $-0.6$  m. As  $\psi_m$  at  $-0.6$  m becomes smaller than  $-0.2$  MPa, water uptake at transitioned towards  $-1.1$  m. In Fig. 5-2A this is reflected by the large amplitudes at  $-0.6$  m and the near flat line at  $-1.1$  m, with some evidence of enhanced activity at that depth starting at October 28, 2005. Fig. 5-2B (intermediate stress) clearly shows that the irrigation on October 25, 2005 was only registered at  $-0.2$  m (no preferential flow at this time). In the no-stress treatment (Fig. 5-2C) influence of root water uptake cannot be discerned below  $-0.6$  m.

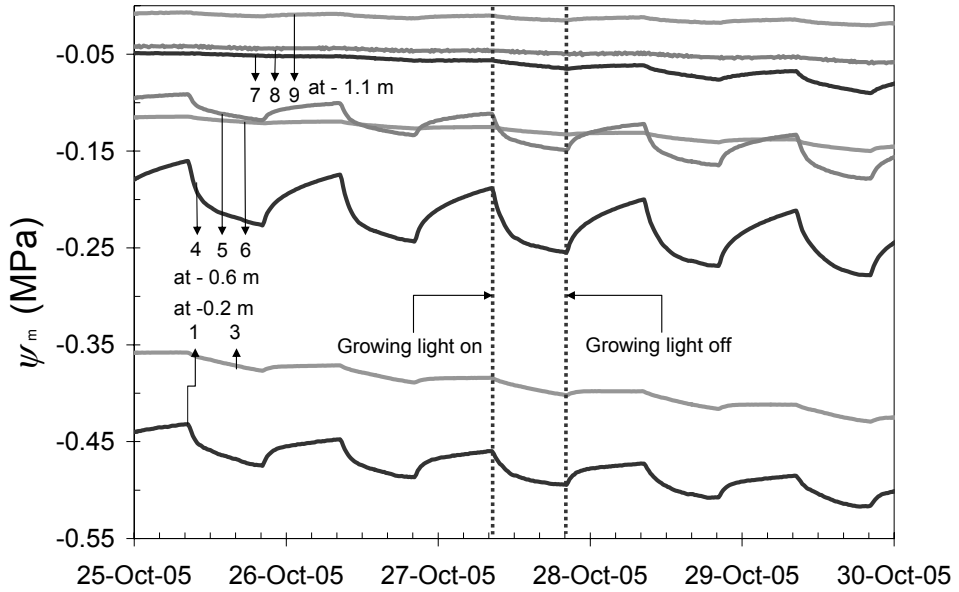


Figure 5.2A. Severe stress; as Fig.5-1, but for a selected period to highlight the diurnal cycle of the matric potential (continued on next page).

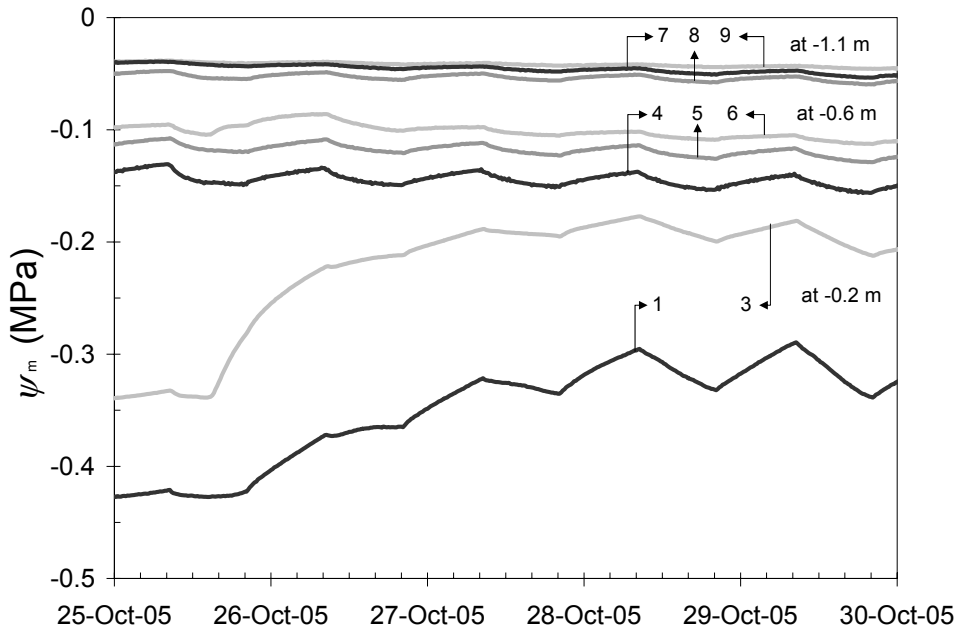


Figure 5.2B. (continued from previous page) Intermediate stress (continued on next page).

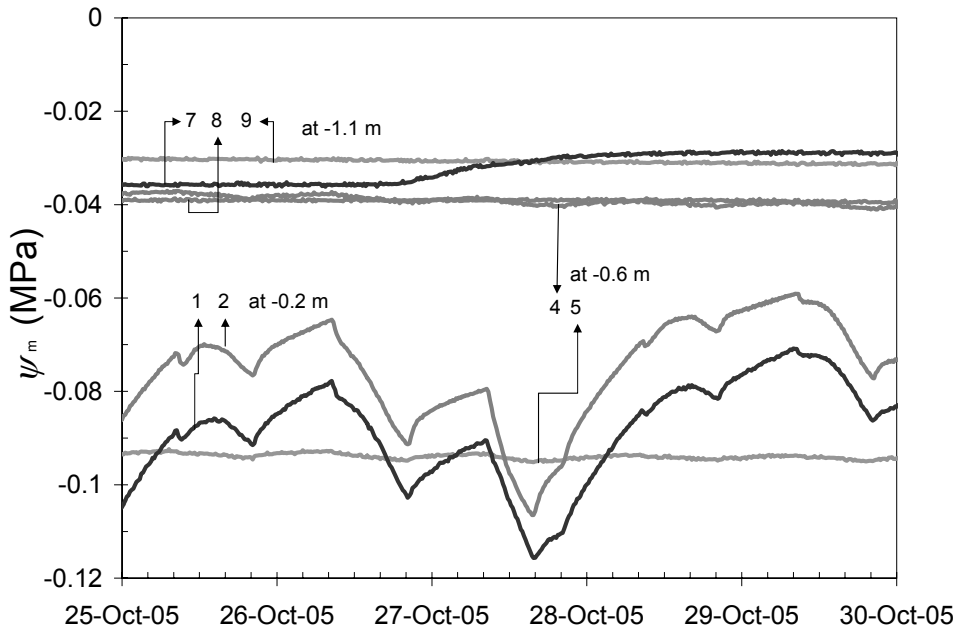


Figure 5.2B. (continued from previous page) No stress.

The declining phase of the diurnal cycle in the severe-stress treatment started with a rapid drop followed by a more gradual descent (Fig. 5-2A), probably reflecting the succession of the stomatal phase by the cuticular phase. Under less-stressed conditions the cuticular phase appears to be lacking, thus indicating the stomata have not closed completely (Figs. 5-2B and 5-2C).

In the stressed lysimeters, the POTs labeled 3 (-0.2 m), 6 (-0.6 m) and 9 (-1.1 m) generally show less diurnal variation and have smoother trends than the other POTs. These POTs were located farthest from the lysimeter centre, where less roots may have grown compared to the other POT locations. An exception is POT 9 in the severe stress treatment, where the maize plants probably invested in root growth due to the extremely low  $\psi_m$  in the upper profile.

The nightly rise in  $\psi_m$  appears to be relatively fast compared to the wetting observed during the evaporation phase in Figs. 5-1A and 5-1B. Possibly, this rewetting of the root zone occurs partially through Darcian flow in the soil driven

by hydraulic gradients, and for another part through water transport through the much more conductive roots from wet regions within the root zone to dry regions (hydraulic lift; Caldwell et al. 1998, Dawson 1993).

### 5.3.2 Rhizotube observations and root length density

Figures 5-3 and 5-4 show the root numbers  $N_r$  of the different treatments on 4 dates corresponding to 18, 32, 48 and 70 days after ceasing the initial frequent irrigations in the intermediate stress and severe stress treatment.

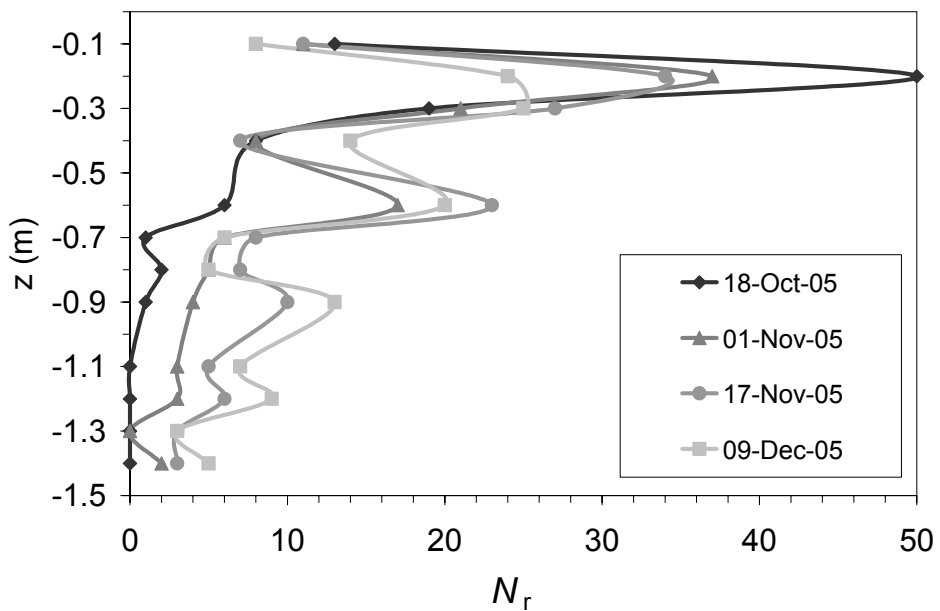


Figure 5-3A. Root numbers  $N_r$  visually observed at the surface ( $\text{cm}^2$ ) of cylindrical, transparent rhizotubes in the cropped lysimeter under severe water stress (see Figs. 4-1 in Chapter 4, and 5-1 for details). (continued on next page)



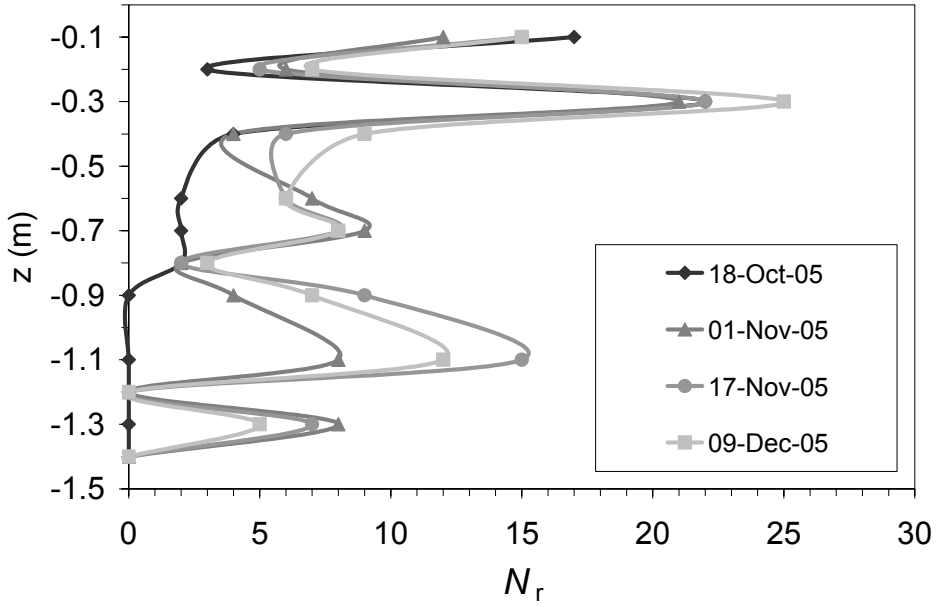


Figure 5-3B. (continued from previous page) Root numbers  $N_r$  visually observed at the surface ( $\text{cm}^2$ ) of cylindrical, transparent rhizotubes in the cropped lysimeter under intermediate water stress (see Figs. 4-1 in Chapter 4, and 5-1 for details). (continued on next page)

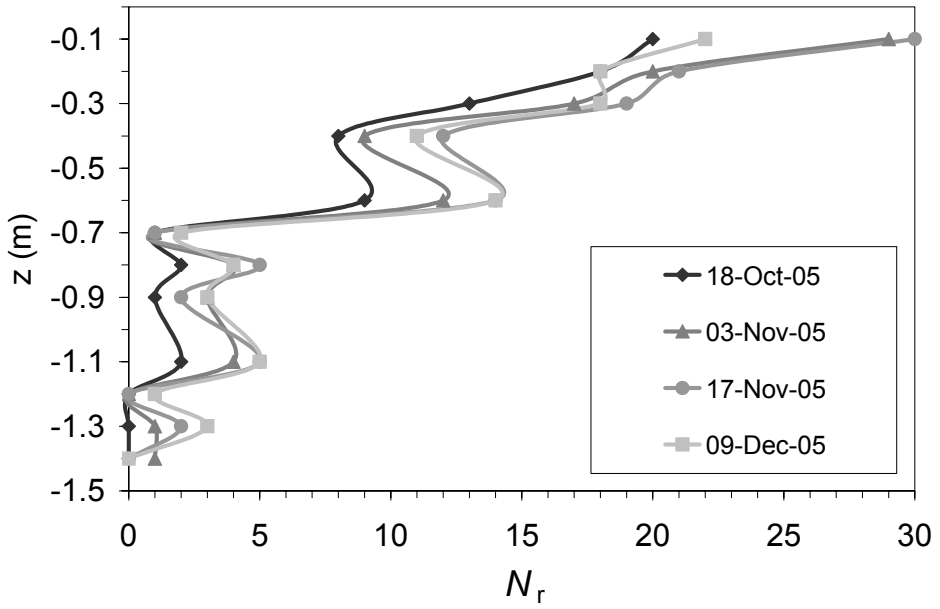
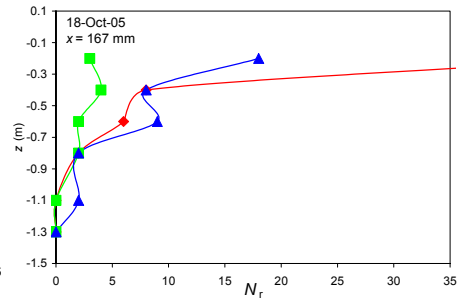
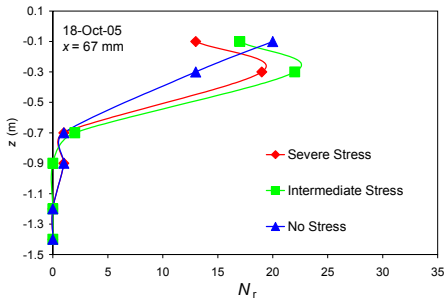
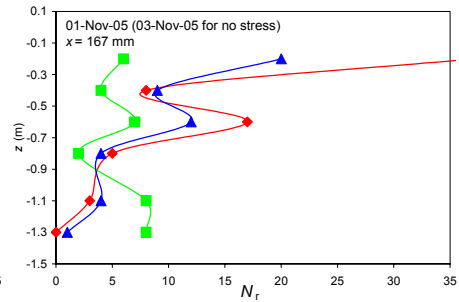
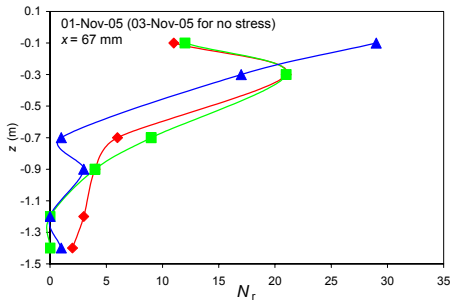


Figure 5-3C. (continued from previous page) Root numbers  $N_r$  visually observed at the surface ( $\text{cm}^{-2}$ ) of cylindrical, transparent rhizotubes in the cropped lysimeter under no water stress (see Figs. 4-1 in Chapter 4, and 5-1 for details).

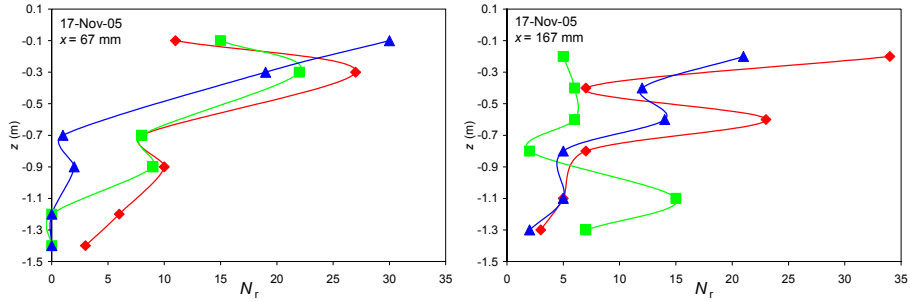


18-Oct-05

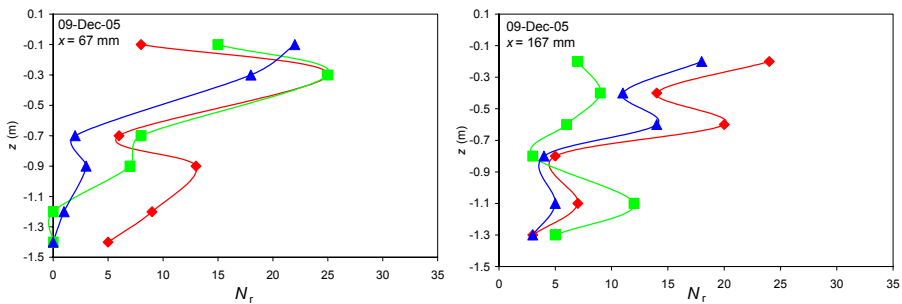


1-Nov-05 (3-Nov-05 for No Stress)

Figure 5-4. Comparison of root numbers ( $N_r$ ) visually observed at the surface ( $\text{cm}^2$ ) of cylindrical, transparent rhizotubes in the three cropped lysimeters under severe, intermediate, and no water stress (see Figs. 4-1 in Chapter 4, and 5-1 for details) for 4 dates. Left: data for rhizotubes at  $x = 67$  mm. Right: data for rhizotubes at  $x = 167$  mm (continued on next page).



17-Nov-05



9-Dec-05

Figure 5-4. (continued from previous page)

On October 18, 2005, the root profiles varied little between treatments, with roots growing predominantly in the upper soil layers. The large root count in the rhizotube at  $-0.2$  m in Fig. 5-3A (severe stress) reflects preferential root growth along the rhizotube. On November 1, 2005, the root counts were still not that different. From then on, the lysimeter under intermediate stress was irrigated again. The severely stressed crop reduced its number of roots in the top soil and expanded its root network at larger depths, particularly at  $-0.6$  m (Fig. 5-3A). The crop under intermediate stress showed similar behavior, but grew relatively many roots at  $-1.1$  m (Fig. 5-3B), despite the fact that the POT data in Fig. 5-1B do not show much evidence of enhanced active root water uptake at that depth at that

time. The crop without water stress maintained a large root density between  $-0.2$  and  $-0.6$  m (Fig. 5-3C).

By November 17, 2005, the crop under intermediate stress had increased its number of shallow roots, probably as a response to the resumed irrigation, even though the soil there was still quite dry (between  $-0.2$  and  $-0.4$  MPa, Fig. 5-1B). Maize roots can grow at water potentials below  $-4$  MPa, and root tips that may survive on vapor transport rapidly elongate if the surrounding soil is wetted again (Portas and Taylor, 1976).

Figure 5-4 shows that compared to the no stress treatment, the intermediate and severe stress treatments provoked root growth in soil that was further away from the stems of the plants. The different root distributions in Figs. 5-3 and 5-4 indicate that the crop invested more in its deeper root system when exposed to water stress and a dry top soil, even though the correlation between root density and root water uptake was not always clear. Also, changing conditions prompted rapid modifications of the root distribution. Several researches noted that water stress may greatly alter root distribution, not only in maize (Box et al., 1989), but also in cotton (Klepper et al. 1973).

The  $L_r$  (Fig. 5-5) that were observed in soil cores taken after the experiment show a completely different distribution over depth compared to the root amounts observed during the experiment. Furthermore, the shape of the  $L_r$  distribution over the depth is comparable for all treatments. The observed root diameter within the rhizotubes was between 0 and 0.13 mm, and although the bulk of the observed  $L_r$ s lies between 0 and 1 mm, the smallest diameter class between 0 and 0.2 mm is severely underrepresented (Fig. 5-6). This is probably a result from the method used to retrieve the roots (Oliveira et al. 2000). Coelho and Or (1999) suggest the measured  $L_r$  to be a measure of potential water uptake areas, as was observed in kiwifruit by Green and Clothier (1995). Although  $L_r$  from soil cores is considered to be the representative quantity to measure (Smit et al. 2000), it necessarily is an integrative measure encompassing the entire history of environmental factors during the plants development.

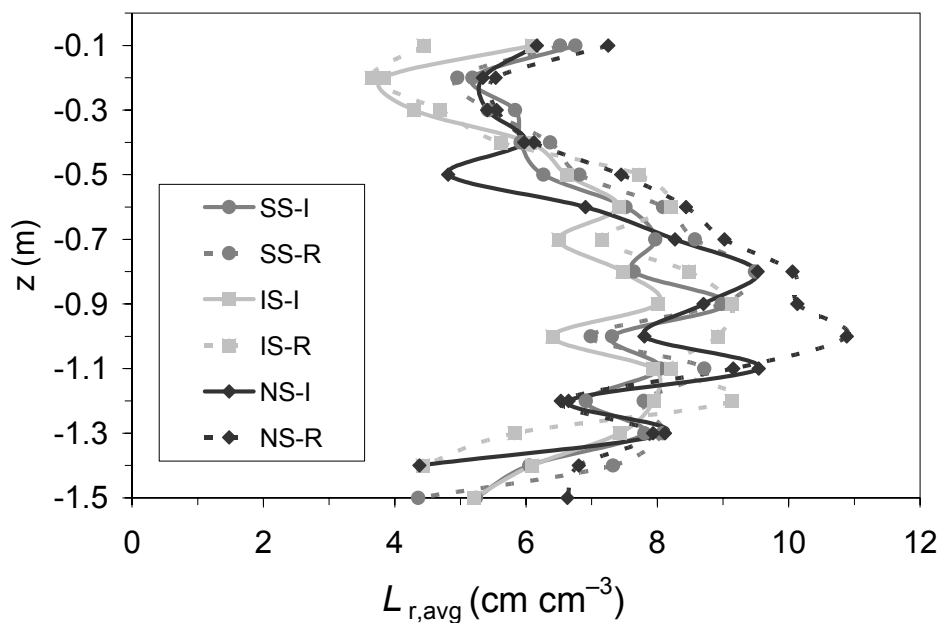


Figure 5-5. Total root length density  $L_r$  ( $\text{cm cm}^{-3}$ ) for no-stress (NS), intermediate stress (IS) and severe stress (SS) treatments determined under the mid plant soil volume where the instruments (I) were located and under the left plant soil volume where the rhizotube (R) were located.  $L_r$  was determined over 10 cm long samples, but is plotted at the minimum depth of each sample.

In contrast, root water uptake patterns may vary rapidly by development of fine roots and root hairs (poorly captured by the  $L_r$  determination), and changes in root conductivity (Coelho and Or, 1999). Rhizotube observation may be a more appropriate method compared to destructive soil core sampling, when the objective is to study root patterns under water limiting conditions.

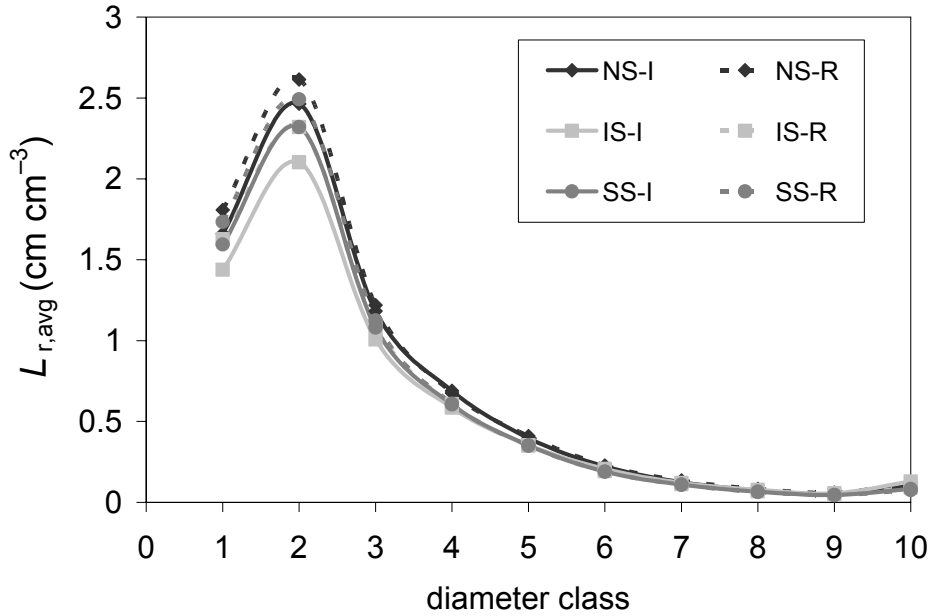


Figure 5-6. Average root length density  $L_{r,avg}$  ( $\text{cm cm}^{-3}$ ) for no-stress (NS), intermediate stress (IS) and severe stress (SS) treatments determined under the mid plant soil volume where the instruments (I) were located and under the left plant soil volume where the rhizotube (R) were located, averaged over number of samples ( $N=14$  for NS-I and NS-R,  $N=15$  for other series). Diameter classes (mm):  $0.0 \leq 1 < 0.2$ ;  $0.2 \leq 2 < 0.4$ ;  $0.4 \leq 3 < 0.6$ ;  $0.6 \leq 4 < 0.8$ ;  $0.8 \leq 5 < 1.0$ ;  $1.0 \leq 6 < 1.2$ ;  $1.2 \leq 7 < 1.4$ ;  $1.4 \leq 8 < 1.6$ ;  $1.6 \leq 9 < 1.8$ ;  $10 > 1.8$ .

## 5.4 Conclusions

In this chapter we explored root water uptake strategies under various levels of water stress. Observation of matric potentials show the ability of maize plants to take up water under extremely dry conditions, and to shift water uptake areas to lower, relatively wetter soil layers. This shift in water uptake to deeper layers seems to occur when the steep dry end of the retention curve is reached at a particular shallower depth. Even though the observations were only made at three depths, the observations are contrary to the minimum energy hypothesis that was formulated for non-stressed plants. Root water uptake continues straight to the steep end of the retention curve, where soil moisture content measurements by for instance TDR are no longer very accurate. Clear target ranges of  $\psi_m$  in which plants prefer to take up water deserves further investigation.

Observations made in rhizotubes showed that water stress provoked root growth at lower soil layers during the experiment, and showed the dynamic response of root growth during periods of water stress and resumed irrigation. This type of behavior (shifted water uptake in combination with root growth) may hold for several plant species. It may be a challenge to include this behavior in unsaturated flow models that include root water uptake, where root systems are usually assumed constant. The comparison between rhizotubes observations and afterwards determined root length density from soil cores suggest that the latter may not reflect conditions during the experiment, and therefore correlates poorly to observed root water uptake patterns.

From the observed root water uptake day-night cycles we could not determine whether the increase in matric potential during the night stems from soil water redistribution or plant water exudation (hydraulic lift). A combined effect might be likely, but specific studies with for instance the use of tracers are necessary to solve this knowledge gap. The use of polymer tensiometers in such studies is invaluable.



### 6.1 Conclusions

Measurement of total soil water potential ( $\psi_{\text{tot}}$ ) is essential for characterization of many unsaturated soil processes. In unsaturated soils, the matric potential ( $\psi_{\text{m}}$ ) is often the largest component of  $\psi_{\text{tot}}$ . In this thesis a new polymer tensiometer (POT) was developed to measure  $\psi_{\text{m}}$ , between 0 and  $-1.6$  MPa. The POT functioned properly for periods comparable to a growing season. The effect of water stress on root water uptake was studied under different irrigation regimes using POTs. This section gives an overview of the conclusions that originate from Chapters 2 to 5, while section 6.2 focuses on directions for future research concerning these POTs.

In Chapter 2, a POT design with a flat ceramic was presented. The ceramic included a  $\gamma\text{-Al}_2\text{O}_3$  membrane that very efficiently retains polymers. Long-term pressure decay (less than  $1 \text{ kPa d}^{-1}$ ) was possibly caused by polymer degradation, or by diffusion of some smaller-sized polymer molecules through the porous membrane. The long-term pressure decay could be adequately quantified by means of calibration, and the readings accordingly corrected. POTs need to be calibrated for temperature variations, as the osmotic pressure  $\pi$  of the polymer solution is dependent on temperature. The abrupt response of  $\pi$  in the polymer chamber to temperature gradients is such that it needs consideration in experimental designs.

Chapters 2 and 3 showed that temperature response times were affected by polymer chamber height, and by the area of the ceramic that is in contact with the polymer solution. Designs that minimized polymer chamber height (approximately 1 mm), while maximizing the ceramic area in contact with polymer solution showed the shortest response times (less than an hour for a 5 °C change). A preferred design therefore will mostly depend on the maximization of the ceramic membrane's surface in contact with the polymer solution, as well as on the minimization of the polymer chamber's height.

The POTs were compared with time domain reflectometry (TDR) probes and conventional, water-filled tensiometers in three evaporation experiments. In the evaporation experiments described in Chapter 3 POTs with ceramic cones were used. Alteration of the shape of the ceramic improved soil contact, and facilitated installation in the soil. The various designs used in Chapters 2 and 3 had repercussions for the level of skill required to manufacture the POTs. Regardless of the designs, all POTs measured until at least  $-1.6$  MPa, and were comparable with conventional tensiometers until the latter cavitated. Matric potentials measured by POTs and converted soil moisture measurements by TDR were also comparable, but mainly revealed the risks associated with converting soil moisture readings in dry soils to matric potentials. In dry soil, the moisture retention curve is such that a small change in moisture content leads to a large change in matric potential. At the same time, as little moisture is left in the soil, the accuracy of the TDR becomes important.

By combining POT and TDR measurements it is possible to observe an *in situ* moisture retention curve. These *in situ* moisture retention curves were comparable to retention curves from soil cores, and could be fitted with the Van Genuchten (1980) curve. Although *in situ* moisture retention curves will never exceed the upper measurement limit of POTs, pairing POT and TDR data will give a unique opportunity to study the dynamics of moisture retention curves in field soils.

In addition to the extended measurement range, POTs are able to regain their full osmotic pressure without user interference after having dried out. The time required to regain pressure by rewetting depended on the polymer chamber height and the ceramic area in contact with the polymer solution. Response times were decreased with decreasing polymer chamber heights, and increasing ceramic area in contact with the polymer solution. Response times of less than 1 day are

feasible. It should be noted that the reported response times in this thesis are an extreme scenario; from completely dry polymer to fully saturated. In practice when the polymer solution does not completely dry, pressure recovery will generally be much faster. POTs thus appear very attractive for field applications because of their much wider measurement range, fast pressure response, and their ability to rewet without user interference.

In Chapter 4 the potential for using POTs in cropped lysimeters under varying levels of water stress was explored. A total of 27 POTs and 27 TDR probes monitored the soil matric potential and the soil moisture content, respectively, in three lysimeters over a period of 4 months. The degree of stress was defined in terms of a minimum soil matric potential as measured by any of the POTs in a given treatment (no stress, intermediate stress and severe stress). The use of POTs provides a means to better define levels of local water stress.

The moisture retention curve of this particular loam showed that volumetric moisture contents were below 0.1 when water stress reached the predefined stress levels. For these low moisture contents, TDR measurements may be of little use, again due to the sensitivity of TDR readings. Effects of water stress levels on the cumulative root length density  $L_{r,z}$  could not be observed. Increased water uptake efficiency from deep roots in combination with slow but continuing root growth in drier soil may explain observed similarities in cumulative root length density.

Soil matric potential profiles indicated that as the topsoil in the lysimeter dried out under water-stressed conditions, root water uptake occurred between 0.3 and 0.5 m depth. The maize plants were able to extract water under very dry conditions, and continued to extract water from those dry regions. Such observations indicate that POTs have the potential to improve experimental analysis of root water uptake in dry soils, and thus they may help unraveling plant root water uptake strategies under various levels of water stress.

In Chapter 5 root water uptake strategies under various levels of water stress were explored further. Observation of matric potentials in Chapter 4 already showed the ability of maize plants to take up water under extremely dry conditions, and to shift water uptake areas to lower, relatively wetter soil layers. This shift in water uptake to deeper layers seems to occur when the steep dry end of the

retention curve is reached at a particular shallower depth. This is contrary to the minimum energy hypothesis that was formulated for non-stressed plants (Dirksen et al. 1994, Adiku et al. 2000). In this hypothesis the root water uptake is controlled by the unsaturated conductivity and the sum of the matric and gravitational potential. Instead root water uptake continues straight to the steep end of the retention curve where the unsaturated conductivity is very low, and even when water is readily available in deeper layers.

Observations made in rhizotubes showed that water stress provoked root growth at lower soil layers during the experiment, but also showed the dynamic response of root growth during periods of water stress and resumed irrigation. This type of behavior (shifted water uptake in combination with root growth) may hold for several plant species, and has implications for the way root water uptake is treated in unsaturated zone modeling (see section 7.2). The comparison between rhizotubes observations and afterwards determined root length density  $L_r$  determined *a posteriori* from soil cores suggest that the latter may not reflect conditions during the experiment, and therefore correlates poorly to observed root water uptake patterns.

From the observed root water uptake day-night cycles we could not determine whether the increase in matric potential during the night stems from soil moisture redistribution or plant water exudation (hydraulic lift). A combined effect is likely, but specific studies with for instance the use of tracers are necessary to bridge this knowledge gap. The use of POTs in such studies is invaluable.

## 6.2 Outlook

### 6.2.1. Polymer tensiometers

POTs are an important instrumental addition to soil physical research to characterize soil physical processes in dry soils. The POTs reported in Chapters 3, 4, and 5 functioned well, but certain aspects of their design may still be improved.

Screening for polymer solutions that would not display any long term pressure decay would reduce the time that is currently needed to calibrate each POT. Furthermore, it is desirable to understand the processes that lead to peaked pressure responses when temperature gradients occur. Instead, combining polymers with

opposite responses of the osmotic pressure to temperature change could reduce these abrupt pressure responses to temperature gradients, and cancel the influence of temperature variations. Preliminary research in this direction showed that the long term sustainability of the osmotic pressure of polymer mixtures may be affected.

The cone-shaped ceramics that are currently used in the POT design include a ceramic membrane that efficiently retains polymers. The fabrication of these ceramics is labor-intensive, and thus costly. Using a ceramic substrate in combination with the use of cross-linked polymers could possibly make the ceramic membrane superfluous, and hence the POT less expensive. Another design alteration would be to make outer surface of the stainless steel casing in which the ceramic is glued smoother, to better facilitate installation in soil.

The pressure transducer used throughout this thesis had a pressure range slightly over 2.0 MPa. Considering the influence of temperature on the osmotic pressure of the polymer solution, the measurements of soil matric potentials are 'limited' to approximately  $-1.6$  MPa. In theory however, when using a transducer with a larger pressure range, measurements of the soil matric potential could be extended even further. This may be interesting for researchers working on dryland ecohydrology, because specialized plants may survive much lower potentials (Wood 2005).

Furthermore, POTs could be applied for determination of unsaturated soil hydraulic properties over a larger continuous range, like the estimation of the unsaturated hydraulic conductivity in either conventional (Arya 2002) or novel (Schneider 2006) experimental setups. In combination with soil moisture content sensors, moisture retentions curves including hysteresis can be derived *in situ*. With the data from Chapter 3, the suitability of moisture retention curve models can be studied.

### 6.2.2 Salinity

A topic that has not been covered in this thesis is the influence of salts in the soil solution on the osmotic pressure of the polymer solution. This is important as it is estimated that 20% of all cultivated land and nearly half of the irrigated land is salt-affected, which has a negative effect on crop yields (Van Schilfgaarde 1994, Munns 2002, Flowers 2004). Soil salinity is an acute problem, primarily due to the

declining quality of irrigation water (Rhoades and Loveday 1990, Ghassemi et al. 1995, Flowers 2004). Consequently, new strategies to enhance crop yield stability on saline soils represent a major research priority (Botella et al. 2005). If POTs are found to be only moderately sensitive to salts, they would be ideal instruments to contribute to such research, as the signal of most soil moisture content sensors is strongly attenuated by soil salinity. Thorough testing of POTs in saline environments is therefore highly necessary.

POTs could also prove useful to study soil matric potentials dynamics to characterize solute transport processes, leaching below waste disposal sites, and multi-phase flow. The suitability of POTs for these research directions merits attention.

### 6.2.3 Plant responses to water stress

In the lysimeter experiment described in Chapters 4 and 5, the maize plants showed shifted water uptake in combination with root growth in water-stressed conditions. As maize is only one species, it is difficult to generalize, and it should be further investigated whether this type of behavior (shifted water uptake in combination with root growth) may hold for more plant species. Furthermore, it would be highly desirable to learn the preferred matric potential range for water uptake for important crops to optimize irrigation strategies. The observations for maize suggest this range depends not only on the crop but also on the soil. Consequently, site-specific irrigation guidelines may be needed, and the POT can be instrumental in developing such farm-oriented recommendations.

It is becoming increasingly clear that root-sourced signals appear to play a key role in regulating stomatal aperture in response to soil water availability (Bacon, 2004). This creates opportunities for both soil scientists and plant physiologist to combine the strengths of their respective disciplines to fill the still existing gaps in our understanding of plant responses.

POTs may prove helpful in determining plant responses to changes in soil water conditions, and in combination with stable isotope discrimination, and measurements of photosynthetic activity and stomatal conductance, help determine water use efficiency in plants. POTs could thus be helpful in distinguishing crops with reduced water requirements. With such crops, agriculture could benefit by reducing the use of groundwater resources. An alternative water-saving irrigation

strategy in which POTs could be useful is partial rootzone drying, in which part of the rootzone is left to dry to a pre-determined level, and only part of the rhizosphere is wetted at each irrigation time. Partial rootzone drying could save water and yet maintain yield as was shown for some grape cultivars, and tomatoes (Loveys et al. 2000, Zegbe et al. 2004) As such, POTs could become a component of a decision support system for water resource management.

#### 6.2.4 Modeling root water uptake

Combining measurement and modeling of root water uptake helps to identify and characterize important processes of plant responses to water limited conditions. In macroscopic models (see Chapter 1) the representation of water uptake by a root system requires little detail of the root system's morphology. Instead, root density profiles (Huck and Hillel 1983) or a root distribution in terms of a potential extraction rate (Feddes et al. 1978, Prasad 1988 in Feddes and Raats 2004) can be used. It may be a challenge to include shifted water uptake in combination with root growth in these unsaturated flow models.

Modeling approaches need to be verified by measurements. At the same time, as measurements are often time-consuming and expensive, models can help to identify important parameters that need to be measured. An example of the latter can be demonstrated by the model R-SWMS (Javaux et al. 2008). The level of detail that is included by incorporating detailed plant properties in this model introduces a number of parameters for which measurements are scarce. This is especially true for root conductivity. Root conductivities are plant- and age-specific, and may vary depending on the applied method and on which specific property was measured (see for maize French and Steudle 1989, Steudle et al. 1993, Doussan et al. 1998, Zwieniecki et al. 2003). By using detailed data such as those from the lysimeter experiment described in Chapter 4 and 5, realistic parameterizations may be obtained without the need for extensive root conductivity measurements.





## Derivation of the total soil water potential

---

The thermodynamic theory following below is an excerpt of Anderson (2005) until Eq. A-16.

The first thermodynamic law states the conservation of energy. The energy content ( $U$ ) of a system may gain or lose energy only by heat flow ( $q$ ) or work ( $w$ ). Note that the variables are given as quantity per mole, and are thus independent of the system size.

$$\Delta U = q + w \quad (\text{A-1})$$

In A-1 the heat added to a system is positive, and the work done on the system is positive. There are different ways possible to do work on a system, for instance gravity

$$w = Mg\Delta z \quad (\text{A-2})$$

Where  $m$  is the mass of the system,  $g$  is the gravity constant, and  $\Delta z$  is the height over which the system is transferred. Work in natural environment usually includes expansion or contraction of systems, as temperature changes at constant pressures can usually not be avoided.

$$w = -P_{\text{ext}}\Delta V \quad (\text{A-3})$$

Where  $P_{\text{ext}}$  is the external pressure working on the system, and  $\Delta V$  is change in volume of the system. In the limit, when infinitesimal increments of  $V$  are taken, the work of expansion is

$$w_{\text{rev}} = w_{\text{max}} = - \int_{V_1}^{V_2} P dV \quad (\text{A-4})$$

There is no need to distinguish between  $P_{\text{ext}}$  and  $P_{\text{int}}$  (the internal pressure of the system, since they are never more than infinitesimally different. In any real or nonreversible expansion, the work is less than the maximum obtainable work, thus (A-4) becomes:

$$- w \leq \int_{V_1}^{V_2} P dV \quad (\text{A-5})$$

Similarly for heat transfer in expansion or contraction processes:

$$- q = \int_{Z_1}^{Z_2} T dZ \quad (\text{A-6})$$

Where  $Z$  is some property of the gas. In processes of constant external pressure, the first law of thermodynamics can be written as:

$$\Delta U = q_p - P\Delta V \quad (\text{A-7})$$

Where  $q_p$  is the heat transferred in the constant pressure process. Where the first law determines that energy cannot be lost, the second law determines in which direction processes will proceed. Processes can take place spontaneously if they are lowering the chemical energy of the system, and they only proceed in the other direction when an external energy source is provided. The directions of the processes can be described by thermodynamic potentials. The most important thermodynamic potential is entropy ( $S$ ). When identifying a thermodynamic

potential, it is necessary to specify the constraints. Thus entropy ( $S$ ) by itself is not a potential; entropy at constant energy and volume ( $S_{U,V}$ ) is a potential. In other words, entropy is not maximized in systems at constant  $T$  and  $P$ , only in systems at constant  $U$  and  $V$ . As  $S=Z$ , Eq. A-6 becomes:

$$q \leq \int_{S_1}^{S_2} TdS \quad (\text{A-8})$$

The second law of thermodynamics implicitly includes the following relationships:

$$dS_{U,V} > 0 \text{ and } dU_{S,V} > 0 \text{ for spontaneous processes} \quad (\text{A-9})$$

$$dS_{U,V} = 0 \text{ and } dU_{S,V} = 0 \text{ equilibrium} \quad (\text{A-10})$$

The first and the second thermodynamics laws can be combined to:

$$dU - TdS + PdV \leq 0 \quad (\text{A-11})$$

A more general formulation that includes all forms of work is given by:

$$dU - TdS + \sum_i X_i dx_i \leq 0 \quad (\text{A-12})$$

Where  $X_i$  is a generalized force and  $dx_i$  a generalized displacement.

Now we have two parameters,  $S_{U,V}$  and  $U_{S,V}$ , that tell which way processes will go, but they refer to processes that only occur at constant values of  $U$  and  $V$ , or of  $S$  and  $V$ . By introducing Gibbs free energy ( $G$ ), it is possible to refer to processes at constant  $T$  and  $P$ :

$$G = U - TS + PV \quad (\text{A-13})$$

The differential form of Eq A-13 is:

$$dG = dU - TdS - SdT + PdV + VdP \quad (\text{A-14})$$

or

$$dG_{T,P} = dU - TdS + PdV \quad (\text{A-15})$$

To describe changes of  $G$  as a result of changes in  $T$  and  $P$ , Eq A-11 and A-14 can be combined to:

$$dG = -SdT + VdP \quad (\text{A-16})$$

The equations given above are limited to constant composition systems. To be able to deal with compositional changes it is necessary to include chemical potentials ( $\mu_j$ ) (Sposito, 1981):

$$\mu_j = \left( \frac{\partial G}{\partial n_j} \right)_{T,P,\hat{n}_j} \quad (\text{A-17})$$

Where  $n_j$  refers to the amount of moles of any individual component  $j$ , and  $\hat{n}_j$  refers to the amount of moles of all components except  $j$ . The difference in chemical potential between water in the soil and pure free water at the same temperature is an expression for the total soil water potential.

### Flory Huggins solution theory

---

Like most substances, polymer solutions show reaction to temperature variations. Key parameter in this process is the dimensionless Flory-Huggins interaction parameter (Flory, 1941; Huggins, 1941). The Flory-Huggins solution theory is a mathematical model of the thermodynamics of polymer solutions and accounts for the dissimilarity in molecular sizes by using a different expression for the entropy of mixing. Although it uses simplifying assumptions (e.g. Nikitas 1984), it generates useful results for interpreting experiments. The result is an equation for the Gibbs free energy change ( $\Delta G_m$ ) for mixing a polymer with a solvent (See Appendix A for Gibbs free energy). The change in Gibbs free energy is in this case a function of the number of moles ( $n_m$ ) and volume fraction ( $\phi$ ).

$$\Delta G_m = RT(n_1 \ln \phi_1 + n_2 \ln \phi_2 + n_1 \phi_2 \chi_{12}) \quad (\text{B-1})$$

Where  $R$  is the gas constant,  $T$  the absolute temperature, subscript 1 the solvent, subscript 2 the polymer, and  $\chi_{12}$  the Flory-Huggins interaction parameter.

The Flory-Huggins interaction parameter accounts for the change in energy of interdispersing polymer and solvent molecules. Using the Flory-Huggins equation, an expression can be obtained, that relates the osmotic pressure ( $\pi$ ) of the polymer and the temperature.

$$\pi = -\frac{RT}{v_s} \left[ \ln(1 - \phi) + \left(1 - \frac{1}{l}\right)\phi + \chi\phi^2 \right] \quad (\text{B-2})$$

Where  $v_s$  is the solution molar volume and  $l$  the polymer chain length.



---

## Bibliography

---

- Adiku, S.G.K., C.W. Rose, R.D. Braddock and H. Ozier-Lafontaine. 2000. On the simulation of root water extraction: examination of a minimum energy hypothesis. *Soil Sci.* 165: 226-236.
- Adiku, S.G.K., H. Ozier-Lafontaine and T. Bajazet. 2001. Patterns of root growth and water uptake of a maize-compea mixture grown under greenhouse conditions. *Plant and Soil* 235: 85-94.
- Agus, S.S. and T. Schanz. 2005. Comparison of four methods for measuring total suction. *Vadose Zone J.* 4: 1087-1095.
- Alami-Younssi, S., A. Larbot, M. Persin, J. Sarrazin and L. Cot. 1995. Rejection of mineral salts on a gamma alumina nanofiltration membrane, application to environmental process. *J. Membrane Sci.* 102: 123-129.
- Allen, R.G., L.S. Pereira, D. Raes and M. Smith. 1998. Crop evapotranspiration: Guidelines for computing crop water requirements. FAO Irrigation and drainage paper 56, FAO, Rome.
- Ameglio, T., J. Morizet, P. Cruiziat and M. Martignac. 1990. The effect of root temperature on water flux, potential and root resistance in sunflower. *Agronomie* 10: 331-340.
- Anderson, G.M. 2005. Thermodynamics of natural systems. Cambridge university press, UK.
- Andraski, B.J. and B.R. Scanlon. 2002. Thermocouple psychrometry, p. 609-642. In J.H. Dane, and G.C. Topp (eds.) *Methods of Soil Analysis. Part 4.* SSSA Book Ser. 5. SSSA, Madison, WI.
- Arya, L.M. 2002. Wind and hot-air methods. *In:* Dane, J.H. and G.C. Topp. *Methods of soil analysis Part 4 Physical Methods*, Soil Science Society of America Book Series No 5, Madison, WI, USA.

- Atkinson, D. 2000. Root characteristics: Why and what to measure. In: A.L. Smit, A.G. Bengough, C. Engels, M. van Noordwijk, S. Pellerin and S.C. van de Geijn (Ed.) *Root methods a handbook*. Springer-Verlag, Heidelberg, D.
- Bacon, M.A. 2004. Water use efficiency in plant biology. *In*: Bacon, M.A. (ed.) *Water use efficiency in plant biology*. Blackwell publishing, Oxford, UK.
- Baker, J.M. and R.J. Lascano. 1989. The spatial sensitivity of time-domain reflectometry. *Soil Sci.* 147: 378-384.
- Bakker, G., M.J. van der Ploeg, G.H. de Rooij, C.W. Hoogendam, H.P.A. Gooren, C. Huijckes, L.K. Koopal and H. Kruidhof. 2007. New polymer tensiometers: Measuring matric pressures down to the wilting point. *Vadose Zone J.* 6: 196-202.
- Begg, J.E. and N.C. Turner. 1976. Crop water deficits. *Ad. Agron.* 28: 161-217.
- Biesheuvel, P.M., R. Raangs and H. Verweij. 1999. Response of the osmotic tensiometer to varying temperatures: modeling and experimental evaluation. *Soil Sci. Soc. Am. J.* 63: 1571-1579.
- Biesheuvel, P.M., A.P. van Loon, R. Raangs, H. Verweij and C. Dirksen. 2000. A prototype osmotic tensiometer with polymeric gel grains. *Eur. J. Soil Sci.* 51: 355-364.
- Blackman, P.G. and W.J. Davies. 1985. Root to shoot communication in maize plants of the effects of soil drying. *J. Exp. Bot.* 36: 39-48.
- Blake, G.R. and K.H. Hartge. 1986. Bulk Density. In A. Klute (ed.) *Methods of Soil Analysis. Part 1*. 2nd ed. Agron. Monogr. 9. ASA and SSSA, Madison, WI.
- Bocking, K.A. and D.G. Fredlund. 1979. Use of the osmotic tensiometer to measure negative pore water pressure. *Geotech. Test. J.* 2(1): 3-10.
- Bohm, W., H. Maduakor and H.M. Taylor. 1977. Comparison of five methods for characterizing soybean rooting density and development. *Agron. J.* 69: 415-419.
- Bolt, G.H. 1976. Soil physics terminology. *Bulletin of the international society of soil science* 49: 26-36.
- Botella, M.A., A. Rosado, R.A. Bressan and P.M. Hasegawa. 2005. Plant adaptive responses to salinity stress. *In*: Jenks, M.A. and P.M. Asegawa (Eds.) *Plant abiotic stress*. Blackwell publishing, Oxford, UK.



- Box, J.E., A.J.M. Smucker and J.T. Ritchie. 1989. Minirhizotron observation techniques for investigating root responses to drought and oxygen stresses. *Soil Sci. Soc. Am. J.* 53: 115-118.
- Boyer, J.S., 1970. Differing sensitivity of photosynthesis to low leaf water potentials in corn and soybean. *Plant Physiol.* 46: 236–239.
- Brooks, J.R. (representing 45 authors). 2004. The cohesion-theory. *New Phytol.* 163: 451-452.
- Brown, D.A. and D.R. Upchurch. 1987. Minirhizotrons: A summary of methods and instruments in current use. In: Taylor, H.M. (Ed.) *Minirhizotron observation tubes: Methods and applications for measuring rhizosphere dynamics*, ASA Special Publication No 50. ASA, Madison, WI, USA.
- Cailloux, M. 1972 Metabolism and the absorption of water by root hairs. *Canadian Journal of Botany* 50:557-573.
- Caldwell, M.M., T.E. Dawson and J.H. Richards. 1998. Hydraulic lift: consequences of water efflux from the roots of plants. *Oecologia* 113: 151-161.
- Campbell, G.S. 1988. Soil water potential measurement: An overview. *Irrigation Sci.* 9: 265-273.
- Campbell, G.S. and G.W. Gee. 1986. Water potential: Miscellaneous methods. In: A. Klute (ed.) *Methods of soil analysis. Part 1.* 2nd ed. Agron. Monogr. 9. ASA and SSSA, Madison, WI.
- Cassel, D.K. and A. Klute. 1986. Water potential: Tensiometry. In A. Klute (ed.) *Methods of Soil Analysis. Part 1.* 2nd ed. Agron. Monogr. 9. ASA and SSSA, Madison, WI.
- Caulfield, M.J., X. Hao, G.G. Qiao and D.H. Solomon. 2003. Degradation on polyacrylamides. Part I. Linear polyacrylamide. *Polymer* 44: 1331-1337.
- Chaves, M.M. 1991. Effects of water deficits on carbon assimilation. *J. Exp. Bot.* 42: 1–16.
- Chaves, M.M. J.S. Pereira, J. Maroco, M.L. Rodrigues, C.P.P. Ricardo, M.L. Osório, I. Carvalho, T. Faria and C. Pinheiro. 2002. How plants cope with water stress in the field. Photosynthesis and growth. *Annals of Botany* 89: 907-916.
- Coelho, E.F. and D. Or. 1999. Root distribution and water uptake patterns of corn under surface and subsurface drip irrigation. *Plant and Soil* 206:123-136.

- Corey, A.T. and A. Klute. 1985. Applications of the potential concept to soil water equilibrium and transport. *Soil Sci. Soc. Am. J.* 49: 3-11.
- Corey, A.T. and S.D. Logsdon. 2005. Limitations of the chemical potential. *Soil Sci. Soc. Am. J.* 69: 976-982.
- Dai, A., K.E. Trenberth and T. Quian. 2004. A global dataset of palmer drought severity index for 1870-2002: Relationship with soil moisture and effects of surface warming. *J. Hydrometeorology* 5: 1117-1130.
- Dane, J.H. and J.W. Hopmans. 2002. Water retention and storage, p. 671-673. *In* J.H. Dane, and G.C. Topp (ed.) *Methods of Soil Analysis. Part 4. SSSA Book Ser. 5. SSSA, Madison, WI.*
- Dane, J.H. and G.C. Topp (ed.) *Methods of Soil Analysis. Part 4. SSSA Book Ser. 5. SSSA, Madison, WI, USA.*
- Davidson, R.L. (ed.). 1980. *Handbook of water-soluble gums and resins.* McGraw-Hill, Inc, New York.
- Davies, W.J. and J. Zhang. 1991. Root signals and the regulation of growth and development of plants in drying soil. *Annu. Rev. Plant Physiol. Plant Mol. Biol.* 42: 55-76.
- Dawson, T.E. 1993. Hydraulic lift and water use by plants: implications for water balance, performance and plant-plant interactions. *Oecologia* 95: 565-574.
- De Vos, R.M. and H. Verweij. 1998. Improved performance of silica membranes for gas separation. *J. Membrane Sci.* 143: 37-51.
- Dirksen, C., M.J. Huber, P.A.C. Raats, S.L. Rawlins, J. van Schilfgaarde, J. Shalhevet and M.Th. van Genuchten. 1994. Interaction of alfalfa with transient water and salt transport in the rootzone. Research report No. 135. U.S. Salinity Laboratory, Riverside, CA, USA.
- Donovan, L.A., M.J. Linton and J.H. Richards. 2001. Predawn plant water potential does not necessarily equilibrate with soil water potential under well-watered conditions. *Oecologia* 129: 328-335.
- Doussan, C., G. Vercambre and L. Pagès. 1998. Modelling of the hydraulic architecture of root systems: an integrated approach to water absorption-Distribution of axial and radial conductances in maize. *Annals of Botany* 81: 225-232.

- Dunbabin, V.M., A.J. Diggle and Z. Rengel. 2002. Simulation of field data by a basic three-dimensional model of interactive root growth. *Plant and soil* 239: 39-54.
- Edlefsen, N.E. and A.B.C. Anderson. 1943. Thermodynamics of soil moisture. *Hilgardia* 15: 31-298.
- Ephrath, J.E., M. Silberbush and P.R. Berliner. 1999. Calibration of minirhizotron readings against root length density data obtained from soil cores. *Plant and soil* 209: 201-208.
- Everett, D.H. 1972. Manual of symbols and terminology for physico-chemical quantities and units. Appendix II. Definitions, terminology and symbols in colloid and surface chemistry, part I. *Pure Appl. Chem.* 31: 579-638.
- Feddes, R.A. and P.A.C. Raats. 2004. Parameterizing the soil-water-plant root system. *In*: Feddes, R.A., De Rooij, G.H. and J.C. van Dam. *Unsaturated-zone modeling: progress, challenges and applications*, Wageningen UR Frontis Series 6, Kluwer academic publishing, the Netherlands.
- Feddes, R.A., P.J. Kowalik and H. Zaradny. 1978. Simulation of field water use and crop yield. *Simulation Monographs Pudoc*, Wageningen, NL.
- Ferré, P.A., J.H. Knight, D.L. Rudolph, and R.G. Kachanoski. 1998. The sample areas of conventional and alternative time domain reflectometry probes. *Water Resources Research* 34: 2971-2979.
- Ferré, P.A. and G.C. Topp. 2002. Time Domain Reflectometry. *In*: J.H. Dane and G.C. Topp (eds.) *Methods of Soil Analysis. Part 4. SSSA Book Ser. 5. SSSA, Madison, WI.*
- Flory, P.J. 1941. Thermodynamics of high polymer solutions. *J. Chem. Phys.* 9: 660-661.
- Flory, P.J. 1942. Thermodynamics of high polymer solutions. *J. Chem. Phys.* 10: 51-61.
- Foley, J.A., R. DeFries, G.P. Asner, C. Barford, G. Bonan, S.R. Carpenter, F.S. Chapin, M.T. Coe, G.C. Daily, H.K. Gibbs, J.H. Helkowski, T. Holloway, E.A. Howard, C.J. Kucharik, C. Monfreda, J.A. Patz, I.C. Prentice, N. Ramankutty and P.K. Snyder. 2005. Global consequences of land use. *Science* 309: 570-574.
- French, J., and E. Steudle. 1989. Axial and radial hydraulic resistance to roots of maize (*Zea Mays* L.). *Plant Physiology* 91: 719-726.

- Gardner, W.R. 1960. Dynamic aspects of water availability to plants. *Soil Sci.* 89: 63-73.
- Garrigues, E., C. Doussan and A. Pierret. 2006. Water uptake by plants: 1- Formation and propagation of a water extraction front in mature root systems as evidenced by 2D light transmission imaging. *Plant and Soil* 283: 83-98.
- Gassemi, F., A.J. Jakeman and H.A. Nix. 1995. Salinization of land and water resources, human causes, extent, management and case studies. University of New South Wales Press Ltd., Sydney
- Gollan, T., J.B. Passioura and R. Munns. 1986. Soil water status affects the stomatal conductance of fully turgid wheat and sunflower leaves. *Aust. J. Plant Physiol.* 13: 459-464.
- Gowing, D.J.G., W.J. Davies and H.G. Jones. 1990. A Positive Root-sourced Signal as an Indicator of Soil Drying in Apple, *Malus x domestica* Borkh. *J. Exp. Bot.* 41: 1535-1540.
- Grace, J. 1999. Environmental controls of gas exchange in tropical rain forests. In: Press, M.C, J.D. Scholes and M.G. Barker (ed.). *Physiological plant ecology: the 39th Symposium of the British Ecological Society.* Blackwell Science, United Kingdom.
- Grant, S.A. and J. Backmann. 2002 Effect of temperature on capillary pressure. *In: Raats, P.A.C., D. Smiles and A.W. Warrick (eds.). Environmental mechanics: water, mass and energy transfer in the biosphere: the Philip volume.* AGU Geophysical Monograph 129, Washington DC.
- Green, S.R. and B.E. Clothier. 1995. Root water uptake by kiwifruit vines following partial wetting of the root zone. *Plant and soil* 173: 317-328.
- Green, S., M. Kirkham and B. Clothier. 2006. Root uptake and transpiration: from measurements and models to sustainable irrigation. *Agric. Water. Management* 86: 165-176.
- Groenvelt, P.H. and G.H. Bolt. 1969. Non-equilibrium thermodynamics of the soil-water system. *J. Hydrol.* 7: 358-388.
- Hainsworth and Aylmore. 1989. Non-uniform soil water extraction by plant roots. *Plant and soil* 113: 121-124.
- Hamblin and Tennant. 1987. Root length density and water uptake in cereals and grain legumes: How well are they correlated? *Aust. J. Agric. Res.* 38: 513-527.

- Hill, J., E. Nelson, D. Tilman, S. Polasky and D. Tiffany. 2006. Environmental, economic, and energy costs and benefits of biodiesel and ethanol biofuels. *Proc. Natl. Acad. Sci. U.S.A.* 103: 11206-11210.
- Hillel, D. 1998. *Environmental soil physics*. Academic Press, San Diego, CA.
- Himmelbauer, M.L., W. Loiskandl and F. Kastanek. 2004. Estimating length, average diameter and surface area of roots using two different image analysis systems. *Plant and Soil* 260: 111-120.
- Hopmans, J.W. and K.L. Bristow. 2002. Current capabilities and future needs of root water and nutrient uptake modeling. *Advances in Agronomy* 77:103-183.
- Hsiao, T.C., E. Acevedo, E. Fereres and D.W. Henderson. 1976. Water stress, growth and osmotic adjustment. *Phil. Trans. R. Soc. Lond. B.* 273: 479-500.
- Hsiao, T.C., W.K. Silk and K. Jing. 1985. Leaf growth and water deficits: biophysical effects. In: Baker, N.R., W.J. Davies and C.K. Ong (ed.), *Control of leaf growth*. Soc. for Exp. Biol. Seminar Series 27, Cambridge University Press, Cambridge, UK.
- Huck, M.G. and D. Hillel. 1983. Model of root growth and water uptake accounting for photosynthesis, respiration, transpiration, and soil hydraulics. *Advances in Irrigation* 2: 273-333.
- Huggins, M.L. 1942a. Theory of solutions of high polymers. *J. Am. Chem. Soc.* 64: 1712-1719.
- Huggins, M.L. 1942b. Some properties of solutions of long-chain compounds. *J. Phys. Chem.* 46: 151-158.
- Huisman, J.A., C. Sperl, W. Bouten and J.M. Verstraten. 2001. Soil water content measurements at different scales: accuracy of time domain reflectometry and ground-penetrating radar. *J. Hydrol.* 245: 48-58.
- Huntington, T.G. 2006. Evidence of intensification of the global water cycle: Review and synthesis. *J. Hydr* 319: 83-95.
- Iwata, S., T. Tabuchi and B.P. Warkentin. 1988. Energy concept and thermodynamics. *In: Soil-water interactions: mechanisms and applications*. Marcel Dekker Inc., New York.
- Javaux, M., T. Schröder, J. Vanderborght, and H. Vereecken. 2008. Use of a Three-Dimensional Detailed Modeling Approach for Predicting Root Water Uptake. *Vadose Zone J.* 7: 1079–1088.

- Johnson, M.G., D.T. Tingey, D.L. Philips and M.J. Storm. 2001. Advancing fine root research with minirhizotrons. *Environmental and experimental botany* 45: 263-289.
- Kirkham, M.B. 2002. The concept of the soil-plant-atmosphere continuum and applications. *In: Raats, P.A.C., D. Smiles and A.W. Warrick (eds.). Environmental mechanics: water, mass and energy transfer in the biosphere: the Philip volume. AGU Geophysical Monograph 129, Washington DC.*
- Klepper, B., H.M. Taylor, M.G. Huck and E.L. Fiscus. 1973. Water relations and growth of cotton in drying soil. *Agronomy J.* 65: 307-310.
- Klute, A. (ed.). 1986a *Methods of Soil Analysis. Part 1. 2nd ed. Agron. Monogr. 9. ASA and SSSA, Madison, WI.*
- Klute, A. 1986b. Water retention: Laboratory methods, p. 635-686. *In A. Klute (ed.) Methods of Soil Analysis. Part 1. 2nd ed. Agron. Monogr. 9. ASA and SSSA, Madison, WI.*
- Koorevaar, P., G. Menelik and C. Dirksen. 1983. *Elements of soil physics. Developments in Soil Science 13, Elsevier.*
- Kramer, P. J. 1980. Drought, stress and the origin of adaptations. *In: Turner, N. C. and P. J. Kramer (eds.). Adaptions of Plants to Water and High Temperature Stress. John Wiley & Sons, New York.*
- Kramer, P.J. 1983. *Water relations of plants. Academic Press, Inc, London, UK.*
- Kroes, J.G. and J.C. van Dam. 2003. Reference manual of SWAP, version 3.03. *Alterra-report 773, Wageningen, NL.*
- Lawlor, D.W. and J.E. Leach. 1985. Leaf growth and water deficits: biochemistry in relation to biophysics. *In: Baker, N.R., W.J. Davies and C.K. Ong (ed.), Control of leaf growth. Soc. for Exp. Biol. Seminar Series 27, Cambridge University Press, Cambridge, UK.*
- Lide, D.R. (ed.) 2005. *CRC Handbook of chemistry and physics. 86<sup>th</sup> ed. CRC Press, Taylor & Francis Group, LLC, Boca Raton, FL.*
- Loveys, B.R., Dry, P.R., Stoll, M. and McCarthy, M.G., 2000. Using plant physiology to improve the water use efficiency of horticultural crops. *Acta Hort.* 537, pp. 187–197.
- Ludlow, M.M. 1980. Adaptive significance of stomatal response to water stress. *In: Turner, N.C. and P.J. Kramer (ed.). Adaptation of Plants to Water and High Temperature Stress. Wiley & Sons, New York.*

- Madsen, H.B., C.R. Jensen and T. Boysen. 1986. A comparison of the thermocouple psychrometer and the pressure plate methods for determination of soil water characteristic curves. *J. Soil Sci.* 37: 357-362.
- Mansfield, T.A. and D.L.R. De Silva. 1994. Sensory systems in the roots of plants and their role in controlling stomatal function in the leaves. *Physiol. Chem. Phys. & Med.* 26: 89-99.
- Maroco, J.P., J.S. Pereira and M.M. Chaves. 1997. Stomatal responses to leaf-to-air vapour pressure deficit in Sahelian species. *Australian J. Plant Phys.* 24: 381-387.
- McMichael, B.L. and J.J. Burke. 1996. Temperature Effects on Root Growth. In: Y. Waisel, A. Eshel and U. Kafkafi (Ed.) *Plant roots: The hidden half*. Marcel Dekker Inc., New York, NY, USA.
- Miller, E.E. and A. Salehzadeh. 1993. Stripper for bubble-free tensiometry. *Soil Sci. Soc. Am. J.* 57: 1470-1473.
- Molyneux, P. 1983. *Water-soluble synthetic polymers: Properties and behavior*, Vol. 1. CRC Press, Inc, FL.
- Molz, F.J. 1981. Models of water transport in the soil-plant system: a review. *Water Res. Res.* 17: 1245-1260.
- Moses, C.L, L.P.N. Rebelo and W.A. Van Hook. 2003. Membrane osmometer for use at moderate applied pressures. *J. Pol. Sci. Part B. Pol. Phys.* 41 (23): 3064-3069.
- Mualem Y. A new model predicting the hydraulic conductivity of unsaturated porous media. *Water Resour. Res.* 1976;12:513-522.
- Munns, R. 2002. Comparative physiology of salt and water stress. *Plant, Cell & Environment* 25, 239–250.
- Nikitas, P. 1984. Generalized Flory-Huggins isotherms for adsorption from solution. *J. Chem. Soc., Faraday Trans I* 80: 3315-3329.
- Nitao, J.J. and J. Bear. 1996. Potentials and their role in transport in porous media. *Wat. Res. Res.* 32: 225-250.
- Noborio, K., R. Horton and C.S. Tan. 1999. Time domain reflectometry probe for simultaneous measurement of soil matric potential and water content. *Soil Sci. Soc. Am. J.* 63: 1500-1505.
- Oliveira, M. d. R. G., M. van Noordwijk, S.R. Gaze, G. Brouwer, S. Bona, G. Mosca and K. Hairiah. 2000. Auger sampling, ingrowth cores and pinbord

- methods. In: A.L. Smit, A.G. Bengough, C. Engels, M. van Noordwijk, S. Pellerin and S.C. van de Geijn (Ed.) Root methods a handbook. Springer-Verlag, Heidelberg, D.
- Or, D. 2001. Who invented the tensiometer? *Soil Sci. Soc. Am. J.* 65: 1-3.
- Or, D. and J.M. Wraith. 1999. A new soil matric potential sensor based on time domain reflectometry. *Water Resources Research* 35 (11): 3399-3407.
- Pagès, L., G. Vercambre, J.-L. Drouet, F. Lecompte, C. Collet and J. Le Bot. 2004. Root Typ : a generic model to depict and analyse the root system architecture. *Plant and Soil* 258: 103-119.
- Passioura, J.B. 2002. Environmental biology and crop improvement. *Functional plant biology* 29: 537-546.
- Peck, A.J. and R.M. Rabbidge. 1966. Soil-water potential: Direct measurement by a new technique. *Science* 151: 1385-1386.
- Peck, A.J. and R.M. Rabbidge. 1969. Design and performance of an osmotic tensiometer for measuring capillary potential. *Soil Sci. Soc. Am. Proc.* 33: 196-202.
- Pohlmeier, A., A. Oros-Peusquens, M. Javaux, M.I. Menzel, J. Vanderborght, J. Kaffanke, S. Romanzetti, J. Lindenmair, H. Vereecken and N.J. Shah. 2008. Changes in soil water content resulting from *Ricinus* root uptake monitored by magnetic resonance imaging. *Vadose Zone J* 7: 1010-1017.
- Polomski, J. and N. Kuhn. 2002. Root research methods. In: Waisel, Y., A. Eshel and U. Kafkaki (eds.) *Plant roots, the hidden half* 3<sup>rd</sup> ed. Marcel Dekker Inc, New York, USA.
- Portas, C.A.M. and H.M. Taylor. 1976. Growth and survival of young plant roots in dry soil. *Soil Science* 121: 170-175.
- Prasad, R. 1988. A linear root water uptake model. *J. Hydrology* 99: 297-306.
- Reece, C.F. 1996. Evaluation of a line heat dissipation sensor for measuring soil matric potential. *Soil Sci. Soc. Am. J.* 60: 1022-1028.
- Rhoades, J.D. and J. Loveday. 1990. Salinity in irrigated agriculture. In: Stewart, B.A. and D.R. Nielsen (Eds.). *Irrigation of agricultural crops*. ASA Monograph 30. Madison, WI.
- Ridley, A.M. and J.B. Burland. 1993. A new instrument for the measurement of soil moisture suction. *Géotechnique* 43: 321-324.



- Romano, N, J.W. Hopmans and J.H. Dane. 2002. Suction table. In J.H. Dane and G.C. Topp (eds.) *Methods of Soil Analysis. Part 4. SSSA Book Ser. 5. SSSA, Madison, WI, USA.*
- Sadras, V.O. and S.P. Milroy. 1996. Soil-water thresholds for the responses of leaf expansion and gas exchange: a review. *Field Crops Res.* 47: 253-266.
- Scheenen, T.W.J., D. van Dusschoten, P.A. de Jager and H. Van As. 2000. Quantification of water transport in plants with NMR imaging. *J. Exp. Bot.* 51: 1751-1759.
- Schneider, K. O. Ippisch and K. Roth. 2006. Novel evaporation experiment to determine soil hydraulic properties. *Hydrol. Earth sys. Sci.* 10: 817-827.
- Schulze, E.D., N.C. Turner, T. Gollan and K.A. Shackel. 1987. Stomatal responses to air humidity and soil drought. *In: Zeiger, Z., G.D. Farquhar and I.R. Cowan (eds.). Stomatal Function. Stanford University Press, CA.*
- Segal, E., T. Kushnir, Y. Mualem and U. Shani. 2008. Microsensing of water dynamics and root distributions in sandy soils. *Vadose Zone J.* 7: 1018-1026.
- Sharp, R.E. and W.J. Davies. 1985. Root growth and water uptake by maize plants in drying soil. *Journal of experimental botany* 36: 1441-1456.
- Sharp, R.E. and W.J. Davies. 1989. Regulation of growth and development of plants growing with a restricted supply of water. *In: Plant under stress*, pp. 72–93, Jones, H.G., Flowers, T.L., Jones, M.B., eds. Cambridge University Press, London
- Smit, A.L., E. George and J. Groenwold. 2000. Root observation and measurements at (transparent) interfaces with soil. *In: Smit, A.L., A.G. Bengough, C. Engels, M. van Noordwijk, S. Pellerin and S.C. van de Geijn. Root methods, a handbook. Springer-Verlag, Heidelberg, Germany.*
- Smith, J.A.C. and H. Griffiths. 1993. *Water deficits, plant responses from cell to community.* BIOS Scientific Publishers, Oxford, UK.
- Somerville, C. and J. Briscoe. 2001. Genetic engineering and water. *Science* 292: 2217.
- Sposito, G. 1981. *Thermodynamics of soil solutions.* Oxford University Press, New York, USA.
- Steudle, E. and C.A. Peterson. 1998. How does water get through roots? *J. Exp. Bot.* 49: 775-788.

- Steudle, E., M. Murrmann, and C.A. Peterson. 1993. Transport of water and solutes across maize roots modified by puncturing the endodermis. *Plant Physiology* 103: 335-349.
- Swanson, R.H. 1975. [I] A thermal flowmeter for estimating the rate of xylem sap ascent in trees. [II] Velocity distribution patterns in ascending xylem sap during transpiration. *Flow, its measurement and control in science and industry* 1: 647-652.
- Tamari S., J.-C. Gaudu and T. Simonneu. 1993. Tensiometric measurement and metastable state of water under tension. *Soil Sci.* 156: 149-155.
- Tarantino A. and L. Mongiovi. 2001. Experimental procedures and cavitation mechanisms in tensiometer measurements. *Geotechnical and Geological Engineering* 19: 189-210.
- Taylor, S.T., Revised and edited by G.L. Ashcroft. 1972. *Physical Edaphology. The physics of irrigated and nonirrigated soils.* W.H. Freeman and company, USA.
- Tingey, D.T. and C. Stockwell. 1977. Semipermeable membrane system for subjecting plants to water stress. *Plant Physiology* 60: 58-60.
- Tollner, E.W., E.L. Ramseur and C. Murphy. 1994. Techniques and approaches for documenting plant root development with X-ray computed tomography. In: Anderson, S.H. and J.W. Hopmans, SSSA Special Publication No. 36. SSSA, Madison, WI.
- Van den Honert, T.H. 1948. Water transport in plants as a catenary process. *Discussions of the Faraday Society* 3: 146-153.
- Van der Ploeg, M.J., H.P.A. Gooren, G. Bakker and G.H. de Rooij. 2008. Matric potential measurements by polymer tensiometers in cropped lysimeters under water-stressed conditions. *Vadose Zone J.* 7:1048-1053.
- Van der Weerd, L., M.M.A.E. Claessens, T. Ruttink, F.J. Vergeldt, T.J. Schaffsma and H. Van As. 2001. Quantitative NMR microscopy of osmotic stress responses in maize and pearl millet. *J. Experimental Botany* 52: 2333-2343.
- Van Genuchten, M. Th. 1980. A closed-form equation for predicting the hydraulic conductivity of unsaturated soils. *Soil Sci. Soc. Am. J.* 44: 892-898.
- Van Schilfgaarde, J. 1994. Irrigation - a blessing or a curse. *Agric. Wat Man.* 25: 203-219.

- Vetterlein, D., H. Marschner and R. Horn. 1993. Microtensiometer technique for in situ measurement of soil matric potential and root water extraction of a sandy soil. *Plant and soil* 149: 263-273.
- Warrick, A.W. 2002. *Soil physics companion*. CRC Press LLC, Florida.
- Wilson, K.B., D.D. Baldocchi and P.J. Hanson. 2001. Leaf age affects the seasonal pattern of photosynthetic capacity and net ecosystem exchange of carbon in a deciduous forest. *Plant, cell and the environment* 24: 571-583.
- Whalley, W.R., J. Lipiec, W. Stepniowski and F. Tardieu. 2000. Control and measurement of the physical environment in root growth experiments. *In: Smit, A.L., A.G. Bengough, C. Engels, M. van Noordwijk, S. Pellerin and S.C. van de Geijn (eds.)*. *Root methods: a Handbook*, Springer, Berlin.
- Wood, A.J. 2005. Eco-physiological adaptations to limited water environments. *In: Jenks, M.A. and P.M. Hasegawa (eds.)* *Plant abiotic stress*. Blackwell publishing, Iowa, USA.
- Wood, A.J. and M.A. Jenks. 2007. Plant desiccation tolerance: Diversity distribution, and real-world applications. *In: Jenks, M.A. and A.J. Wood. 2007 Plant desiccation tolerance*. Blackwell publishing, Iowa, USA.
- Wright. 1977. The relation between leaf water potential and the levels of abscisic acid and ethylene in excised wheat leaves. *Planta* 134:183-189.
- Young, M.H. and J.B. Sisson. 2002. Tensiometry. *In J.H. Dane and G.C. Topp (eds.)* *Methods of Soil Analysis. Part 4. SSSA Book Ser. 5. SSSA, Madison, WI*.
- Zegbe, J.A., M. H. Behboudian and B. E. Clothier. 2004. Partial rootzone drying is a feasible option for irrigating processing tomatoes. *Agricultural Water Management* 68: 195-206
- Zegelin, S.J., I. White and D.R. Jenkins. 1989. Improved field probes for soil water content and electrical conductivity measurement using time domain reflectometry. *Water Resources Research* 25: 2367-2376.
- Zimmerman, U., H. Schneider, L.H. Wegner and A. Haase. Water ascent in tall trees: does evolution of land plants rely on a highly metastable state? *New Phyt.* 162: 575-615.
- Zwieniecki, M.A. and L. Boersma. 1997. A technique to measure root tip hydraulic conductivity and root water potential simultaneously. *J. Exp. Bot.* 48: 333-336.

Zwieniecki, M.A., M.V. Thompson, and N.M. Holbrook. 2003. Understanding the hydraulics of porous pipes: Tradeoffs between water uptake and root length utilization. *Journal of Plant Growth Regulation* 21: 315-323.

---

## Samenvatting

---

Door wereldwijde klimaatverandering kunnen droogten vaker voorkomen en ze kunnen daarbij ook heviger zijn. Het watergebruik in de landbouw is nog altijd groeiend, maar de hoeveelheid water dat voor irrigatie gebruikt kan worden is eindig. Het begrijpen van wateropname door plantenwortels onder water limiterende omstandigheden neemt dan ook toe. Stroming van water van de bodem de wortel in wordt gedreven door een potentiaal gradiënt die bestaat tussen water in de bodem en water in de wortel. Deze gradiënt wordt onder andere bepaald door de mate waarin bodemdeeltjes kracht uitoefenen op (trekken aan) het in de bodem aanwezige water; dit wordt ook wel de matrische potentiaal genoemd. In de onverzadigde bodem, is de matrische potentiaal vaak de grootste component van de totale potentiaal van het bodemwater. Tensiometers worden algemeen gebruikt om het drukequivalent van de matrische potentiaal te meten. Helaas kunnen conventionele tensiometers maar tot een matrische potentiaal van  $-0.09$  MPa meten. Dit is een gevolg van het met water gevulde reservoir in de conventionele tensiometers. Het gebruik van tensiometers die met een polymeeroplossing worden gevuld in plaats van water vergroot het meetbereik tot voorbij een matrische potentiaal van  $-1.6$  MPa (bijna twintig keer meer in vergelijking met water gevulde tensiometers). Dit proefschrift beschrijft de ontwikkeling van dergelijke polymeertensiometers, die bestaan uit een druksensor met ingebouwde temperatuursensor, een roestvrij staalomhulsel, en een ceramische plaat met een membraan om lekkage van de polymeeroplossing te verhinderen.

Het verloop van druk op lange termijn, temperatuureffecten en responstijden van de polymeertensiometers werden getest onder laboratoriumomstandigheden. De polymeertensiometers werden ook getest in drie herpakte bodems: zandige leem, zand en leem. Na enkele maanden continu gebruik werd een langzame daling

van de osmotische druk waargenomen. Voor deze daling werd een correctie op de metingen ontwikkeld.

De osmotische potentiaal van een polymeer oplossing is temperatuursafhankelijk en vereist calibratie voordat de tensiometer in de bodem geïnstalleerd wordt. Responstijden als gevolg van veranderingen in omgevingstemperatuur konden worden verkort door het volume polymeeroplossing in de tensiometer te minimaliseren en tegelijkertijd het keramisch oppervlak dat in contact stond met de polymeer oplossing te maximaliseren. Op deze manier werden responstijden acceptabel voor gebruik in het laboratorium en veldexperimenten. Bodemcontact werd vergroot door gebruik te maken van massieve, kegelvormige keramieken in plaats van keramische plaatjes.

Door de combinatie van matrische potentialen gemeten met een polymeertensiometer en vochtgehalten gelijktijdig gemeten door middel van time domain reflectometry, kon de *in situ* vochtretentie karakteristiek van een bodem bepaald worden over het meetbereik van beide instrumenten. Vochtretentie karakteristieken die apart in het laboratorium bepaald werden, werden gebruikt om vochtmetingen van time domain reflectometry om te rekenen naar matrische potentialen. Daarbij kwam naar voren dat de precisie van TDR en die van de conversie een grote rol gaat spelen bij lage vochtgehalten. De vergelijking van indirect verkregen matrische potentialen met van de polymeertensiometers laat dan ook vooral het risico zien om dergelijke indirect verkregen potentialen te gebruiken bij lage vochtgehalten.

Vervolgens werd met een lysimeter experiment de geschiktheid van polymeertensiometers om matrische potentialen te registreren in de aanwezigheid van wateropname door plantenwortels getest. Door te variëren in de hoeveelheid irrigatie kon in de lysimeters hevige, gemiddelde en geen water stress condities voor maïs (*Zea Mays, L.*) gemaakt worden. De door de polymeertensiometers gemeten matrische potentiaal leverde nauwkeuriger niveaus van water stress op dan wanneer de metingen waren gedaan met conventionele methoden. De van tevoren gekozen stress niveaus bevonden zich in het steile, droge eind van de vochtkarakteristiek. Hier zijn volumetrische vochtgehalte metingen minder informatief, simpelweg omdat er weinig vocht overblijft.

Waarnemingen met polymeertensiometers liet zien dat maïs planten in staat zijn om zelfs in een hele droge bodem water op te nemen en om de wateropname te verschuiven naar lagere, relatief nattere gedeelten van de bodem. Deze verschuiving lijkt samen te hangen met het bereiken van het steile, droge gedeelte van de vocht karakteristiek in een ondieper gedeelte van het bodemprofiel. Foto's van het wortelstelsel gedurende het experiment door middel van rhizobuizen lieten zien dat het optreden van water tekorten ervoor zorgt dat wortels dieper in de bodem gaan groeien en dat deze wortelgroei dynamisch is gedurende periodes van water tekorten en hervatte irrigatie.

Polymeertensiometers zijn op dit moment de enige instrumenten die matrische potentialen in het steile, droge gedeelte van de vocht karakteristiek kunnen meten in een veldexperiment. De resultaten die gepresenteerd zijn in dit proefschrift laten zien dat polymeertensiometers een belangrijke instrumentele toevoeging zijn om bodemfysische processen in droge bodems te karakteriseren.





---

# Curriculum Vitae

---

Martine Johanna van der Ploeg, 3 juni 1978, Alkmaar

1990-1995

HAVO, Agnes College, Leiden.

1995-1997

VWO, Aquino College, Leiden.

1997-2003

Studie Bodem, water en atmosfeer, Wageningen Universiteit, specialisatie Hydrologie.

2001

Afstudeeronderzoek University of Life Sciences, Noorwegen.

2002-2003

Stage bij Duchás, Heritage Service of Ireland, Ierland.

2003-2008

Promotieonderzoek bij de leerstoelgroep Bodemnatuurkunde, Ecohydrologie en Grondwaterbeheer.

2008-heden

Postdoc bij de leerstoelgroep Bodemnatuurkunde, Ecohydrologie en Grondwaterbeheer.

December 2008

Certificaat Netherlands Research School for Socio-Economic and Natural Sciences of the Environment (SENSE), belangrijkste activiteiten:

deelname aan de cursus Environmental soil physics (Heidelberg, 2004)

deelname aan de cursus Advanced soil physics (Wageningen, 2003-2004)

deelname aan de cursus Uncertainty modelling and analysis (Wageningen, 2004)

deelname aan the International seminar AQUA, Citizenship through the theme of water: participatory report (Collengo, 2004)



This research was financially supported by the Dutch Technology Foundation STW (project 05828).